CONTENTS (Continued)

CONTENTS

I 49.77:1219 NASA 1.60:1219/v.1

MAY 30 1978

NASA Technical Paper 1219

COMPLETED ORIGINAL

A Digital Computer Program for the Dynamic Interaction Simulation of Controls and Structure (DISCOS)

Volume I

Carl S. Bodley, A. Darrell Devers,
A. Colton Park, and Harold P. Frisch

MAY 1978

NASA

165

NAS1.60:1219/v.1

NASA Technical Paper 1219

A Digital Computer Program for the Dynamic Interaction Simulation of Controls and Structure (DISCOS)

Volume I

Carl S. Bodley, A. Darrell Devers,
and A. Colton Park
Martin Marietta Corporation
Denver, Colorado

Harold P. Frisch
Goddard Space Flight Center
Greenbelt, Maryland

National Aeronautics
and Space Administration

**Scientific and Technical
Information Office**

1978

All measurement values are expressed in the International System of Units (SI) in accordance with NASA Policy Directive 2220.4, paragraph 4.

PREFACE

This document, prepared by the Dynamics and Loads Section, Martin Marietta Corporation, Denver Division, under Contract NAS5-11996, presents the results of a study for the purpose of developing a computer program system for dynamic simulation and stability analysis of passive and actively controlled spacecraft. The study was performed from May 1973 to April 1975 and was administered by the Goddard Space Flight Center, National Aeronautics and Space Administration, Greenbelt, Maryland, under the direction of Joseph P. Young.

Upon delivery, the computer program and associated documentation was checked in detail by Harold P. Frisch. This document incorporates both the original Martin work and the supplementary material prepared at the Goddard Space Flight Center.

The digital computer program, DISCOS (Dynamic Interaction Simulation of Controls and Structure), has been extensively annotated and tested on a range of problems that should have exposed nearly all theoretical errors and programming bugs.

From its inception in 1973, DISCOS has been designed to grow as new needs and more efficient computational techniques develop. This feature makes it impossible to define a final version. To circumvent this problem, the official release version will contain only those additions to the delivered program that enhance program documentation and user interface capability and correct programming errors.

Included in this version are more than 10,000 comment cards and a capability to routinely direct the computer to output on the line printer virtually all computation along with explanatory alphanumeric statements. A large percentage of the comment cards are in subroutines DEF1, DEF2, . . ., and DEF5. These subroutines are composed entirely of comment cards and provide the user with an area in the source file for keeping documentation current. In particular, subroutine DEF5 contains a narrative description of the program and its current capabilities.

For the uninitiated reader, it probably would be best to speed-read subroutine DEF5 to obtain a quick overview of the capabilities of the program and the solution techniques applied before reading this document.

The potential user should be aware of the fact that DISCOS is not intended for simple problems. It is primarily for problems which were heretofore intractable. Consequently, the theoretical basis for the program is highly advanced, and the computation algorithms are designed for the efficient processing of the equations associated with large multidegree-of-freedom systems.

As an aid to the user, the paper on which the derivation of the coupled flexible-body equations of motion is based and a paper that outlines the solution method and comments on results obtained from several DISCOS applications appear as reference material at the end of Volume I. Volume I contains all relevant theoretical work.

Volume II describes the DISCOS program and its support programs. The user is encouraged to refer to the comment cards provided in all DISCOS subroutines for additional descriptive information. The comment cards found in the DISCOS subroutines are intended to provide a link between the computer code and the theoretical equations provided in Volume I.

To effectively interface with the program, the user must be able to write the subroutines that will define all non-gyroscope forces and torques. The user is provided with a clean interface. When the load vector associated with the effects of springs, dampers, motors, gas jets, etc. is defined and properly stored in the computer memory, DISCOS will automatically transform it into the appropriate generalized form required by the formulation.

The inclusion of effects such as aerodynamic loading and thermodynamic deformation is more difficult. However, the methodology is analogous to that used for including gravity-gradient effects.

The methodology for including loads associated with springs, dampers, motors, gas jets, constraints, etc. is found in Volume II and in the comment cards of the appropriate subroutines referred to in Volume II.

DISCOS is probably the most powerful computational tool to date for the computer simulation of actively controlled coupled multiflexible-body systems. It is not an easy program to understand and effectively apply, but it is not intended for simple problems. The user is expected to have an extensive working knowledge of rigid- and flexible-body dynamics, finite-element techniques, numerical methods, and frequency-domain analysis.

A DIGITAL COMPUTER PROGRAM FOR THE DYNAMIC INTERACTION SIMULATION OF CONTROLS AND STRUCTURE (DISCOS) VOLUME I

Carl S. Bodley, A. Darrell Devers, and A. Colton Park
Martin Marietta Corporation
Denver, Colorado

and

Harold P. Frisch
Goddard Space Flight Center
Greenbelt, Maryland

I. INTRODUCTION

Modern society has derived numerous and varied benefits from Earth-orbiting satellites. These benefits include prediction of extreme changes in weather, exploration of mineral and water resources, materials research, medical research and experimentation, solar-system studies, and increased communications and defense capabilities. The design and ultimate development of these satellites requires extensive analytical and experimental studies to ensure complete confidence in the overall ability of the total system to perform its required functions.

Two of the most important and potentially most difficult of these studies are the analysis of dynamic response and the prediction of stability characteristics. In recent years, the National Aeronautics and Space Administration (NASA) and members of the aerospace industry have expended much effort in analyzing these phenomena. Although these are worthy efforts, most have been somewhat limited in scope because of the extreme complexity of the problems. Factors that make these studies so complex are: (1) the imposition of a spin rate for either stabilization or artificial gravity; (2) the dynamic interaction of this spin rate with large flexible appendages; (3) the complex environmental loadings, including gravity gradient and solar radiation; and (4) the intricate control logic required for maintaining stability or for executing orbital maneuvers.

The authors at Martin Marietta Corporation acknowledge the assistance provided by Goddard Space Flight Center (GSFC) personnel. Harold Frisch and James Donohue contributed valuable technical comments and suggestions throughout the program. In particular, they

developed the basic approach to be used for data input, defined exactly what should be included in the transfer function and stability analysis portion of the program, and defined eight of the eleven demonstration problems. They provided the associated data that were used to verify both the nonlinear time response and linear transfer function and the stability analysis portions of the program. Raymond Welch provided the subroutine used to generate root-locus plots. Dr. William Case provided valuable advice on interfacing with NASTRAN output and generated the demonstration problem used to validate the interface subroutine (NASFOR).* During the early program development stage, Dr. James Mason offered significant advice on the need to compute internal forces at the interconnect points. Reginald Mitchell contributed invaluable advice on requirements for making the program compatible with the GSFC IBM 360/95 computer system. In addition, he supplied the contractor with a 360-compatible plot package, furnished the contractor with a self-authored subroutine for reading NASTRAN output, and was responsible for running all demonstration problems on the 360/95 computer. Finally, the authors acknowledge the encouragement and efforts of Joseph P. Young, Technical Monitor, who made numerous valuable comments and suggestions throughout the study.

A. Overview

The state-of-the-art dynamic response analysis of a system of connected bodies is currently restricted to topological systems of connected rigid bodies with (possibly) flexible terminal bodies. Because of the complex orbiting configuration and mechanical systems proposed for future space programs, the limitations of the current technology are severely restrictive. This document presents a more comprehensive formulation that is capable of considering any body of the total system as flexible and that is not restricted to a specific connection arrangement.

Applications of such methods and program systems are numerous and include simulation of the Space Shuttle payload deployment/retrieval mechanism, solar-panel-array deployment, antenna deployment, analysis of multispin satellites, and analysis of large, highly flexible satellites.

This approach provides a general-purpose modeling capability for dynamic simulation and stability analysis of passive and actively controlled spacecraft. In particular, the following items are considered:

- Time-domain solution of the nonlinear differential equations of motion that describe total or nominal response† of the complete spacecraft system idealized as a collection of interconnected flexible (or rigid) bodies
- Linearization of the governing differential equations by numerical means

*The NASFOR subroutine has been superseded by a special NASTRAN DMAP program and associated preprocessor program written by Harold P. Frisch.

†In certain cases, the total response of the dynamic system may be considered to be equilibrium state motion (nominal response) plus perturbation motion with respect to the equilibrium state.

- Time-domain solution of the linearized differential equations that describe the perturbation response of the complete spacecraft system about some predetermined (calculated or user-specified) nominal motion
- General frequency-domain stability analysis corresponding to the linearized spacecraft representation
- Provision for arbitrary (explicitly time-dependent) loadings and environmental interaction, such as gravity gradient and thermally induced deformations resulting from solar radiation

B. Description of the Physical System

The physical system undergoing analysis may be generally described as a cluster of contiguous, flexible structures (bodies) that comprise a mechanical system such as a spacecraft. The entire system (spacecraft) or portions thereof may be either spinning or nonspinning. Member bodies of the spacecraft are capable of undergoing large relative excursions such as those of appendage deployment or rotor/stator motions. The general system of bodies is, by its inherent nature, a feedback system in which inertial forces (such as those due to centrifugal and Coriolis acceleration) and the restoring and damping forces are motion-dependent. Also, the system may possess a control system in which certain position and rate errors are actively controlled through the use of reaction control jets, servomotors, or momentum wheels.

Bodies of the system may be interconnected by linear or nonlinear springs and dampers, by a mechanism that is a combination of gimbal and slider block, or by any combination of these. Also, any two bodies of the system may be free (one from the other) and possess six degrees of relative motion freedom. Several or all of the six degrees of relative motion freedom between two bodies may also be a prescribed function of time (including zero motion).

For further introduction of the physical system, consider an illustrative example, such as the system of bodies of figure 1, and let this example be the prototype for all subsequent discussion and development.

In figure 1, a nontopological tree configuration has been deliberately indicated. There are five hinges and four bodies, thus one closed path. Consecutive integer labels are used for body reference points, hinges, sensor points,* and momentum wheels. The numerical order in each of the four label sets may be random; however, it is understood that body 1 (which may be any body of the system) is associated with hinge 1.

For each body of the system, there is a body-fixed, right-handed reference frame, whose origin may be at the body's mass center or at some structural hard point on the body. (A body's elastic deformation is measured in its reference frame.)

*A "sensor point" is any point at which kinematic data must be obtained (e.g., where an attitude sensor is located).

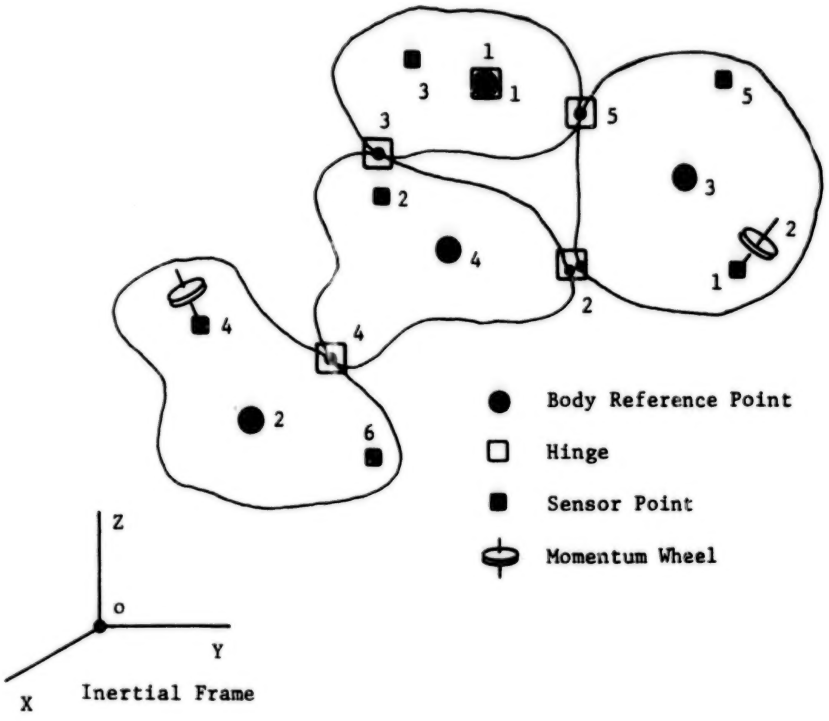

Figure 1. Labeling scheme for example system.

In this document, a hinge is defined as a pair of structural hard points (see figure 2) with a point situated on each of two contiguous bodies. In figure 2, point p and point q comprise a hinge. Clearly, a typical body may contain one or more hinge points, but a hinge may be associated with only two bodies. Hinge 1 is given special consideration. It is also a pair of points; but one of the pair is coincident with the reference point of body 1, and the other point of the pair is coincident with the inertial origin. Thus, motion "across the hinges" is used to represent system motion. The reference point of body 1 is located with respect to the inertial origin by an inertially referenced position vector. The attitude of the reference frame of body 1, with respect to the inertial frame, is represented by three Euler angles. Thus, six position/attitude coordinates are associated with hinge 1.

Each of the remaining hinges is considered in a manner somewhat similar to that of hinge 1. Referring to figure 2, note that there is an orthogonal reference frame attached to point p and another to point q. The triad of point p may have a "natural" (or undeformed) misalignment with respect to the triad of body point m, plus additional misalignment caused by elastic deformation. The same relationship is true concerning points n and q.

Now six relative position/attitude coordinates are associated with the hinge of points p and q. Point q is located from point p with a p-frame referenced position vector. The attitude of the q-frame with respect to the p-frame is represented by three Euler rotations. Thus, if NH is the number of system hinges, 6 X NH position coordinates are to be used in

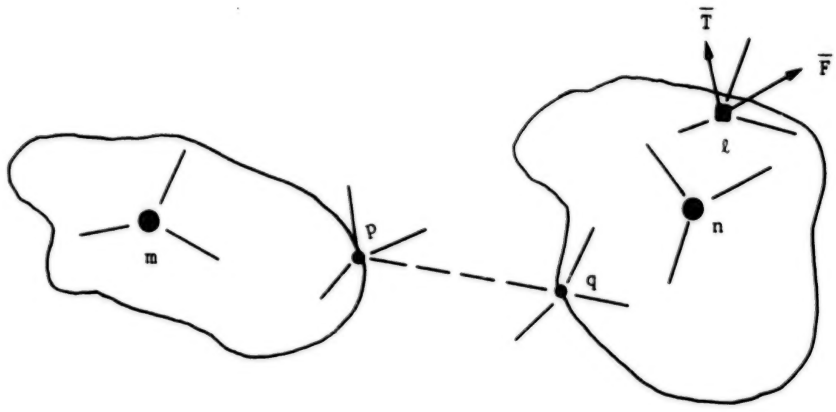

Figure 2. Typical contiguous bodies of the system.

conjunction with modal displacement coordinates for defining the system's position state. Note that only the time-variable position coordinates of the 6 X NH set of candidates are considered as state-vector elements. (The position coordinates whose rates are constrained to zero are not included; however, the position coordinates themselves need not be zero.)

The system of bodies usually has a number of so-called sensor points. A sensor point is defined as a structural hard point with an attached right-handed orthogonal reference frame that is used for a variety of purposes. A sensor point may be used to enable the program system to monitor the position, attitude, or the rates associated with a specific structural hard point. For example, a rate gyro, a star tracking device, or another motion/position sensing device is physically situated at a sensor point. Also, a sensor point is used as a point of application of a force or torque vector (see figure 2).

The system of bodies may contain built-in momentum wheels, of which some are constant speed wheels and others are variable speed. The variable speed momentum wheels are motor driven; the shaft torque results from a given control law. Each momentum wheel of the system must be associated with a sensor point because, for a general flexible body, the gyroscopic coupling is influenced by elastic motion.

As is indicated in figure 1, the system may be in a nontopological tree configuration. The methods employed in this development are such that closed-loop configurations (generally referred to as nontopological) may be considered. If every body of the N-Body system is rigid, there may be no closed loops because such a system has an indeterminate "load path." To accommodate closed loops, the system must contain sufficient structural flexibility (compliance), and therefore modal displacement coordinates, so that the kinematic equations of interconnection constraint are algebraically consistent.

The program development is such that none, several, or all bodies of the N-Body system may be flexible. The system may be "forced" by environmental factors such as gravity, gravity gradient, solar pressure, thermal gradient, and aerodynamic drag.

The computer program system described herein falls into several categories of capability:

- Synthesis and time-domain solution of the nonlinear differential equations of motion of the complete spacecraft system idealized as a collection of interconnected flexible (or rigid) bodies
- Linearization of the governing equations by numerical means
- Time-domain solutions of the linearized equations that describe perturbation response of the complete spacecraft system about some predetermined (calculated or user-specified) nominal motion
- General frequency-domain stability analysis corresponding to the linearized spacecraft representation

II. EQUATIONS OF STATE/TIME-DOMAIN SIMULATION

A. Introductory Discussion

The state equations* that govern dynamic response of a system of interconnected flexible bodies, which may be actively or passively controlled and which may be "forced" by environmental factors such as solar pressure, gravity gradient, aerodynamic drag, etc., are presented here in a concise summary form as:

$$\{\dot{U}\}_j = [m]_j^{-1} \left(\{G\}_j + [b]_j^T \{\lambda\} \right) \tag{II-1}$$

$$\{\dot{\xi}\}_j = [S_\xi]_j \{U\}_j \tag{II-2}$$

$$\{\dot{\beta}\} = \sum_j [B]_j \{U\}_j \tag{II-3}$$

$$\{\dot{\delta}\} = f\left(\{\beta\}, \{\dot{\beta}\}, \{\xi\}, \{\dot{\xi}\}, \{\delta\} \right) \tag{II-4}$$

subject to the constraint equations

$$\sum_j [b]_j \{U\}_j = \{\dot{\alpha}\} \tag{II-5}$$

*For the interested reader, Reference Paper I describes the development of these equations in more detail.

In equations II-1 through II-5 the index, j, ranges from 1 through the number of bodies of the system. Equations II-1 through II-4 represent n first order, nonlinear, ordinary differential equations whereas equation II-5 represents m additional conditions of kinematic constraint. Thus, the dimension of the state space for a given system of controlled bodies is (n-m). That is, n-m state variables are required for defining the configuration at any instant of time, t.

State variables of the configuration space include absolute velocities, $\{U\}_j$; modal displacements, $\{\xi\}_j$; position coordinates (both angular and cartesian position), $\{\beta\}$; and additional variables, $\{\delta\}$, that will subsequently be referred to as control variables. These variables are associated with the differential equations that define a given control law. However, they may reflect any other auxiliary differential equations that are necessary for defining the overall feedback system (for example, they may include thermal equilibrium states or other state variables necessary for a complete definition of the state-dependent environment)

The right-hand sides of equations II-1 through II-4 are functionally dependent on all the state variables and time, although the relationships may be termed only implicit at this point. Let it suffice that, in a way of introduction, a description of the nature of the governing equations II-1 through II-5 be given here and more explicit development and discussion follow in subsequent sections.

Equation II-1 represents the dynamic equilibrium equations for the typical j^{th} body of the system. They are of the form shown whether the body is treated as rigid or flexible. They state, in effect, that a deformation dependent mass matrix, $[m]_j$, postmultiplied by a vector of relative accelerations, $\{\dot{U}\}_j$, produces a vector of inertial forces that is balanced by all other state- and time-dependent forces, $\{G\}_j$, and interconnection constraint forces, $[b]_j^T \{\lambda\}$. The vector, $\{G\}_j$, includes inertial forces due to centrifugal and Coriolis acceleration, as well as elastic restoring forces, damping forces, control actuator forces, and so forth. The constraint forces, $[b]_j^T \{\lambda\}$, are necessary in order to satisfy the kinematic constraint equation (II-5); elements of the vector $\{\lambda\}$ are actually Lagrange multipliers, evaluated and used in the solution process.

Equation II-2 simply represents a selection transformation because the vector of modal velocities, $\{\dot{\xi}\}_j$, is a subvector of $\{U\}_j$. Equation II-3, used to develop $\{\dot{\beta}\}$, represents a kinematical transformation, transforming nonholonomic velocities to time derivatives of position coordinates. Finally, equation II-4 is an auxiliary differential equation that is user-defined and may be used to implement control dynamics and other feedback effects.

The constraint equation (II-5) represents kinematic conditions of a form similar to those of equation II-3. In either case, there is a velocity transformation. Equation II-5 might be termed an active set of kinematic conditions, and those of equation II-3, a passive set. The active set is used to calculate m of the dependent elements of the $\{U\}_j$ vectors in terms of

the remaining independent elements and the prescribed velocities, $\{\dot{\alpha}\}$, some of which may be zero and others user-defined functions of time. Thus, the constraint equations are of a general form because nonholonomic, rheonomic conditions may be so represented. If the $\{U\}_j$ vectors satisfy the required conditions of equation II-5, the position rates, $\{\dot{\beta}\}$, may be evaluated by the passive conditions of equation II-3, resulting in a kinematically consistent system.

Note that m equations of constraint are represented by equation II-5. There are also m Lagrange multipliers in the vector, $\{\lambda\}$. In studies of dynamic systems, the Lagrange multipliers and the dependent velocities and accelerations are often entirely eliminated from the governing equations. Such is not the case in this development in which Lagrange multipliers are involved in the equations for two reasons: (1) to monitor the multipliers as a function of system motion, as they are interconnection forces and torques, and (2) for numerical implementation, it is convenient to calculate and use the $\{\lambda\}$ vector in equation II-1. The Lagrange multipliers are calculated by differentiating equation II-5 and combining that result with equation II-1 giving:

$$\{\lambda\} = \left(\sum_j [b]_j\ [m]_j^{-1}\ [b]_j^T\right)^{-1} \left[\{\ddot{\alpha}\} - \sum_j \left([\dot{b}]_j\ \{U\}_j + [b]_j\ [m]_j^{-1}\ \{G\}_j\right)\right] \quad \text{(II-6)}$$

Note the following functional dependencies:

$$[b]_j = f\left(\{\beta\}_j, \{\xi\}_j\right) \quad \text{(II-7)}$$

$$[B]_j = f\left(\{\beta\}_j, \{\xi\}_j\right) \quad \text{(II-8)}$$

thus,

$$\{\dot{\beta}\} = f\left(\{\beta\}, \{\xi\}, \{U\}\right) \quad \text{(II-9)}$$

$$\{\dot{\xi}\}_j = f\left(\{U\}_j\right) \quad \text{(II-10)}$$

$$\{\dot{\delta}\} = f\left(\{\beta\}, \{\dot{\beta}\}, \{\xi\}, \{\dot{\xi}\}, \{\delta\}\ ;\ t\right) \tag{II-11}$$

$$\{G\}_j = f\left(\{\xi\}, \{U\}, \{\delta\}\ ;\ t\right) \tag{II-12}$$

$$[m]_j = f\left(\{\xi\}_j\right) \tag{II-13}$$

$$[\dot{b}]_j = f\left(\{\beta\}, \{\dot{\beta}\}, \{\xi\}, \{\dot{\xi}\}\right) \tag{II-14}$$

thus,

$$\{\lambda\} = f\left(\{\xi\}, \{\beta\}, \{U\}, \{\dot{\xi}\}, \{\dot{\beta}\}, \{\dot{\delta}\}\ ;\ t\right) \tag{II-15}$$

and

$$\{\dot{U}\} = f\left(\{\xi\}, \{\beta\}, \{U\}, \{\dot{\xi}\}, \{\dot{\beta}\}, \{\ddot{\delta}\}\ ;t\right) \tag{II-16}$$

where, in the foregoing notation, the elements of the matrices/vectors on the left are functions of the elements of the vectors on the right. The chronology of evaluations indicated must be followed in the solution process.

The differential equations of motion for the system are therefore of the general form:

$$\dot{y}_i = f(y_1, y_2, \ldots, y_{n-m}; t) \tag{II-17}$$

and the state vector and its time derivative are arranged as follows:

$$\{y\} = \begin{bmatrix} \{U\}_1 \\ \{U\}_2 \\ \vdots \\ \{U\}_{NB} \\ \{\xi\}_1 \\ \{\xi\}_2 \\ \vdots \\ \{\xi\}_{NB} \\ \beta_1 \\ \beta_2 \\ \vdots \\ \beta_{N\beta} \\ \delta_1 \\ \delta_2 \\ \vdots \\ \delta_{N\delta} \end{bmatrix} \qquad \{\dot{y}\} = \begin{bmatrix} \{\dot{U}\}_1 \\ \{\dot{U}\}_2 \\ \vdots \\ \{\dot{U}\}_{NB} \\ \{\dot{\xi}\}_1 \\ \{\dot{\xi}\}_2 \\ \vdots \\ \{\dot{\xi}\}_{NB} \\ \dot{\beta}_1 \\ \dot{\beta}_2 \\ \vdots \\ \dot{\beta}_{N\beta} \\ \dot{\delta}_1 \\ \dot{\delta}_2 \\ \vdots \\ \dot{\delta}_{N\delta} \end{bmatrix}$$

where NB is the total number of bodies of the system, Nβ is the total number of position coordinates necessary for orienting the system, and Nδ is the total number of auxiliary (control) differential equations required.

Now, if the $\{y\}$ vector is known (numerically) from prescribed initial conditions or from numerical integration of $\{\dot{y}\}$, the primary task of the solution process is to numerically establish the $\{\dot{y}\}$ vector. The $\{\dot{y}\}$ vector is numerically (step by step) integrated to produce an incremented $\{y\}$ vector, and thus a sequence of time-point solutions.

To summarize, a narrative description of the steps (numerical evaluations) necessary for producing $\{\dot{y}\}$ given $\{y\}$, follows.

The matrices, $[B]_j$ and $[b]_j$, are kinematic coefficients that depend on position and modal displacement variables and are evaluated as the first step.

Now, if available numerical techniques (also computer software and hardware) were absolutely accurate, the $\{U\}_j$ vectors resulting from numerical integration of the $\{\dot{U}\}_j$ vectors would satisfy the constraint equation II-5. Because this is not the case, the second step of the solution process is to calculate the dependent elements of the $\{U\}_j$ vectors by using equation II-5. In fact, because of anticipated numerical inaccuracies, only the independent elements of the $\{\dot{U}\}_j$ vectors are obtained by numerical integration. Only n-m "integrators" are involved in the solution process even though all of the elements of the $\{\dot{U}\}_j$ vectors are numerically evaluated (by use of equation II-1); good numerical resolution is found in the independent $\{\dot{U}\}_j$ elements because the Lagrange multipliers $\{\lambda\}$ were used.

A kinematically consistent system results from satisfying equation II-5. The $\{U\}_j$ vectors may now be used with the selection and kinematic transformations as indicated by equations II-2 and II-3 to numerically produce all the modal velocities, $\{\dot{\xi}\}_j$, and position coordinate rates, $\{\dot{\beta}\}$, completing the third step of the process.

Sufficient calculation has been completed to this point to evaluate the control variable rates according to equation II-4, producing $\{\dot{\delta}\}$. During the process of calculating the $\{\dot{\delta}\}$ vector, all of the required control actuator torques (or forces) are calculated because sufficient numerical information is available. All of the constituents of the torques/force vectors, $\{G\}_j$, are now available, and $\{G\}_j$, $[m]_j$, and $[\dot{b}]_j$ are therefore numerically evaluated, which completes the fourth step of the process. (Refer to the functional expressions of equations II-11 through II-14.)

With reference to equation II-6, note that there is now sufficient numerical information to evaluate $\{\lambda\}$, which is then used in equation II-1 to calculate the $\{\dot{U}\}_j$, completing the fifth and final step of the process.

Note that, in the above discussions, the solution process may be carried out through completion, providing the state vector is numerically known. At any step of a simulation, the $\{y\}$ vector is known, of course, as the result of numerical integration. The initial state vector is another matter. It is difficult, if not impossible, for a user to prescribe $\{U\}_j$ vectors that are kinematically consistent with the conditions of equation II-5; also, the nonholonomic velocities of $\{U\}_j$, when considered as a complete set, are of a somewhat abstract nature. The user is in a much better position to prescribe initial values of $\{\dot{\beta}\}$ and $\{\dot{\xi}\}$–the initial velocities that are physically meaningful to him. Thus, to initiate the simulation (that is, to create an initial state vector from information the user is in a position to prescribe) the following preliminary steps must be taken.

The user must prescribe initial values of the $\{\xi\}_j$, $\{\dot{\xi}\}_j$, $\{\beta\}$, $\{\dot{\beta}\}$, and $\{\delta\}$ vectors and the variable speed momentum-wheel spin velocities, $\dot{\theta}$. Now, in that the prescribed position rates, $\{\dot{\alpha}\}$, are explicitly dependent on time and are always available, kinematic equations II-3 and II-5 may be used together to establish initial values of all $\{U\}_j$. The question inevitably arises: Are the number of equations represented by II-3 and II-5 sufficient to solve for the elements of the $\{U\}_j$? Consider the typical $\{U\}_j$ vector. Note that there are six reference-frame velocities in each $\{U\}_j$ (namely, ω_x, ω_y, ω_z, u, v, and w). Six relative velocities are also associated with each hinge. Now, if the system is a topological tree configuration, equations II-3 and II-5 comprise exactly the required number of equations to establish the reference-frame velocities; that is, there are as many hinge points as there are bodies, and, even if every body were rigid, the system would be determinate. In this case, the initial sets of six reference-frame velocities are computed by equations II-3 and II-5; the prescribed initial $\{\xi\}$ vectors and momentum-wheel spin velocities are simply placed in the appropriate $\{U\}_j$ vectors, and the initial state vector is thus defined.

If the system is not a topological tree configuration, then there are more equations (II-3 and II-5) to be satisfied than there are reference frame velocities. (In other words, there are more hinges than bodies.) In this case, elements of the $\{\dot{\xi}\}_j$ vectors must take on the responsibility of helping to satisfy the kinematic conditions. For each hinge in excess of the number of system bodies, there must be at least six deformation modes, represented by ξ coordinates, and they must be distributed throughout the system in such a way that the kinematic conditions of equation II-5 are independent. Clearly then, when there are more hinges than bodies (nontopological tree), one or more of the bodies must be flexible for the system to be determinate. When the configuration is nontopological, the user will specify initial values for all of the $\dot{\xi}$, but he must acknowledge that they are not all independent and that the dependent ones (automatically determined by the program) are calculated and replace the values that he has specified.

From these considerations, note that the initial state vector is created by the program from information that is user-supplied and that is physically meaningful to him. In the event of a nontopological tree configuration, the user's only concern in regard to initial conditions is whether he has supplied an adequate description of system flexibility for the system's kinematical equations to be determinate.

B. Derivation of Equations of Dynamic Equilibrium

The differential equations of motion and auxiliary equations that characterize a physical system may take any one of several equivalent forms. Equivalent form means that the same physical system can be characterized by more than one set of mathematical variables; in any case, the number of variables must be the same. For example, the motion equations for a rigid body could be derived by using Lagrange's equations (resulting in six second-order equations), or the Newton-Euler equations could be used when translational motion is represented by three second-order equations, whereas rotational motion is represented by

six first-order equations (three moment-momentum equations and three attitude equations). In each case, there are twelve state variables.

There are a variety of alternative methods of analytical dynamics that one may select from to develop the final (programmable) equation format. A timely and valuable commentary accompanies the comprehensive comparative evaluation of these methods in a recent report by Likens (Reference 1). The basis for this development is effectively included in his discussion.

The intent here is not to highlight any particular method of analytical dynamics as being superior to the others. Clearly, the methods are all equivalent if they are developed through completion without any compromising simplifications. The choice of method is made after considering the requirements associated with a particular problem or computer simulation program. This development begins with a Lagrangian approach; then, algebraic manipulation is used to derive the format of equations II-1 through II-5.

Lagrange's equations for the general situation appear as

$$\frac{d}{dt}\left(\frac{\partial T}{\partial \dot{q}_j}\right) + \frac{\partial D}{\partial \dot{q}_j} - \frac{\partial T}{\partial q_j} + \frac{\partial V}{\partial q_j} = Q_j + \sum_{i=1}^{m} a_{ji}\,\lambda_i \qquad \text{(II-18a)}$$

$$\text{for } (j=1, 2, \cdots n)$$

$$\sum_{j=1}^{n} a_{ij}\,\dot{q}_j + a_{it} = 0 \qquad \text{(II-18b)}$$

$$\text{for } (i=1, 2, \cdots m)$$

In these equations, T and V are system kinetic and potential energies, respectively, and D is the Rayleigh dissipation function (accounting for internal damping). The generalized constraint forces

$$\sum_{i} a_{ji}\,\lambda_i$$

augment the generalized forces, Q_j (that arise because of the action of external factors), and are necessary for satisfying the additional conditions of constraint of equation II-18b. The form of equation II-18 is complete and general, in that it includes unconservative forces

(explicitly time dependent), Q_j, and dissipative forces, $\partial D/\partial \dot{q}_i$, and the auxiliary constraint equation (II-18b) are in an all-encompassing form because holonomic conditions may be so represented. The coefficients, $(a_{ij}, j = 1, 2, \cdot\cdot, n; t)$, may depend explicitly on the time, (t); therefore, the constraint conditions as shown account for both rheonomic and scleronomic situations.

In the equations, n is the number of generalized coordinates involved in the representation, and m is the number of auxiliary conditions of constraint. Note that, although the q_j are generalized coordinates (as they must be for the Lagrangian formulation), they are independent *only* in the isolated case when m = 0 or when there are no auxiliary constraint conditions. Some engineers share a misconception on this point: that, if the variables, q_i, are not independent, they are not generalized coordinates. In view of the m constraint equations, this is simply a set of generalized coordinates that are not independent.

In cases where all of the constraint equations are holonomic, it is theoretically possible to eliminate m of the q_i in terms of the remaining n-m. However, if any of the constraint conditions are nonholonomic, a Lagrange multiplier, $\{\lambda_i\}$, must be used in conjunction with that equation. Of course, Lagrange multipliers may be used for either holonomic or nonholonomic constraints.

In that the simulation program includes mathematical representation of active or passive control for elements of the spacecraft system, some state equations involve control variables in addition to equation II-18. The manner in which the additional control equations enter into the composite system state equations is the same whether they are in the form given by equation II-1 or that of equation II-18. In either case, the control system state variables retain their identity, although the control forces/torques necessary to "close the loop" are transformed differently. In the case of Lagrange's equations, the control torques contribute to the generalized forces, Q_j, whereas, in the case of summary equation II-1, they contribute to elements of $\{G\}$ and may be interpreted as ordinary forces or torques, acting at a structural hard point (or at a sensor point). Therefore, discussion of the control system will be postponed until later, and the "mainline" motion equations will be emphasized until the point is reached at which the control system coupling can be clearly indicated.

To "solve" Lagrange's equations of motion, the explicit form of the kinetic and potential energy functions, the dissipation function D, and the form of the transformation relating ordinary Cartesian position coordinates (positioning the typical system particle or element) to the generalized coordinates, q_i must first be defined; the form of the transformation is necessary for expressing generalized forces, Q_j, in terms of external ordinary forces. After the form of the energy functions and coordinate transformation is defined, the indicated differentiations (equation II-18) are performed. A system of ordinary second-order differential equations, which in many cases are nonlinear and which require solution using numerical integration techniques, have been explicitly defined, but the motion equations have not yet been solved.

With numerical implementation and digital programming in mind, the form of the ordinary differential equations is recasted. First of all, they should result in canonical first-order form (the highest time derivatives appear uncoupled on the left-hand side). Also, complicated combinations of generalized velocities and displacements should be grouped so that such groups may be replaced with new variable names. These new variables have been called "quasi-coordinates" in the literature. This will simplify the required computer programming and minimize arithematic computation. Also, it helps considerably in organizing the numerical algorithms necessary for evaluating the left-hand side of the state equations. Thus, recasting the form of the governing equations is sufficiently justified.

The recasting process is begun by defining the forms of kinetic and potential energy and the required transformation. First, note that bodies of the system of flexible bodies are tentatively treated as if they are completely independent of each other. The influence of any body on another is accounted for by the additional constraint conditions and the Lagrange multipliers. Thus, if kinetic and potential energies for the typical body are expressed and Lagrange's equations are applied to it, the ordinary differential equations pertaining to it are simply a subset of equation II-18, and the total system through the representative form of the typical body will have been accounted for.

The generalized coordinates chosen to represent the configuration of the typical body include three Euler angles to indicate attitude of the body fixed-axis system relative to an inertial frame, three projections (components) of the position vector from the origin of the inertial frame to the origin of the body fixed-reference system onto the inertial axes, and N elastic displacement coordinates. Note that the origin of the body fixed-axis system need not necessarily coincide with the body center of mass. Also, the elastic displacement coordinates may be measurements of displacement at a discrete set of points on the body, or they may be coordinates associated with normal vibration modes. In either case, they represent displacements measured in the body axis system. For the r^{th} flexible body, its generalized coordinates are tabulated as:

$$\{q_r\} = \begin{bmatrix} \phi \\ \theta \\ \psi \\ X \\ Y \\ Z \end{bmatrix} \begin{matrix} \left.\vphantom{\begin{matrix}a\\b\\c\end{matrix}}\right\} \text{Attitude Euler Angles} \\ \left.\vphantom{\begin{matrix}a\\b\\c\end{matrix}}\right\} \text{Body's Reference Point Position Coordinates} \end{matrix} \qquad \begin{bmatrix} \xi_1 \\ \xi_2 \\ \cdot \\ \cdot \\ \xi_N \end{bmatrix}_r \left.\vphantom{\begin{matrix}a\\b\\c\\d\\e\end{matrix}}\right\} \text{Elastic Displacement Coordinates}$$

A transformation now exists that relates a set of nonholonomic velocities to the generalized velocities that are extensively used in recasting the equations. The transformation appears as:

$$\begin{bmatrix} \omega_x \\ \omega_y \\ \omega_z \\ \hdashline u \\ v \\ w \\ \hdashline \dot{\xi}_1 \\ \dot{\xi}_2 \\ \vdots \\ \dot{\xi}_N \end{bmatrix} = \left[\begin{array}{ccc:ccc:ccc} \pi_{11} & \pi_{12} & \pi_{13} & & & & & & \\ \pi_{21} & \pi_{22} & \pi_{23} & & & & & & \\ \pi_{31} & \pi_{32} & \pi_{33} & & & & & & \\ \hdashline & & & \gamma_{11} & \gamma_{12} & \gamma_{13} & & & \\ & & & \gamma_{21} & \gamma_{22} & \gamma_{23} & & & \\ & & & \gamma_{31} & \gamma_{32} & \gamma_{33} & & & \\ \hdashline & & & & & & 1 & & \\ & & & & & & & 1 & \\ & & & & & & & & \ddots \\ & & & & & & & & 1 \end{array}\right] \begin{bmatrix} \dot{\phi} \\ \dot{\theta} \\ \dot{\psi} \\ \hdashline \dot{X} \\ \dot{Y} \\ \dot{Z} \\ \hdashline \dot{\xi}_1 \\ \dot{\xi}_2 \\ \vdots \\ \dot{\xi}_N \end{bmatrix} \qquad \text{(II-19)}$$

where, in equation II-19, the vector of nonholonomic velocities, $\{U\}$, contains the three projections, $(\omega_x, \omega_y, \omega_z)$, of the angular velocity vector, $\bar{\omega}$, onto the body fixed axes ($\bar{\omega}$ is the angular velocity of the body reference frame), the three projections of the reference point translational velocity, (u, v, w), onto the body fixed axes, and the displacement rates, $\{\dot{\xi}\}$. The elements of the transformation, γ_{ij} (i, j = 1, 2, 3), are direction cosines; the submatrix, $[\gamma]$, is an orthonormal rotation transformation relating the attitude of the body fixed-axis system to the inertial frame. The submatrix, $[\pi]$, is also a rotation transformation; however, it is not orthonormal because it relates vector components based on an orthogonal basis to those of a skew (nonorthogonal) basis (namely, the axes about which Euler rotations are measured).

In short,

$$\{U\} = [\beta] \{\dot{q}\} \qquad \text{(II-20)}$$

Clearly the elements of $[\beta]$ are functions of the three Euler angles. Twelve sets of Euler angles are possible. Any one set is valid for use in subsequent development; the resulting equation form is independent of selection from the twelve sets of angles.

Elements of the transformation, $[\beta]$, may be explicitly defined in terms of three of the generalized coordinates (the Euler angles).

The kinetic-energy expression for the r^{th} body is most easily expressed (initially) in terms of the nonholonomic velocities, $\{U\}$, after which $[\beta]$ is used to replace $\{U\}$ with $[\beta]\ \{\dot{q}\}$. The kinetic energy is then expressed completely in terms of generalized displacements and velocities—the form necessary for applying equation II-18.

Kinetic energy for the typical body is

$$T = \tfrac{1}{2} \int_V \bar{v} \cdot \bar{v} \sigma dV \qquad \text{(II-21)}$$

where $\bar{v}$ is the velocity field, and σ is mass density, and where integration is carried out over the volume, V, of the body.

The inertial position of any point, p, of the body (figure 3) is:

$$\bar{r} = \bar{X}_R + \bar{\rho}_0 + \bar{\eta} \qquad \text{(II-22)}$$

where $\bar{X}_R$ is the inertial position of the body's reference point (R is the origin of the body axis system), $\bar{\rho}_0$ positions the point p′ (which coincides with p in the undeformed configuration) from point R, and $\bar{\eta}$ (x, y, z, t) is a measure of elastic displacement.

The vectors $\bar{\rho}_0$ and $\bar{\eta}$ are referenced to the body axis system, thus

$$\bar{\rho}_0 = \begin{bmatrix} \bar{i} & \bar{j} & \bar{k} \end{bmatrix} \begin{bmatrix} x \\ y \\ z \end{bmatrix} \qquad \text{(II-23)}$$

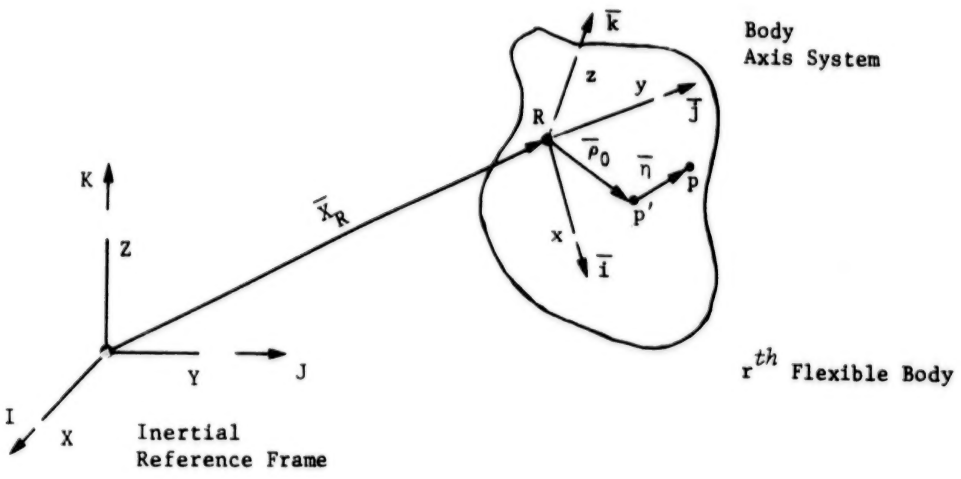

Figure 3. The r^{th} flexible body.

and

$$\bar{\eta}\ (x, y, z, t) = \left[\bar{i}\ \ \bar{j}\ \ \bar{k}\right] \sum_{k=1}^{N} \left(\begin{bmatrix} \phi_{xk}\ (x, y, z) \\ \phi_{yk}\ (x, y, z) \\ \phi_{zk}\ (x, y, z) \end{bmatrix} \xi_k\ (t) \right) \qquad \text{(II-24)}$$

the elastic displacement $\bar{\eta}$ is represented as the superposition of a finite number of single valued space functions, $\bar{\phi}_k$.

The velocity field, $\bar{v}$, is obtained as

$$\bar{v} = \frac{d\bar{r}}{dt} = \bar{v}_R + \bar{\omega} \times \left(\bar{\rho}_0 + \bar{\eta} \right) + \sum_{k=1}^{N} \bar{\phi}_k\ \dot{\xi}_k \qquad \text{(II-25)}$$

with

$$\bar{v}_R = \frac{d\bar{X}_R}{dt}$$

The velocity of the reference point, R, may be expressed in terms of components referenced to either the inertial frame or the body frame; that is,

$$\bar{v}_R = \begin{bmatrix} I & J & K \end{bmatrix} \begin{bmatrix} \dot{X} \\ \dot{Y} \\ \dot{Z} \end{bmatrix} \qquad \text{(II-26)}$$

also

$$\bar{v}_R = \begin{bmatrix} \bar{i} & \bar{j} & \bar{k} \end{bmatrix} \begin{bmatrix} u \\ v \\ w \end{bmatrix}$$

The unit vectors, $\{\bar{i}, \bar{j}, \bar{k}\}$, $\{I, J, K\}$, are related through the rotation transformation, $[\gamma]$, and it follows that

$$\begin{bmatrix} u \\ v \\ w \end{bmatrix} = [\gamma] \begin{bmatrix} \dot{X} \\ \dot{Y} \\ \dot{Z} \end{bmatrix} \qquad \text{(II-27)}$$

To be concise, the repeated index summation convention is introduced at this point. With this convention, when any two factors of a term have the same index, summation over the range of that index is implied, and the Σ sign is deleted. For example, the third term on the right of equation II-25 is

$$\bar{\phi}_k \dot{\xi}_k$$

and represents

$$\sum_{k=1}^{N} \bar{\phi}_k \dot{\xi}_k$$

Now, if equation II-25 is substituted into equation II-21, the kinetic energy is

$$
\begin{aligned}
T = \tfrac{1}{2} \int_V \Big\{ & \bar{v}_R \cdot \bar{v}_R + [\bar{\omega} \times (\bar{\rho}_0 + \bar{\eta})] \cdot [\bar{\omega} \times (\bar{\rho}_0 + \bar{\eta})] \\
& + \bar{\phi}_k \cdot \bar{\phi}_j \, \dot{\xi}_k \, \dot{\xi}_j \\
& + 2 \, \bar{v}_R \cdot [\bar{\omega} \times (\bar{\rho}_0 + \bar{\eta})] + 2 \bar{v}_R \cdot \bar{\phi}_k \, \dot{\xi}_k \\
& + 2 \, [\bar{\omega} \times (\bar{\rho}_0 + \bar{\eta})] \cdot \bar{\phi}_k \, \dot{\xi}_k \Big\} \, \sigma dV
\end{aligned}
\qquad \text{(II-28)}
$$

or, integrating term by term over V,

$$
\begin{aligned}
T = {} & \tfrac{1}{2} \, m \begin{bmatrix} u & v & w \end{bmatrix} \begin{Bmatrix} u \\ v \\ w \end{Bmatrix} \\
& + \tfrac{1}{2} \begin{bmatrix} \omega_x & \omega_y & \omega_z \end{bmatrix} \begin{bmatrix} J_{xx} & -J_{xy} & -J_{xz} \\ -J_{yx} & J_{yy} & -J_{yz} \\ -J_{zx} & -J_{zy} & J_{zz} \end{bmatrix} \begin{bmatrix} \omega_x \\ \omega_y \\ \omega_z \end{bmatrix} \\
& + \tfrac{1}{2} \, e_{jk} \, \dot{\xi}_j \, \dot{\xi}_k \\
& + \begin{bmatrix} u & v & w \end{bmatrix} \begin{bmatrix} 0 & S_z & -S_y \\ -S_z & 0 & S_x \\ S_y & -S_x & 0 \end{bmatrix} \begin{bmatrix} \omega_x \\ \omega_y \\ \omega_z \end{bmatrix} \\
& + \begin{bmatrix} u & v & w \end{bmatrix} \begin{bmatrix} a_{xk} \\ a_{yk} \\ a_{zk} \end{bmatrix} \dot{\xi}_k
\end{aligned}
\qquad \text{(II-29)}
$$

$$+ \begin{bmatrix} \omega_x & \omega_y & \omega_z \end{bmatrix} \begin{bmatrix} d_{xk} \\ d_{yk} \\ d_{zk} \end{bmatrix} \dot{\xi}_k \qquad \text{(II-29) continued}$$

where the following was used:

$$m = \int_V \sigma dV \qquad \text{(II-30)}$$

$$J_{xx} = \int_V [(y + \phi_{yj}\, \xi_j)^2 + (z + \phi_{zj}\, \xi_j)^2]\ \sigma dV \qquad \text{(II-31)}$$

$$= J_{xxo} + 2(b_{yyj} + b_{zzj})\, \xi_j + (c_{yjyk} + c_{zjzk})\, \xi_j\, \xi_k$$

with

$$b_{yyj} = \int_V y\, \phi_{yj}\ \sigma dV$$

$$b_{zzj} = \int_V z\, \phi_{zj}\ \sigma dV \qquad \text{(II-32)}$$

and

$$c_{yjzk} = \int_V \phi_{yj}\, \phi_{zk}\ \sigma dV$$

Also used was

$$a_{xk} = \int_V \phi_{xk} \, \sigma dV \tag{II-33}$$

$$e_{jk} = \int_V \left(\phi_{xj} \, \phi_{xk} + \phi_{yj} \, \phi_{yk} + \phi_{zj} \, \phi_{zk} \right) \sigma dV \tag{II-34}$$

and

$$S_x = \int_V \left(x + \phi_{xj} \, \xi_j \right) \sigma dV \tag{II-35}$$

$$= S_{xo} + a_{xj} \, \xi_j$$

$$d_{xk} = \int_V \left[\left(y + \phi_{yj} \, \xi_j \right) \phi_{zk} - \left(z + \phi_{zj} \, \xi_j \right) \phi_{yk} \right] \sigma dV \tag{II-36}$$

$$= b_{yzk} - b_{zyk} + \left(c_{yjzk} - c_{zjyk} \right) \xi_j$$

and also,

$$J_{xy} = \int_V \left(x + \phi_{xj} \, \xi_j \right) \left(y + \phi_{yj} \, \xi_j \right) \sigma dV \tag{II-37}$$

$$= J_{xyo} + \left(b_{xyj} + b_{yxj} \right) \xi_j + c_{xjyk} \, \xi_j \, \xi_k$$

All other quantities involved in equation II-29 are obtained by cyclic permutation of the indexes, x, y, and z. Finally, because the kinetic energy is of quadratic form in the elements of $\{U\}$, it may be expressed as a triple matrix product

$$T = \tfrac{1}{2} \left\lfloor U \right\rfloor [m] \, \{U\} \tag{II-38}$$

with

$$[m] = \left[\begin{array}{ccc|ccc|ccc} J_{xx} & -J_{xy} & -J_{xz} & 0 & -S_z & S_y & d_{x1} & d_{x2} & \cdots \; d_{xN} \\ & J_{yy} & -J_{yz} & S_z & 0 & -S_x & d_{y1} & d_{y2} & \cdots \; d_{yN} \\ & & J_{zz} & -S_y & S_x & 0 & d_{z1} & d_{z2} & \cdots \; d_{zN} \\ \hline & & & m & 0 & 0 & a_{x1} & a_{x2} & \cdots \; a_{xN} \\ & & & & m & 0 & a_{y1} & a_{x2} & \cdots \; a_{yN} \\ & & & & & m & a_{z1} & a_{z2} & \cdots \; a_{zN} \\ \hline & \text{(symmetric)} & & & & & e_{11} & e_{12} & \cdots \; e_{1N} \\ & & & & & & & e_{22} & \cdots \; e_{2N} \\ & & & & & & & & \cdots \; e_{NN} \end{array}\right] \qquad \text{(II-39)}$$

or in short,

$$[m] = \left[\begin{array}{c|c|c} J & -S & d \\ \hline S & m & a \\ \hline d^T & a^T & e \end{array}\right] \qquad \text{(II-40)}$$

Using equations II-40, II-19, and II-38 gives

$$T = \tfrac{1}{2} \left\lfloor \dot{q} \right\rfloor [\beta]^T \; [m] \; [\beta] \; \{\dot{q}\} \qquad \text{(II-41)}$$

Clearly, the elements of [m] depend only on the ξ_k; the elements of $[\beta]$ depend on the Euler angles, and kinetic energy is therefore a function of generalized velocities and the generalized coordinates themselves. Thus, the functional notation,

$$T = T\left(q_1, q_2, \cdots q_n; \dot{q}_1, \dot{q}_2, \cdots \dot{q}_n\right)$$

is applicable; terms such as $\partial T/\partial q_j$ will come about and play an important role in the simulation.

To continue, it is necessary to express the potential energy, V, and dissipation function, D. Assume that the elastic strain energy can be written as a positive definite quadratic form in the elastic displacement coordinates, or

$$V = \tfrac{1}{2} \lfloor \xi \rfloor [k] \{\xi\} \tag{II-42}$$

the symmetric matrix, [k], is developed by standard finite-element techniques such as those embodied in NASTRAN. If $\{\xi\}$ is a set of normal modal coordinates, then [k] is diagonal with the j^{th} diagonal element appearing as

$$k_{jj} = \omega_j^2 \tag{II-43}$$

where ω_j is the j^{th} natural frequency. Of course, normalization of the eigenvectors (mode shapes) is assumed so that the generalized mass for the j^{th} vibration mode is unity.

Now, because

$$\begin{aligned} \{\xi\} &= [0 \mid 0 \mid I_N] \{q\} \\ &= [S_\xi] \{q\} \end{aligned} \tag{II-44}$$

it follows that

$$V = \tfrac{1}{2} \lfloor q \rfloor [S_\xi]^T [k] [S_\xi] \{q\} \tag{II-45}$$

Similarly, D is written as

$$D = \tfrac{1}{2} \lfloor \dot{q} \rfloor [S_\xi]^T [C] [S_\xi] \{\dot{q}\} \tag{II-46}$$

where matrix, [C], developed by standard finite-element techniques, is equivalent viscous damping for the structure.

Refer back to Lagrange's equations (II-18a and II-18b), and reexpress them in matrix format as follows:

$$\begin{aligned}\frac{d}{dt}\left([\beta]^T\ [m]\ [\beta]\ \{\dot{q}\}\right) = &-[S_\xi]^T\left([k]\ [S_\xi]\ \{q\} + [C]\ [S_\xi]\ \{\dot{q}\}\right)\\ &+\{Q\} + \tfrac{1}{2}\left\{\lfloor\dot{q}\rfloor\ [\beta_{,j}]^T\ [m]\ [\beta]\ \{\dot{q}\}\right\}\\ &+\tfrac{1}{2}\left\{\lfloor\dot{q}\rfloor\ [\beta]^T\ [m]\ [\beta_{,j}]\ \{\dot{q}\}\right\}\\ &+\tfrac{1}{2}\left\{\lfloor\dot{q}\rfloor\ [\beta]^T\ [m_{,j}]\ [\beta]\ \{\dot{q}\}\right\} + [a]^T\{\lambda\}\end{aligned} \qquad \text{(II-47)}$$

and

$$[a]\ \{\dot{q}\} = -\{a_t\} \qquad \text{(II-48)}$$

What is meant by $[\beta_{,j}]$ and $[m_{,j}]$ is the partial derivative of each element of $[\beta]$ and $[m]$ with respect to the j^{th} generalized coordinate.

Now, define the ordinary momenta (see Reference Paper II):

$$\begin{aligned}\{p\} &= [m]\ [\beta]\ \{\dot{q}\}\\ &= [m]\ \{U\}\end{aligned} \qquad \text{(II-49)}$$

Also, because

$$\{U\} = [\beta]\ \{\dot{q}\}$$

it follows that

$$\{\dot{q}\} = [\beta]^{-1}\ \{U\} \qquad \text{(II-50)}$$

Using equations II-49, II-50, II-47, and II-48,

$$\begin{aligned}\{\dot{p}\} = &- [\beta]^{-1T} [S_\xi]^T \left([k] [S_\xi] \{q\} + [C] [S_\xi] \{\mathring{q}\} \right) \\ &+ [\beta]^{-1T} \{Q\} + [\beta]^{-1T} \left(\left\{ \lfloor \dot{q} \rfloor [\beta_{,j}]^T \{p\} \right\} - [\dot{\beta}]^T \{p\} \right) \\ &+ \tfrac{1}{2} [\beta]^{-1T} \left\{ \lfloor U \rfloor [m_{,j}] \{U\} \right\} + [\beta]^{-1T} [a]^T \{\lambda\}\end{aligned} \tag{II-51}$$

and

$$[a] [\beta]^{-1} \{U\} = \{-a_t\} \tag{II-52}$$

On studying equations II-51 and II-52, several observations can be made: First of all, recall the form of $[\beta]$ and $[S_\xi]$ (equations II-19 and II-44). It is clear from these forms that

$$[\beta]^{-1T} [S_\xi]^T \equiv [S_\xi]^T \tag{II-53}$$

and that

$$[S_\xi] \{q\} = \{\xi\} \tag{II-54}$$

and

$$[S_\xi] \{\mathring{q}\} = \{\dot{\xi}\} \tag{II-55}$$

Also, because the elements of $[m]$ depend only on ξ_k, the first six elements of

$$\left\{ \lfloor U \rfloor [m_{,j}] \{U\} \right\}$$

are null; therefore

$$[\beta]^{-1T} \left\{ \lfloor U \rfloor [m_{,j}] \{U\} \right\} = \left\{ \lfloor U \rfloor [m_{,j}] \{U\} \right\} \tag{II-56}$$

Further, note that matrix $[\beta]^{-1T}$ transforms the generalized forces, $\{Q\}$, to forces "acting in the quasi-coordinates," or call

$$\{G_{ex}\} = [\beta]^{-1T}\{Q\} \tag{II-57}$$

thus, $\{G_{ex}\}$ contains ordinary forces and moments attributable to external sources and corresponds to time derivatives of the ordinary momenta.

Because the transformation, $[\beta]$, depends only on the Euler angles, it follows that only the first six elements of the column

$$[\beta]^{-1T}\left(\left\{\left[\dot{q}\right]\left[\beta_{,j}\right]\{p\}\right\} - [\dot{\beta}]^{T}\{p\}\right)$$

are nonzero, and, after considerable algebraic manipulation, this column may be reexpressed as

$$[\tilde{\Omega}]\{p\}$$

or

$$[\tilde{\Omega}]\{p\} = \left[\begin{array}{ccc:ccc:ccc} 0 & \omega_z & -\omega_y & 0 & w & -v & & & \\ -\omega_z & 0 & \omega_x & -w & 0 & u & & & \\ \omega_y & -\omega_x & 0 & v & -u & 0 & & & \\ \hdashline & & & 0 & \omega_z & -\omega_y & & & \\ & & & -\omega_z & 0 & \omega_x & & & \\ & & & \omega_y & -\omega_x & 0 & & & \\ \hdashline & & & & & & & & \\ & & & & & & & & \\ & & & & & & & & \\ & & & & & & & & \end{array}\right] \left[\begin{array}{c} p(\omega_x) \\ p(\omega_y) \\ p(\omega_z) \\ \hdashline p(u) \\ p(v) \\ p(w) \\ \hdashline \dot{p}(\xi_1) \\ \cdot \\ \cdot \\ \cdot \\ \dot{p}(\xi_N) \end{array}\right] \tag{II-58}$$

With these observations and definitions, equations II-51 and II-52 may be reexpressed as

$$\{\dot{p}\} = \{G_{ex}\} - \begin{bmatrix}0\\k\end{bmatrix}\{\xi\} - \begin{bmatrix}0\\C\end{bmatrix}\{\dot{\xi}\} + [\tilde{\Omega}]\{p\} + \tfrac{1}{2}\left\{\lfloor U \rfloor [m_{,j}]\{U\}\right\} + [b]^T\{\lambda\} \tag{II-59}$$

and

$$[b]\{U\} = \{\dot{\alpha}\} \tag{II-60}$$

where

$$[b] = [a][\beta]^{-1} \tag{II-61}$$

was used, and

$$\{\dot{\alpha}\} = -\{a_t\} \tag{II-62}$$

Note that constraint equation II-60 is now expressed in terms of the nonholonomic velocities, $\{U\}$; the coefficients, $[b]$, are obtained directly from relatively simple, vectorial expressions of kinematic constraint. The same $[b]$ coefficients are transposed and used to multiply $\{\lambda\}$, producing constraint forces/torques corresponding to the ordinary momenta.

If the $\{G\}$ vector is now defined as

$$\{G\} = \{G_{ex}\} - \begin{bmatrix}0\\k\end{bmatrix}\{\xi\} - \begin{bmatrix}0\\C\end{bmatrix}\{\dot{\xi}\} + [\tilde{\Omega}][m]\{U\} + \tfrac{1}{2}\left\{\lfloor U \rfloor [m_{,j}]\{U\}\right\} - [\dot{m}]\{U\} \tag{II-63}$$

it follows that dynamic equilibrium equations for the typical r^{th} body may be written as

$$\{\dot{U}\}_r = [m]_r^{-1}\left(\{G\}_r + [b]_r^T\{\lambda\}\right) \tag{II-64}$$

to be used in conjunction with system kinematic constraint equations

$$\sum_r [b]_r \{U\}_r = \{\dot{\alpha}\} \tag{II-65}$$

which is the same form as that given by equations II-1 and II-5.

The last three terms of $\{G\}$ given in equation II-63 are inertial forces that involve velocities and displacements of the body. The matrix [m] is an instantaneous inertia matrix, depending on instantaneous values of the deformation coordinates, $\{\xi\}$. The centrifugal and Coriolis effects are completely accounted for within the framework of the assumed velocity field (given by equation II-25). These effects would not be accounted for if "tangential" velocity due to elastic displacement were neglected (i.e., if it were assumed that $|\bar{\omega} \times \bar{\eta}| << |\bar{\omega} \times \bar{\rho}_0|$. In this case, the inertia would be constant and independent of $\{\xi\}$.

An accurate definition of the dynamic equilibrium equations clearly hinges on a complete and accurate definition of the constituents of the $\{G\}_r$ vector, which includes the inertia matrix, $[m]_r$. Also, the kinematic coefficients, $[b]_r$, must be developed in an exact fashion. Kinematics and a more explicit development of $\{G\}$ are given in subsequent sections.

C. Kinematics and System Topology

From a Lagrangian formulation, all of the generalized forces, not derivable from a potential function, ordinarily appear as $\{Q\}$ on the right side of Lagrange's equations of motion. Internal damping forces have been accounted for with the use of Rayleigh's dissipation function, D, and, for generalized constraint forces, by Lagrange's multipliers.

Thus, the remaining generalized forces to deal with include those that are attributable to external factors such as aerodynamic drag, solar pressure, and other commonly encountered environmental loadings.

Control forces (servodrive torques, reaction jets, etc.) are also treated as if they are external. They are not explicitly external, of course, because they depend on time through position and rate errors that are functions of elements of the state vector and on control system state variables that arise from a given control law.

Assume that there is a finite number of points on the typical body at which a force vector (or torque) is known to act. Each of these force/torque vectors contributes to the generalized forces, $\{Q\}$. The generalized forces are calculated by expressing the virtual work of the external ordinary forces in terms of virtual displacements of the points of force application. The transformation that relates ordinary coordinates to generalized coordinates is then used to define the explicit form of the generalized forces. For example, suppose that a force $\bar{f}_p$, and torque, $\bar{T}_p$, act at point p of the typical body. Their virtual work is

$$\delta W = \bar{f}_p \cdot \delta \bar{r}_p + \bar{T}_p \cdot \delta \bar{\theta}_p \tag{II-66}$$

Note that the virtual rotation, $\delta\bar{\theta}_p$, was treated as a vector quantity. This is valid, even though a general rotation is not a vector quantity, because the virtual rotation is infinitesimal and is therefore a vector. Further, because virtual displacements are infinitesimal, $\delta\bar{r}_p$ and $\delta\bar{\theta}_p$ may be expressed in terms of virtual displacements of the quasi-coordinates; that is,

$$\delta\bar{r}_p = \begin{bmatrix}\bar{i} & \bar{j} & \bar{k}\end{bmatrix} \left(\begin{bmatrix}\delta r_1 \\ \delta r_2 \\ \delta r_3\end{bmatrix} + \begin{bmatrix} 0 & (z_p + \eta_{zp}) & -(y_p + \eta_{yp}) \\ -(z_p + \eta_{zp}) & 0 & (x_p + \eta_{xp}) \\ (y_p + \eta_{yp}) & -(x_p + \eta_{xp}) & 0 \end{bmatrix} \begin{bmatrix}\delta\theta_x \\ \delta\theta_y \\ \delta\theta_z\end{bmatrix} + \begin{bmatrix}\phi_{xj}(x_p, y_p, z_p) \\ \phi_{yj}(x_p, y_p, z_p) \\ \phi_{zj}(x_p, y_p, z_p)\end{bmatrix} \delta\xi_j \right) \tag{II-67}$$

and

$$\delta\bar{\theta}_p = \begin{bmatrix}\bar{i} & \bar{j} & \bar{k}\end{bmatrix} \left(\begin{bmatrix}\delta\theta_x \\ \delta\theta_y \\ \delta\theta_z\end{bmatrix} + \begin{bmatrix}\sigma_{xj}(x_p, y_p, z_p) \\ \sigma_{yj}(x_p, y_p, z_p) \\ \sigma_{zj}(x_p, y_p, z_p)\end{bmatrix} \delta\xi_j \right) \tag{II-68}$$

where $(\delta r_1, \delta r_2, \delta r_3)$ are components of virtual displacement of the body's reference point, R; $(\delta\theta_x, \delta\theta_y, \delta\theta_z)$ are components of virtual rotation of the body axis system; and $(\sigma_{xj}, \sigma_{yj}, \sigma_{zj})$ are components of the j^{th} space function, $\bar{\sigma}_j$, representing elastic rotation at point, p (modal slopes, for example).

Now, assume that the force and torque vectors, ($\bar{f}_p$ and $\bar{T}_p$), are referenced to the body axis system; they may therefore be written as

$$\bar{f}_p = \begin{bmatrix}\bar{i} & \bar{j} & \bar{k}\end{bmatrix} \begin{bmatrix}f_{xp} \\ f_{yp} \\ f_{zp}\end{bmatrix} \tag{II-69}$$

and

$$\bar{T}_p = \left\lfloor \bar{i} \;\; \bar{j} \;\; \bar{k} \right\rfloor \begin{bmatrix} T_{xp} \\ T_{yp} \\ T_{zp} \end{bmatrix} \tag{II-70}$$

Note that virtual displacements of the quasi-coordinates are related to virtual generalized displacements by the same transformation that relates nonholonomic velocities to generalized velocities (equation II-19). It follows that the virtual work attributable to $\bar{f}_p$ and $\bar{T}_p$ may be written as

$$\delta W = \left\lfloor \delta q \right\rfloor [\beta]^T \begin{bmatrix} 1 & & & & -(z_p + \eta_{zp}) & y_p + \eta_{yp} \\ & 1 & & z_p + \eta_{zp} & & -(x_p + \eta_{xp}) \\ & & 1 & -(y_p + \eta_{yp}) & x_p + \eta_{xp} & \\ & & & 1 & & \\ & & & & 1 & \\ & & & & & 1 \\ \sigma_{x1})_p & \sigma_{y1})_p & \sigma_{z1})_p & \phi_{x1})_p & \phi_{y1})_p & \phi_{z1})_p \\ \vdots & \vdots & \vdots & \vdots & \vdots & \vdots \\ \sigma_{xN})_p & \sigma_{yN})_p & \sigma_{zN})_p & \phi_{xN})_p & \phi_{yN})_p & \phi_{zN})_p \end{bmatrix}_{(6 + N \times 6)} \begin{bmatrix} T_{xp} \\ T_{yp} \\ T_{zp} \\ f_{xp} \\ f_{yp} \\ f_{zp} \end{bmatrix} \tag{II-71}$$

The virtual work is also expressed as

$$\delta W = \left\lfloor \delta q \right\rfloor \{Q\}$$

and, because δq_j is arbitrary and independent (treated as independent in the face of Lagrange multipliers and constraint equations), it follows that

$$\{Q\} = [\beta]^T [b_p]^T \begin{Bmatrix} T_p \\ f_p \end{Bmatrix} \tag{II-72}$$

Equations II-71 or II-72 have a noteworthy geometrical interpretation. Note that the first three lines of

$$[b_p]^T \begin{Bmatrix} T_p \\ f_p \end{Bmatrix}$$

are components of the resultant torque vector, $\bar{T}_p + (\bar{\rho}_0 + \bar{\eta}) \times \bar{f}_p$, acting at the body's reference point, R. The second three lines are components of the resultant force vector, $\bar{f}_p$, whereas the j^{th} line, $(j > 6)$, corresponds to the standard procedure (of structural dynamicists) for calculating $Q_{\xi j}$, or, as it is usually expressed, generalized forces acting in deformation modes are

$$\{Q\} = [\phi]^T \{T\}$$

Also, recalling the form of $[\beta]$ (equation II-19), note that $[\pi]^T$ resolves the resultant torque vector (about orthogonal body axes) to components about skew axes about which Euler rotations are measured, whereas $[\gamma]^T$ resolves the resultant force vector (about orthogonal body axes) to components along the inertial axes. Further, note that $[b_p]$ is a matrix of coefficients that relates the velocity of any point, p, to the vector, $\{U\}$. This provides additional insight as to why the same coefficients that are used in kinematic constraint equation II-60 are used (in transposed form) to multiply $\{\lambda\}$-producing resultant constraint forces.

Thus, the remarkable duality of purpose associated with [b]-type coefficients has been emphasized. They are initially expressed by writing simple kinematic velocity relationships. The coefficients, $[b]^T$, are then used to transform discrete ordinary forces and torques to equivalent forces and torques acting through the body's reference point, R. The matrix, $[\beta]$, which is also a velocity transformation, is transposed to produce the transformation to generalized forces (if they are desired).

For ordinary momenta equations, the desire is simply to express $\{G_{ex}\}$, which (following equation II-57) is given by

$$\begin{aligned}\{G_{ex}\}_p &= [\beta]^{-1T}\{Q\} \\ &= [\beta]^{-1T}[\beta]^T[b_p]^T\begin{Bmatrix}T_p\\ f_p\end{Bmatrix} \\ &= [b_p]^T\begin{Bmatrix}T_p\\ f_p\end{Bmatrix}\end{aligned} \qquad \text{(II-73)}$$

This $\{G_{ex}\}_p$ given by equation II-73 reflects only the contribution of the force/torque acting at a single point, p. The total $\{G_{ex}\}$ must be obtained by summing all the points of the body at which forces and torques act, or

$$\{G_{ex}\} = \sum_{i=1}^{NP}[b_{p_i}]^T\begin{Bmatrix}T_{p_i}\\ f_{p_i}\end{Bmatrix} \qquad \text{(II-74)}$$

Kinematic coefficients, $[b_p]$, such as those of the previous example, will be required throughout in the formulation of the state equations. They are used to synthesize the constraint equations and to produce $\{G\}$, and they are involved in the velocity transformation of equation II-3. It is therefore advantageous to think of a "bank" or collection of all the required kinematic coefficients to be put together in a semiautomatic fashion by using input specifications to the digital program.

1. Sensor Point Kinematics–Force/Torque Transformations

Consider the typical structural hard point, s (figure 4). Assume that a right-handed triad is fixed to point s and that the elements of the triad are unit vectors labeled $\bar{\ell}$, $\bar{m}$, and $\bar{n}$. Now, body, n (which has point s on it), also has a right-handed triad fixed to point n. Suppose that, even when body n is in an undeformed state, the s-triad is misaligned with respect to the n-triad. When the body deforms, there may be further angular misalignment between the two triads. Thus, the relationship linking the two sets of unit vectors is

$$\begin{bmatrix}\bar{\ell}\\ \bar{m}\\ \bar{n}\end{bmatrix} = \left[{}_sR_{s'}\right]\left[{}_{s'}R_n\right]\begin{bmatrix}\bar{i}\\ \bar{j}\\ \bar{k}\end{bmatrix} \qquad \text{(II-75)}$$

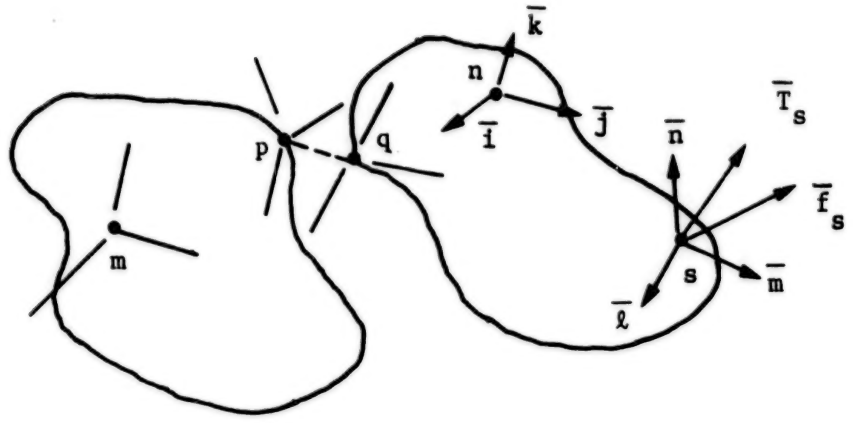

Figure 4. Two typical contiguous bodies of the system.

where $[{}_sR_{s'}]$ and $[{}_{s'}R_n]$ are orthonormal rotation transformations, the first relating the "naturally" misaligned triads via constant Euler rotations and the second accounting for additional rotation due to the body's deformation point s.

The structural deformation at point s is assumed to be sufficiently small that the Euler rotations associated with $[{}_{s'}R_n]$ may be evaluated through the use of

$$\begin{bmatrix} \theta_1 \\ \theta_2 \\ \theta_3 \end{bmatrix} = [\sigma_s] \{\xi\} \tag{II-76}$$

where $[\sigma_s]$ is a (3 X N) matrix of modal rotation amplitudes at point s. (Each of the N columns corresponds to a deformation mode.) Concisely denote the traids associated with points n and s by $\{\bar{e}_n\}$ and $\{\bar{e}_s\}$, respectively. The relationship linking the two sets of unit vectors may then be expressed as

$$\{\bar{e}_s\} = \left[{}_sR_n\right] \{\bar{e}_n\} \tag{II-77}$$

In subsequent kinematic development, there is a requirement for expressing the absolute velocity of a typical s-point and the angular velocity of the typical s-triad in terms of velocity states of a given body. Picture a six-long vector (column) of velocity components (three

rotational and three translational) that are projections of $\bar{\omega}_s$ and $\bar{v}_s$ onto the s-traid axes. It is related to the $\{U\}_n$ vector for the body by the transformation

$$\begin{bmatrix} \omega_{xs} \\ \omega_{ys} \\ \omega_{zs} \\ \hline u_s \\ v_s \\ w_s \end{bmatrix}^{(s)} = \left[\begin{array}{c|c|c|c} {}_sR_n & [0] & {}_sR_n & [\sigma_s] \\ \hline {}_sR_n & [S_{ns}^{(n)}] & {}_sR_n & [h_s] \end{array}\right] \begin{bmatrix} \omega_x \\ \omega_y \\ \omega_z \\ \hline u \\ v \\ w \\ \hline \dot{\xi}_1 \\ \dot{\xi}_2 \\ \cdot \\ \cdot \\ \cdot \\ \dot{\xi}_N \end{bmatrix}^{(n)} \tag{II-78}$$

where $[h_s]$ and $[\sigma_s]$ represent matrices of displacement and rotation amplitudes, respectively, and $[S_{ns}^{(n)}]$ is an antisymmetric matrix accounting for a vector cross product, or

$$[S_{ns}^{(n)}] = \begin{bmatrix} 0 & z_s + \eta_{zs} & -(y_s + \eta_{ys}) \\ -(z_s + \eta_{zs}) & 0 & x_s + \eta_{xs} \\ y_s + \eta_{ys} & -(x_s + \eta_{xs}) & 0 \end{bmatrix} \tag{II-79}$$

The superscripts in equations II-78 and II-79 are used to indicate the frame to which the velocity components are referenced.

Kinematic coefficients such as those of equation II-78 are generated for each so-called sensor point of the system of bodies. They are used by the simulation program to produce contributions to $\{G_{ex}\}$ from given force/torque components in the manner indicated by equation II-74.

2. *Hinge-Point Kinematics*

Kinematics associated with hinges follows a line of development somewhat similar to that of sensor points. Consider the points, p and q (figure 4), to be two structural hard points associated with a given hinge. All necessary kinematic information pertinent to the hinge is obtained through expressing the velocity of point q relative to point p and in expressing the relative angular velocity between the q- and p-frames. It is convenient that the angular velocity components are projections onto skew axes (Euler angle rates) and that translational velocity components are projections onto the axes of the p-triad. The six relative velocity components may be assembled into a column matrix as

$$\{\dot{\beta}\}_k = \begin{bmatrix} \{\dot{\theta}\} \\ \{\dot{\Delta}\} \end{bmatrix}_k \tag{II-80}$$

where $\{\dot{\theta}\}_k$ represents the three relative Euler angle rates and $\{\dot{\Delta}\}_k$ represents the three relative translational velocity components all of which pertain to the k^{th} hinge. The column of relative velocities may now be expressed as

$$\{\dot{\beta}\}_k = [b_p]_k \{U\}_m + [b_q]_k \{U\}_n \tag{II-81}$$

with

$$[b_p] = \left[\begin{array}{c|c|c} -[\pi]^{-1}[{}^qR_p][{}^pR_m] & [0] & -[\pi]^{-1}[{}^qR_p][{}^pR_m][\sigma_p] \\ \hline -[{}^pR_m][S^{(m)}_{mp}] & -[{}^pR_m] & -[{}^pR_m][h_p] \end{array}\right] \tag{II-82}$$

and

$$[b_q] = \left[\begin{array}{c|c|c} [\pi]^{-1}[{}^qR_n] & [0] & [\pi]^{-1}[{}^qR_n][\sigma_q] \\ \hline [{}^pR_q][{}^qR_n][S^{(n)}_{nq}] & [{}^pR_q][{}^qR_n] & [{}^pR_q][{}^qR_n][h_q] \end{array}\right] \tag{II-83}$$

In equations II-82 and II-83, the rotation transformations, $[{}_pR_m]$ and $[{}_qR_n]$, are developed to include the effects of structural deformation as indicated in equation II-75; the rotation

transformations, $[\pi]^{-1}$ and $[{}_{p}R_{q}]$, are developed in standard fashion using the three Euler rotations, $\{\theta\}_{k}$.

For further discussion, consider the system of bodies shown in figure 5. Topology of the system is simply indicated by an integer array, called "ITOPOL," as follows:

	1	2	3	4	5	6	7	8	← Hinge number
[ITOPOL] =	1	2	4	3	5	6	7	7	← Body (n) relative to
	0	3	2	6	3	1	5	2	← Body (m)

The [ITOPOL] array, which is the actual input to the simulation program, is used to define system topology as indicated. Now, with reference to the example shown in figure 5 and the corresponding (ITOPOL) array, the form of the velocity transformation may be written

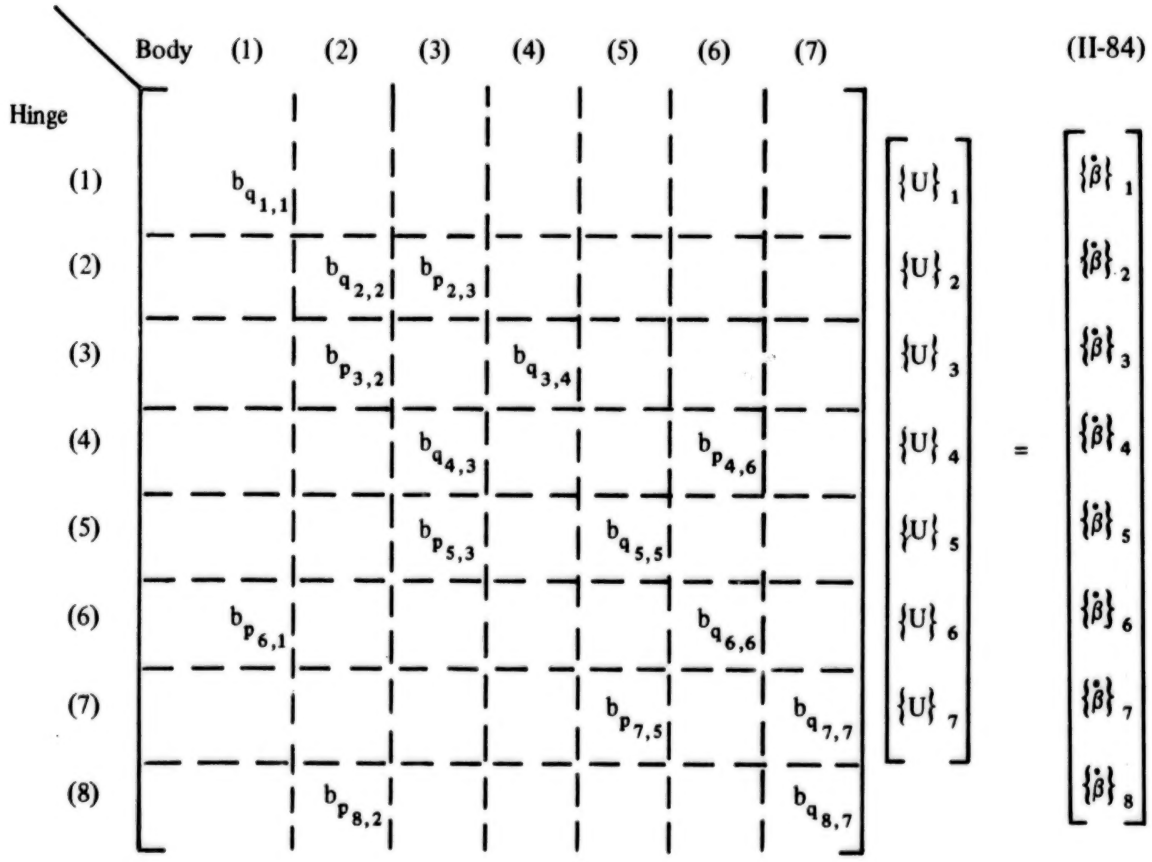

(II-84)

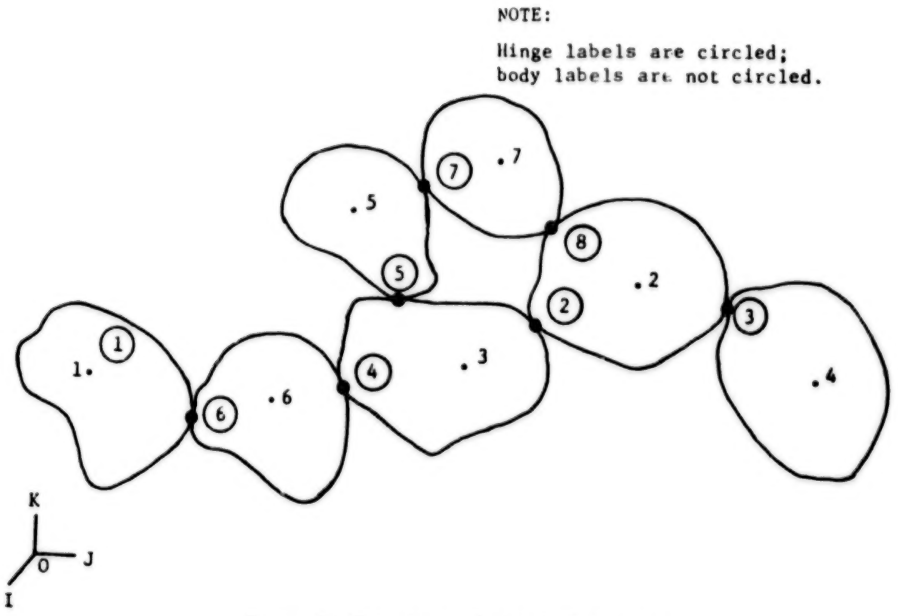

Figure 5. Topology of a typical system.

where $[b_{p_{i,j}}]$ and $[b_{q_{i,j}}]$ are matrices as defined in equations II-82 and II-83 (with i = Hinge number and j = Body number). The velocity transformations of equation II-84 represent the "bank" of all hinge kinematic coefficients previously mentioned and produces every possible velocity component pertinent to hinges. Referring to basic system equations II-3 and II-5, note that selected lines, or equations, from the bank (equation II-84) are taken to represent constraint equations or position coordinate rate equations. The $[B]_j$ and $[b]_j$ coefficients of equations II-3 and II-5 are simply subpartitions extracted from equation II-84.

To implement calculation of Lagrange's multipliers (equation II-6), it is necessary to develop time derivatives of $[b]_j$ coefficients. In a manner similar to the foregoing, in which all $[b]_j$ coefficients are extracted from the complete collections, the $[\dot{b}]_j$ matrices come from a collection of matrices whose members are $[\dot{b}_{q_{i,j}}]$ and $[\dot{b}_{p_{i,j}}]$, which are developed in Appendix C.

D. Development of the $\{G\}_j$ Force Vector

The equations of dynamic equilibrium for the j^{th} body of the system are given in an earlier section as equation II-1. As noted there, the right-hand side includes a so-called $\{G\}_j$ vector, which accounts for all state-dependent forces except for those of interconnection constaint. In equation II-63, the $\{G\}_j$ vector is presented in a somewhat more-developed form.

The purpose of this section is to provide more explicit development of the elements that contribute to $\{G\}_j$. All contributions in the following expression may be accounted for (omitting the j subscript, understanding that the typical, or j^{th} body, is being dealt with):

$$\{G\} = \{G_{ex}\} - \begin{bmatrix} 0 \\ \hline k \end{bmatrix} \{\xi\} - \begin{bmatrix} 0 \\ \hline C \end{bmatrix} \{\dot{\xi}\} + [\tilde{\Omega}]\,[m]\,\{U\} + \tfrac{1}{2}\left\{\left[U\right]\,[m_{,k}]\,\{U\}\right\} - [\dot{m}]\,\{U\} + \{G_{mw}\} + \{G_{gg}\} \qquad \text{(II-85)}$$

Although the first term, $\{G_{ex}\}$, has been discussed in the previous section (equation II-74), note here that the ordinary force/torque components that produce $\{G_{ex}\}$ may be considered as a miscellaneous force vector. Its presence provides the program user latitude for including a variety of additional effects. Clearly, it is the implement through which control forces/torques are "fed back" to the dynamic system.

The second and third terms of equation II-85 have been previously introduced. There is no implicit restriction on the stiffness and damping matrices, [k] and [C], nor is there a restriction on definition of the $\{\xi\}$ coordinates; in the majority of cases, they will likely be coordinates associated with orthonormal vibration modes. However, they may be physical (ordinary-discrete) displacement coordinates as well. In the latter case, the [k] and [C] matrices are usually coupled.

The last two terms of equation II-85 are included to account for momentum-wheel coupling and gravity effects, respectively. The treatment given to built-in momentum wheels is such that, in addition to producing a contribution to $\{G\}$, there is also a required extension to the form of the $[m]_j$ matrices because momentum wheels are *inertially* coupled. Thus, there is sufficient requirement for a dedicated development concerning momentum wheels. The next two sections deal exclusively with momentum-wheel and gravity effects, respectively.

The remaining terms that contribute to $\{G\}$ are basic inertial effects and involve the matrices, [m], $[m_{,k}]$, and $[\dot{m}]$. With reference to equation II-39, the form, [m], is given, corresponding to the case with available single-valued space functions $\bar{\phi}_k$. Ordinarily, access to such a description of the structure's deformation modes is not possible because of the structural complexity of typical spacecraft. The analyst should always be able to obtain, as data, matrices of modal amplitude ratios (mode shapes) and the corresponding structural mass matrix (generated by finite element techniques). To accommodate data based on the more practical definition of structural characteristics, it is necessary to recast the inertia matrices, [m], in a similar but more general format. The generality of the development of paragraph II.B is not compromised by extending the form of the inertia matrix. The extended, or more general, inertia matrix is developed in Appendix A, but here, for purposes of developing

inertial contributions to the $\{G\}$ vector, the resulting form is accepted and the kinetic energy expression is presented as

$$T = \tfrac{1}{2} [U] \left([m_o] + [m_1]_j \xi_j + [m_2]_{jk} \xi_j \xi_k \right) \{U\} \qquad \text{(II-86)}$$

with the repeated index summation convention implied, and with $[m_o]$ of the form

$$[m_o] = \left[\begin{array}{c|c|c} J & -S & d \\ \hline S & m & a \\ \hline d^T & a^T & e \end{array}\right] \qquad \text{(II-87)}$$

that is, it is identical to the [m] given by equation II-39 except that it is constant, independent of deformation. The constant inertia matrix, $[m_o]$, as given by equation II-87, is always of the form shown regardless of the choice of "modal" columns. The form of the matrices, $[m_1]$ and $[m_2]$, is such as to accommodate the general situation; that is, their definition includes inertial integrals as defined for a continuous system (equations II-30 through II-37) or as defined by structural mass matrices that are called "lumped" or "consistent."

The inertia matrix associated with ξ_j is

$$[m_1]_j = \left[\begin{array}{ccc|ccc|c} 2b_1 & -b_4 & -b_5 & \alpha_1 & \alpha_2 & \alpha_3 & \left[(C_{yz})_{jk}\right] \\ & 2b_2 & -b_6 & \alpha_4 & \alpha_5 & \alpha_6 & \left[(C_{zx})_{jk}\right] \\ & & 2b_3 & \alpha_7 & \alpha_8 & \alpha_9 & \left[(C_{xy})_{jk}\right] \\ \hline & & & 0 & 0 & 0 & 0\ 0\ 0 \\ & & & & 0 & 0 & 0\ 0\ 0 \\ & & & & & 0 & 0\ 0\ 0 \\ \hline & & & & & & 0\ 0\ 0 \\ \text{(symmetric)} & & & & & & 0\ 0 \\ & & & & & & 0 \end{array}\right]_j \qquad \text{(II-88)}$$

and the one associated with $\xi_j\ \xi_k$ is

$$[m_2]_{jk} = \left[\begin{array}{ccc|c|c} C_{11} & -C_{12} & -C_{13} & & \\ & C_{22} & -C_{23} & 0 & 0 \\ & & C_{33} & & \\ \hline & & & 0 & 0 \\ \hline \text{(symmetric)} & & & & 0 \end{array}\right]_{jk} \qquad \text{(II-89)}$$

Now, for N-deformation modes associated with a given body, it is understood that the range of the indices, j and k, is N; the coefficients, $(C_{11})_{jk}$, $(C_{12})_{jk}$, $\cdots (C_{xy})_{jk}$, are therefore stored as 9 (N X N) arrays of inertial integrals, whereas $(b_1)_j$, $(b_2)_j$, $\cdots (b_6)_j$ and $(\alpha_1)_j$, $(\alpha_2)_j$, $\cdots (\alpha_9)_j$ are stored as a (6 X N) array and a (9 X N) array, respectively. Thus, from a programming standpoint, note that $9N^2 + 15N$ storage locations are required for accommodating the inertial integrals necessary to account for the deformation-dependent mass matrix. Of course, if a particular body is rigid (N = 0), then only the first (6 X 6) diagonal partition of $[m_o]$ is used.

When the body is flexible (N > 0), the inertia matrix is calculated from deformation states (ξ_j) and inertia integrals in the manner indicated by equation II-86; the redundant operations due to symmetry and null operations are avoided in the digital code.

Having an instantaneous numerical evaluation of the inertia matrix, the term, $[\tilde{\Omega}]\ [m]\ \{U\}$, is calculated and added to $\{G\}$, consistent with the expression of equation II-58.

It is now possible to express explicitly, the combination of the remaining two inertial force vectors in terms of the inertial integrals given in equations II-88 and II-89. For further development, the combination may be defined as

$$\{G_c\} = \left\{ [U]\ [m_{,k}]\ \{U\} \right\} - [\dot{m}]\ \{U\} \qquad \text{(II-90)}$$

Thus, the first element of $\{G_c\}$, corresponding to ω_x, is

$$
\begin{aligned}
(G_c)_1 = \Big\{ & -2\omega_x (b_1)_j + \omega_y (b_4)_j + \omega_z (b_5)_j \\
& -u (\alpha_1)_j - v (\alpha_2)_j - w (\alpha_3)_j \\
& -(C_{yz})_{jk} \dot{\xi}_k - 2\omega_x (C_{11})_{\ell j} \xi_\ell \\
& +\omega_y [(C_{12})_{\ell j} + (C_{12})_{j\ell}] \xi_\ell + \omega_z [(C_{13})_{\ell j} + (C_{13})_{j\ell}] \xi_\ell \Big\} \dot{\xi}_j
\end{aligned}
\tag{II-91}
$$

The second element, corresponding to ω_y, is

$$
\begin{aligned}
(G_c)_2 = \Big\{ & \omega_x (b_4)_j - 2\omega_y (b_2)_j + \omega_z (b_6)_j \\
& -u (\alpha_4)_j - v (\alpha_5)_j - w (\alpha_6)_j \\
& -(C_{zx})_{jk} \dot{\xi}_k + \omega_x [(C_{12})_{\ell j} + (C_{12})_{j\ell}] \xi_\ell \\
& -2\omega_y (C_{22})_{\ell j} \xi_\ell + \omega_z [(C_{23})_{\ell j} + (C_{23})_{j\ell}] \xi_\ell \Big\} \dot{\xi}_j
\end{aligned}
\tag{II-92}
$$

The third element, corresponding to ω_z, is

$$
\begin{aligned}
(G_c)_3 = \Big\{ & \omega_x (b_5)_j + \omega_y (b_6)_j - 2\omega_z (b_3)_j \\
& -u (\alpha_7)_j - v (\alpha_8)_j - w (\alpha_9)_j \\
& -(C_{xy})_{jk} \dot{\xi}_k + \omega_x [(C_{13})_{\ell j} + (C_{13})_{j\ell}] \xi_\ell \\
& + \omega_y [(C_{23})_{\ell j} + (C_{23})_{j\ell}] \xi_\ell - 2\omega_z (C_{33})_{\ell j} \xi_\ell \Big\} \dot{\xi}_j
\end{aligned}
\tag{II-93}
$$

The fourth element, corresponding to u, is

$$(G_c)_4 = -\left\{\omega_x (\alpha_1)_j + \omega_y (\alpha_4)_j + \omega_z (\alpha_7)_j\right\} \dot{\xi}_j \qquad \text{(II-94)}$$

The fifth element, corresponding to v, is

$$(G_c)_5 = -\left\{\omega_x (\alpha_2)_j + \omega_y (\alpha_5)_j + \omega_z (\alpha_8)_j\right\} \dot{\xi}_j \qquad \text{(II-95)}$$

The sixth element, corresponding to w, is

$$(G_c)_6 = -\left\{\omega_x (\alpha_3)_j + \omega_y (\alpha_6)_j + \omega_z (\alpha_9)_j\right\} \dot{\xi}_j \qquad \text{(II-96)}$$

Finally, for the element k + 6, corresponding to an inertial force acting in the ξ_k coordinate,

$$\begin{aligned}
(G_c)_{k+6} &= \omega_x^2 \left[(C_{11})_{kj} \xi_j + (b_1)_k\right] \\
&+ \omega_y^2 \left[(C_{22})_{kj} \xi_j + (b_2)_k\right] \\
&+ \omega_z^2 \left[(C_{33})_{kj} \xi_j + (b_3)_k\right] \\
&- \omega_x \omega_y \left\{\left[(C_{12})_{kj} + (C_{12})_{jk}\right] \xi_j + (b_4)_k\right\} \\
&- \omega_x \omega_z \left\{\left[(C_{13})_{kj} + (C_{13})_{jk}\right] \xi_j + (b_5)_k\right\} \\
&- \omega_y \omega_z \left\{\left[(C_{23})_{kj} + (C_{23})_{jk}\right] \xi_j + (b_6)_k\right\} \\
&+ \omega_x \left[(\alpha_1)_k u + (\alpha_2)_k v + (\alpha_3)_k w\right]
\end{aligned} \qquad \text{(II-97)}$$

$$+ \omega_y \left[(\alpha_4)_k u + (\alpha_5)_k v + (\alpha_6)_k w\right]$$

$$+ \omega_z \left[(\alpha_7)_k u + (\alpha_8)_k v + (\alpha_9)_k w\right]$$

(II-97) continued

$$+ \left\{ \omega_x \left[(C_{yz})_{kj} - (C_{yz})_{jk}\right] + \omega_y \left[(C_{zx})_{kj} - (C_{zx})_{jk}\right] \right.$$

$$\left. + \omega_z \left[(C_{xy})_{kj} - (C_{xy})_{jk}\right] \right\} \dot{\xi}_j$$

On examining the composition of the inertial force $(G_c)_{k+6}$, note that the first six bracketed terms represent centrifugal forces (distance X omega-squared) acting in the deformation coordinates, whereas the last bracketed terms of equation II-97 represent Coriolis forces (velocity X omega).

E. Momentum-Wheel Coupling

The spacecraft system undergoing analysis may have several "built-in" momentum wheels. A momentum wheel is usually defined as a cylindrical or disk-shaped mass that spins about an axis that is fixed to a structural hard point of a given body. The wheel can be either spun up or despun by an electric motor whose rotor is part of the rotating mass. The shaft torque that acts to accelerate the wheel also acts on the body in a negative sense, providing active attitude control. The shaft torque is generally governed by a control law that "senses" attitude and rate errors of the body. In this development, a momentum wheel is assumed to be inertially symmetric about its spin axis.

To develop the inertial coupling effects of the typical momentum wheel, consider three unit-vector bases:

$$\left[\bar{e}_n\right] = \left[\bar{i}, \bar{j}, \bar{k}\right] \qquad \text{(II-98)}$$

$$\left[\bar{e}_s\right] = \left[\bar{\ell}, \bar{m}, \bar{n}\right] \qquad \text{(II-99)}$$

$$\left[\bar{e}_w\right] = \left[\bar{\ell}', \bar{m}', \bar{n}'\right] \qquad \text{(II-100)}$$

The first triad is the body-reference triad for body n, the second is a sensor-point triad (fixed to point s), and the third triad is fixed in the momentum wheel. One of the three unit vectors of $\lfloor \bar{e}_s \rfloor$ is coincident with one of the unit vectors of $\lfloor \bar{e}_w \rfloor$ (i.e., either $\bar{\ell}$, $\bar{m}$, or $\bar{n}$ may be the spin axis depending on the preference of the analyst). In figure 6, $\bar{n} = \bar{n}'$ is shown as the common, or spin, axis.

The absolute angular velocity of the $\lfloor \bar{e}_w \rfloor$ frame can be expressed as

$$\bar{\omega}_w = \lfloor \bar{e}_w \rfloor \; [{}_wR_s] \left(\{\omega_s\} + \{P_w\} \dot{\theta} \right) \tag{II-101}$$

where $\{P_w\}$ is an elementary three-long position vector (null except for unity in the first, second, or third locations corresponding to $\bar{\ell}$, $\bar{m}$, or $\bar{n}$ being the spin axis), and θ is the relative angular speed of the $\lfloor \bar{e}_w \rfloor$ frame with respect to the $\lfloor \bar{e}_s \rfloor$ frame.

With the inertial characteristics assumed (axisymmetry) for the wheel and with the velocity expression of equation II-101, the total angular momentum vector for the wheel may be written as

$$\begin{aligned} \bar{h} &= \lfloor \bar{e}_w \rfloor \; [J_w] \; \{\omega_w\} \\ &= \lfloor \bar{e}_s \rfloor \; [J_w] \left(\{\omega_s\} + \{P_w\} \dot{\theta} \right) \end{aligned} \tag{II-102}$$

with $[J_w]$ diagonal with all diagonal values equal to J_T except for the position corresponding to the spin axis, J_s. J_T is the mass moment of inertia about any axis perpendicular to the spin axis, and J_s is the spin inertia for the wheel.

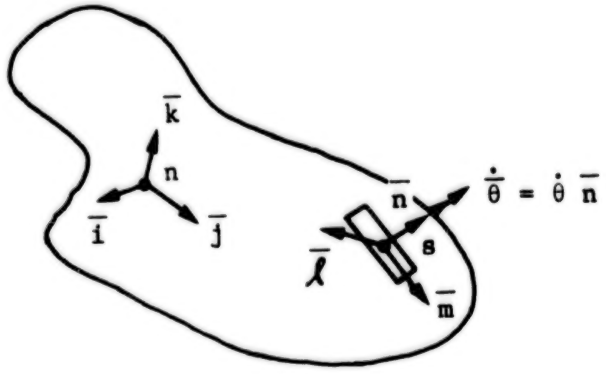

Figure 6. Typical body/momentum-wheel relationship.

The torque acting on the wheel (resolved to the $[\bar{e}_s]$ frame) is

$$\begin{aligned}\bar{T} &= [e_s]\ \{T\} = \frac{d}{dt}\ \bar{h} \\ &= [e_s]\left([J_w]\ \{\dot{\omega}_s\} + \{P_w\}\ J_s\ \ddot{\theta} - [\Omega_s]\ [J_w]\ \{\omega_s\} - [\Omega_s]\ \{P_w\}\ J_s\ \dot{\theta}\right)\end{aligned} \tag{II-103}$$

where an SK* operator is defined so that

$$[\Omega_s] = SK^*\ \{\omega_s\}$$

or

$$\begin{bmatrix} 0 & \omega_{s3} & -\omega_{s2} \\ -\omega_{s3} & 0 & \omega_{s1} \\ \omega_{s2} & -\omega_{s1} & 0 \end{bmatrix} = SK^* \begin{bmatrix} \omega_{s1} \\ \omega_{s2} \\ \omega_{s3} \end{bmatrix} \tag{II-104}$$

The torque acting on body n at point s due to the wheel is $-\bar{T}$, and it drives the body's quasi-coordinate as

$$\begin{aligned}\{G'_{mw}\} = -\ [\hat{b}_s]^T \Big(&[J_w]\ [\hat{b}_s]\ \{\dot{U}\}_n + [J_w]\ \dot{[\hat{b}_s]}\ \{U\}_n + \{P_w\}\ J_s\ \ddot{\theta} \\ &- [\Omega_s]\ [J_w]\ \{\omega_s\} - [\Omega_s]\ \{P_w\}\ J_s\ \dot{\theta}\Big)\end{aligned} \tag{II-105}$$

with

$$[\hat{b}_s] = \left[{}_sR_n \right]\ \left[I \mid O \mid \sigma_s \right] \tag{II-106}$$

and also, as can easily be shown,

$$\dot{[\hat{b}_s]}\ \{U\}_n = [SK^*(\left[{}_sR_n \right]\ [\sigma_s]\ \{\dot{\xi}\}_n)]\ [\hat{b}_s]\ \{U\}_n \tag{II-107}$$

Now, the shaft torque is simply the projection of $\overline{T}$ onto the spin axis, or

$$T_s = \left\lfloor P_w \right\rfloor \{T\}$$
$$= J_s \left\lfloor P_w \right\rfloor [\hat{b}_s] \{\dot{U}\}_n + J_s \left\lfloor P_w \right\rfloor \dot{[\hat{b}_s]} \{U\}_n + J_s \ddot{\theta} \qquad \text{(II-108)}$$

Equations II-105 and II-108 permit the coupled equations for body n and several momentum wheels to be expressed as

$$\left[\begin{array}{c|c|c} m_n + \hat{b}_1^T J_{w1} \hat{b}_1 + \hat{b}_2^T J_{w2} \hat{b}_2 & \hat{b}_1^T P_{w1} J_{s1} & \hat{b}_2^T P_{w2} J_{s2} \\ \hline J_{s1} P_{w1}^T \hat{b}_1 & J_{s1} & 0 \\ \hline J_{s2} P_{w2}^T \hat{b}_2 & 0 & J_{s2} \end{array}\right] \left[\begin{array}{c} \{\dot{U}\}_n \\ \hline \ddot{\theta}_1 \\ \hline \ddot{\theta}_2 \end{array}\right] =$$

$$\left[\begin{array}{c} \{\hat{G}\}_n + [b]_n^T \{\lambda\} \\ \hline 0 \\ \hline 0 \end{array}\right] + \left[\begin{array}{c} \sum_w [\hat{b}_s]^T [\Omega_s] [J_w] \{\omega_s\} - \sum_w [\hat{b}_s]^T [J_w] \dot{[\hat{b}_s]} \{U\}_n \\ \hline 0 \\ \hline 0 \end{array}\right] \qquad \text{(II-109)}$$

$$+ \left[\begin{array}{c} -\sum_w [b_s]^T (SK^* \{P_w\}) [\hat{b}_s] \{U\}_n J_s \dot{\theta} \\ \hline T_{s1} - J_{s1} \left\lfloor P_{w1} \right\rfloor \dot{[\hat{b}_1]} \{U\}_n \\ \hline T_{s2} - J_{s2} \left\lfloor P_{w2} \right\rfloor \dot{[\hat{b}_2]} \{U\}_n \end{array}\right]$$

The inertially coupled body/momentum-wheel equations (for two wheels) are shown as equation II-109 simply for the purpose of indicating the form. Note that, within the equations, there effectively resides the original form of the dynamic-equilibrium equations for body n; namely,

$$[m]_n \{\dot{U}\}_n = \{\hat{G}\}_n + [b]_n^T \{\lambda\} \qquad \text{(II-110)}$$

which govern if no momentum wheels are associated with body n. In equation II-110, the caret (^) has been placed over G to represent the right-hand side force vector that excludes momentum-wheel effects.

Now, on further study of the form of equation II-109, note that, if the "locked" momentum-wheel effects are already included in the definition of $[m]_n$ (which is the standard practice when inertially coupling systems together), the (1, 1) partition of the coefficients on the left of equation II-109 becomes simply $[m]_n$. Also, the second column on the right of equation II-109 is absorbed in $\{\hat{G}\}_n$, having already been accounted for in the development of dynamic-equilibrium equations.

It therefore follows that, in order to implement momentum-wheel coupling with one of the flexible bodies, it is only necessary to extend the $\{U\}_n$ vector to contain momentum-wheel spin values, $(\dot{\theta})$, to extend the inertia (except for the [1, 1] partition) as indicated in equation II-109 and to add to the right-hand side force vector

$$\{G_{mw}\} = -\begin{bmatrix} \sum_w [\hat{b}_s]^T (SK^* \{P_w\}) [\hat{b}_s] \{U\}_n J_s \dot{\theta} \\ \hline T_{s1} - J_{s1} \lfloor P_{w1} \rfloor [\dot{\hat{b}}_1] \{U_n\} \\ \hline T_{s1} - J_{s2} \lfloor P_{w2} \rfloor [\dot{\hat{b}}_2] \{U_n\} \end{bmatrix} \qquad \text{(II-111)}$$

The values for shaft torque T_s that appear in $\{G_{mw}\}$ are established by a given control law if the wheels are to be considered variable speed. If a given momentum wheel is of constant speed (used only for "gyroscopic damping"), the torque equation for it is deleted from the form of equation II-109; however, its effects are still included in the upper partition of the vector, $\{G_{mw}\}$ (the gyroscopic torque due to constant $\dot{\theta}$).

Clearly, the equations of dynamic equilibrium for a body, after having been augmented to include momentum-wheel coupling, are still of the general form

$$\{\dot{U}\}_j = [m]_j^{-1} \left(\{G\}_j + [b]_j^T \{\lambda\} \right) \qquad \text{(II-112)}$$

F. Gravity-Gradient Effects

Attitude dynamics of orbiting spacecraft can be significantly influenced by the gravitational force that is distributed according to the system's position and deformation state. The gravitational force per unit mass varies (in a central force field) simply because different mass particles are at different distances from the Earth's center of mass. Figure 7 describes the geometry associated with a typical elastic body.

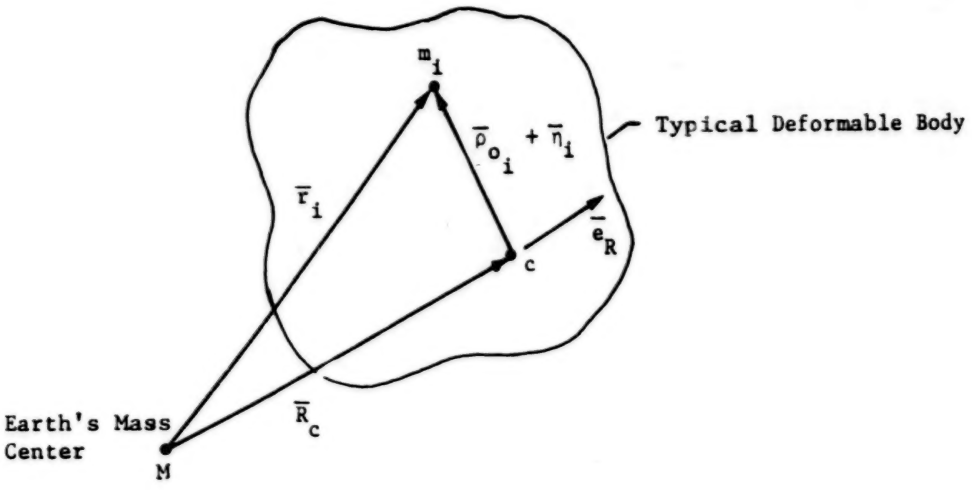

Figure 7. Geometry for gravity effects on a typical body.

For a central force field, the gravitational force per unit mass is given as

$$\left(\frac{\bar{F}}{m}\right)_i = -\frac{GM}{r_i^2}\,\frac{\bar{r}_i}{r_i} \tag{II-113}$$

which, to a first-order approximation, is

$$\left(\frac{\bar{F}}{m}\right)_i = -g_c\left[\bar{e}_R + \frac{\bar{\rho}_{o_i} + \bar{\eta}_i}{R_c} - 3\bar{e}_R\left(\bar{e}_R \cdot \frac{\bar{\rho}_{o_i} + \bar{\eta}_i}{R_c}\right)\right] \tag{II-114}$$

where

GM = the Earth's gravitational constant

m_i = the typical mass particle

g_c = local gravitational acceleration

$\bar{e}_R$ = a unit vector directed along $\bar{R}_c$

c = the origin of the body reference system

The virtual work due to gravitational force can be written as

$$\delta W_g = \sum_i \left(\frac{\bar{F}}{m}\right)_i \cdot \delta \bar{r}_i \, m_i$$

$$= \int_V \left(\frac{\bar{F}}{m}\right) \cdot \delta \bar{r} \, \sigma dV \qquad \text{(II-115)}$$

with m_i replaced by differential mass σdV.

The virtual displacement field is expressed in terms of virtual displacements of the quasi-coordinates as

$$\delta \bar{r} = \delta \bar{r}_c + \delta \bar{\theta}_c \times (\bar{\rho}_0 + \bar{\eta}) + \delta \bar{\eta} \qquad \text{(II-116)}$$

In combining equation II-115 with equation II-116, the torque about point c, due to gravity-gradient effects, is

$$\left(\bar{T}_c\right)_g = g_c \bar{e}_R \times \bar{S} + \frac{3g_c}{R_c} \bar{e}_R \times \left(\bar{\bar{J}} \cdot \bar{e}_R\right) \qquad \text{(II-117)}$$

where

$\bar{S}$ = the first mass moment about point c

$\bar{\bar{J}}$ = the instantaneous inertia tensor (deformation dependent) for the body

The resultant force due to gravity effects is

$$\left(\bar{F}_c\right)_g = -g_c m \bar{e}_R - \frac{g_c}{R_c} \bar{S} + \frac{3g_c}{R_c} \left(\bar{e}_R \cdot \bar{S}\right) \bar{e}_R \qquad \text{(II-118)}$$

and the force acting in the k^{th} deformation coordinate, ξ_k, is

$$\left(G_{\xi_k}\right)_g = - g_c \left\{ \int_V \bar{\phi}_k \cdot \bar{e}_R \sigma dV + \frac{1}{R_c} \int_V \bar{\phi}_k \cdot \left(\bar{\rho}_o + \bar{\eta}\right) \sigma dV \right.$$

$$\left. -3 \frac{\bar{e}_R}{R_c} \cdot \int_V \bar{\phi}_k \left[\bar{e}_R \cdot \left(\bar{\rho}_o + \bar{\eta}\right) \right] \sigma dV \right\} \qquad \text{(II-119)}$$

Now, the unit vector, $\bar{e}_R$, has projections onto the body axis system that continually vary as the body changes attitude. The unit vector, $\bar{e}_R$, is expressed in terms of direction cosines, and the three unit vectors associated with the body-reference frame are expressed as

$$\bar{e}_R = \left[\bar{e}_B\right] \left\{\gamma_g\right\} \qquad \text{(II-120)}$$

Also defined are

$$\left[\tilde{\gamma}_g\right] = SK^* \left\{\gamma_g\right\} \qquad \text{(II-121)}$$

$$\bar{S} = \left[\bar{e}_B\right] \left\{S\right\} \qquad \text{(II-122)}$$

$$\left[\tilde{S}\right] = SK^* \left\{S\right\} \qquad \text{(II-123)}$$

$$\left\{a\right\}_k = \int_V \left\{\phi\right\}_k \sigma dV \qquad \text{(II-124)}$$

With these definitions and the force and torque expressions of equations II-117, II-118, and II-119, it follows that the first three elements of the contribution to the right-hand force vector due to gravity effects are

$$\left\{G_{gg}\right\}_{1,2,3} = g_c \left[\tilde{S}\right] \left\{\gamma_g\right\} - \frac{3g_c}{R_c} \left[\tilde{\gamma}_g\right] \left[J\right] \left\{\gamma_g\right\} \qquad \text{(II-125)}$$

The second three elements are

$$\left\{G_{gg}\right\}_{4,5,6} = - g_c m \left\{\gamma_g\right\} + \frac{g_c}{R_c} \left(3 \left\{\gamma_g\right\} \left[\gamma_g\right] - [I]\right) \left\{S\right\} \qquad \text{(II-126)}$$

The force due to gravity acting in the k^{th} deformation mode is

$$\begin{aligned} G_{\xi_k} = & - g_c \left[\gamma_g\right] \left\{a\right\}_k - \frac{g_c}{R_c} \left[\frac{(b_1)_k + (b_2)_k + (b_3)_k}{2} + e_{kj}\xi_j\right] \\ & + \frac{3g_c}{2R_c} \left\{ \left(1 - 2\gamma_{g1}^2\right) \left[(b_1)_k + (C_{11})_{kj}\xi_j\right] \right. \\ & \quad + \left(1 - 2\gamma_{g2}^2\right) \left[(b_2)_k + (C_{22})_{kj}\xi_j\right] \\ & \quad + \left(1 - 2\gamma_{g3}^2\right) \left[(b_3)_k + (C_{33})_{kj}\xi_j\right] \\ & + 2\gamma_{g1}\gamma_{g2} \left[(b_4)_k + (C_{12})_{..}\xi_j + (C_{12})_{jk}\xi_j\right] \\ & + 2\gamma_{g1}\gamma_{g3} \left[(b_5)_k + (C_{13})_{kj}\xi_j + (C_{13})_{jk}\xi_j\right] \\ & \left. + 2\gamma_{g2}\gamma_{g3} \left[(b_6)_k + (C_{23})_{kj}\xi_j + (C_{23})_{jk}\xi_j\right] \right\} \end{aligned} \qquad \text{(II-127)}$$

where the inertia integrals, $\left(b_n\right)_k$, (n = 1, 2, •• 6), and $\left(C_{\ell m}\right)_{kj}$, (ℓ, m = 1, 2, 3), are consistent with the development given in paragraph II.D and Appendix A.

G. Provision for Inclusion of Thermal Environments

All problems associated with thermally induced deflections have in common the requirement that, to determine the effect of solar heating, the spacecraft's attitude relative to the Sun must be known. This required information can be extracted at any point in time from the state vector. It is then necessary to have a model of the response of the flexible structure, either static or dynamic, to solar heating.

Considerable work has been done on modeling flexible appendages in thermal environments (References 2 through 4), and the results indicate that the response depends on the radiation properties of the booms and the attitude relative to the Sun.

The simulation program accounts for time-dependent thermal deformations in the following manner. It is assumed that a model exists whereby the structural deformation of a flexible boom (or appendage) resulting from solar heating can be determined from elements of the state vector and time. This deformation is subtracted from the actual deformation, and the difference is premultiplied by the appendage stiffness matrix. The result is a vector of modified, generalized restoring forces for the appendage, which is summed into the $\{G\}_j$ vector for the appendage body.

In terms of the development given in paragraphs II.B and II.D where $-[k]\{\xi\}$ is seen to be the generalized restoring forces (in the deformation coordinates), note that $-[k]\{\xi\}$ is replaced with $-[k](\{\xi\} - \{\xi_e\})$. The thermal deformation state, $\{\xi_e\}$, is that which must be established from a thermal deformation model.

In this way, a closed-loop response analysis can be achieved, using external subroutines to develop the thermal deformations. Some problems may require only open-loop operation if the variations of $\{\xi_e\}$ in time is slow with respect to general dynamic response.

Rather than building a rigid (or irrevocable) model of thermal deformation, the dynamic simulation program provides the user with an interface whereby he can formulate and code a particular model. Thus, latitude with respect to user requirements is retained.

III. SYNTHESIS AND ANALYSIS OF THE LINEARIZED SYSTEM

Developments to this point have described the analytical techniques used to synthesize the nonlinear characteristics of a dynamical system consisting of an assembly of interconnected flexible (or rigid) bodies. Particular emphasis has been placed on spacecraft systems in which individual bodies that comprise the system may be either spinning or nonspinning and may have large excursions with respect to each other.

This section presents a comprehensive summary of the techniques developed for synthesis and analysis of the linearized dynamic system with particular emphasis on frequency-domain techniques. For the purposes of this discussion, it is convenient to redefine the nature of the system under consideration and, in describing the techniques, to consider the total dynamic system as a *plant* subject to a *controller* rather than as a spacecraft system consisting of interconnected bodies that may be subjected to a control system.

Linearization of the nonlinear state equations is necessary for applying the powerful analytical techniques associated with linear system stability synthesis. When a nonlinear system can be reduced to a linear system in the vicinity of a particular state of interest, it is much more desirable to work with the linearized state equations. An additional feature related to the linearized system permits the analyst to observe linearized perturbation time-response characteristics for the system. The linearized time response can be easily automated by recursive formulas, which are generally more efficient than nonlinear numerical integration algorithms.*

A. Introductory Discussion

The main-line nonlinear time-domain analysis is structured to assemble a collection of interconnected bodies, including a control law. The general form of the governing equations may be concisely indicated as

$$\dot{Y}^i = F\left(Y^i, t\right) \quad i = 1, 2, \ldots \tag{III-1}$$

and the form of the function, F, is the essence of the nonlinear time-domain solution. In fact, it can be stated that equation III-1 is the fundamental basis for the entire DISCOS program. Algorithms for evaluating the nonlinear state-vector time derivatives (and auxiliary equations) are centered in a subprogram and its supporting routines. These functional algorithms are used for linearizing the governing equations about a specified state. In addition, it is desirable to introduce some new variables, including sensor signals, X_{ss}, and control torques, B. These new variables extend the number of equations, and the additional expressions are linearized along with the basic state equations. Additional remarks concerning the use and manipulation of the additional variables are given in a later section. The remainder of this subsection will address specifics relating to the linearization process.

Attention is first focused on a single variable, $\dot{y}_k$, and its dependence on the system state, Y^i, through a known (though possibly nonlinear) functional relationship. Arguments begin by considering an initial system state, Y^i (o), and a functional algorithm with which to evaluate the expression, $\dot{y}_k = d/dt\ y_k$. The unknown, $\dot{y}_k$, is first expressed in terms of a Taylor's series expansion about the given state, Y^i (o), as

$$\dot{y}_k = \dot{y}_k(o) + \frac{\partial \dot{y}_k}{\partial Y^j} dY^j + \frac{\partial^2 \dot{y}_k}{\partial Y^j \partial Y^\ell} dY^j dY^\ell + \ldots \tag{III-2}$$

*Reference Paper I provides a broadbrush narrative description of the theoretical development given in this section.

Because the interest here lies in the linear part only, the series is truncated for all partial derivatives greater than one and

$$\dot{y}_k - \dot{y}_k(o) = \frac{\partial \dot{y}_k}{\partial Y^j} dY^j = \dot{y}_{k,j} dY^j \qquad \text{(III-3)}$$

The task at hand, then, is to establish the partial derivatives indicated as $\dot{y}_{k,j}$, thus yielding an expression (for all $\Delta\dot{Y}^i = \dot{Y}^i - \dot{Y}^i(o)$, $i = 1, 2, \cdots$) of the form

$$\Delta\dot{Y}^i = H_{i,j} \Delta Y^j \qquad \text{(III-4)}$$

Because it would be nearly impossible (certainly impractical) to generalize the determination of the partial derivatives as explicit analytical expressions involving the independent state variables, a numerical approach has been adopted. This task is accomplished by employing numerical perturbation techniques in conjunction with quadratic functions to establish the desired partial derivatives. Symbolically, determination of elements of $H_{i,j}$ is attempted so that

$$\dot{Y}^i = \dot{Y}^i(o) + H_{i,j} \Delta Y^j \qquad \text{(III-5)}$$

where it is assumed that:

- The functions, $\dot{Y}^i$, are indeed linear, sufficiently near the state, $Y^i(o)$
- The functions, $\dot{Y}^i$, although possibly nonlinear, can be represented as a quadratic (or lower order) in the neighborhood of $Y^i(o)$

The basic approach is concisely summarized in two steps:

- Establish quadratic coefficients for $\dot{Y}^i$ in the vicinity of the state, $Y^i(o)$
- Evaluate the partial derivatives, $H_{i,j}$, at the state, $Y^i(o)$, using the quadratic coefficients and perturbation values on the independent variables.

B. Linearization Process

With reference to figure 8, the quadratic formula can be stated in matrix form as

$$f(\eta) = \begin{bmatrix} \eta^2 & \eta & 1 \end{bmatrix} \begin{Bmatrix} d \\ e \\ f \end{Bmatrix} \qquad \text{(III-6)}$$

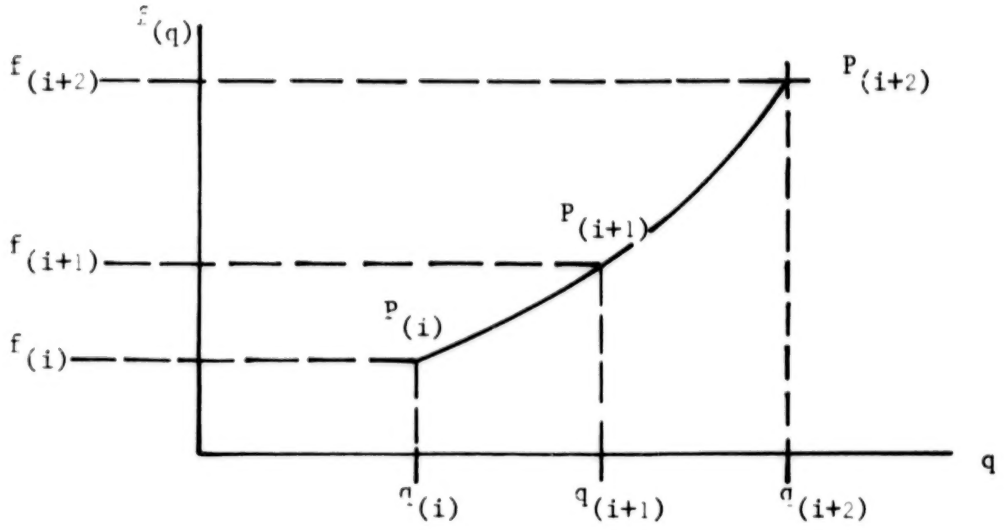

Figure 8. The quadratic formula.

where η is a local spatial coordinate with origin corresponding to $q_{(i)}$, and it is desired to establish the derivative, $\partial f/\partial q$, evaluated at $q_{(i)}$.

In general, the required partial derivative is

$$\frac{\partial f}{\partial q} = \frac{\partial f}{\partial \eta}\,\frac{\partial \eta}{\partial q} \qquad \text{(III-7)}$$

Because the three values, $f_{(i)}$, $f_{(i+1)}$, $f_{(i+2)}$, are evaluated by the previously discussed functional algorithm, these values satisfy equation III-6. More specifically, consider

$$\begin{Bmatrix} f_i \\ f_{i+1} \\ f_{i+2} \end{Bmatrix} = \begin{bmatrix} \eta_i^2 & \eta_i & 1 \\ \eta^2_{i+1} & \eta_{i+1} & 1 \\ \eta^2_{i+2} & \eta_{i+2} & 1 \end{bmatrix} \begin{Bmatrix} d \\ e \\ f \end{Bmatrix} \qquad \text{(III-8)}$$

and, by matrix manipulation, it follows that

$$f(\eta) = \begin{bmatrix} \eta^2 & \eta & 1 \end{bmatrix} \begin{bmatrix} \eta^2_i & \eta_i & 1 \\ \eta^2_{i+1} & \eta_{i+1} & 1 \\ \eta^2_{i+2} & \eta_{i+2} & 1 \end{bmatrix}^{-1} \begin{Bmatrix} f_i \\ f_{i+1} \\ f_{i+2} \end{Bmatrix} \qquad \text{(III-9)}$$

where the local coordinate, η, is defined as

$$\eta = \frac{q - q_i}{q_{i+2} - q_i} \qquad \text{(III-10)}$$

and it can be noted that

$$\eta_i = 0; \quad \eta_{i+2} = 1; \quad \frac{\partial \eta}{\partial q} = \frac{1}{q_{i+2} - q_i} \qquad \text{(III-11)}$$

It then follows that

$$f(\eta) = \begin{bmatrix} \eta^2 & \eta & 1 \end{bmatrix} \begin{bmatrix} 0 & 0 & 1 \\ \eta^2_{i+1} & \eta_{i+1} & 1 \\ 1 & 1 & 1 \end{bmatrix}^{-1} \begin{Bmatrix} f_i \\ f_{i+1} \\ f_{i+2} \end{Bmatrix} \qquad \text{(III-12)}$$

and, if $\eta_{i+1} = 1/2$ is specified and it is noted that $f_{(i)} = f_{(\eta=i)}$,

$$f(\eta) = \begin{bmatrix} \eta^2 & \eta & 1 \end{bmatrix} \begin{bmatrix} 0 & 0 & 1 \\ 1/4 & 1/2 & 1 \\ 1 & 1 & 1 \end{bmatrix}^{-1} \begin{Bmatrix} f_{(0)} \\ f_{(1/2)} \\ f_{(1)} \end{Bmatrix} \qquad \text{(III-13)}$$

$$f(\eta) = \begin{bmatrix} \eta^2 & \eta & 1 \end{bmatrix} \begin{bmatrix} 2 & -4 & 2 \\ -3 & 4 & -1 \\ 1 & 0 & 0 \end{bmatrix} \begin{Bmatrix} f_{(0)} \\ f_{(1/2)} \\ f_{(1)} \end{Bmatrix} \tag{III-14}$$

$$f'(\eta) = \begin{bmatrix} 2\eta & 1 & 0 \end{bmatrix} \begin{bmatrix} 2 & -4 & 2 \\ -3 & 4 & -1 \\ 1 & 0 & 0 \end{bmatrix} \begin{Bmatrix} f_{(0)} \\ f_{(1/2)} \\ f_{(1)} \end{Bmatrix} \tag{III-15}$$

and, in particular,

$$\left.\frac{\partial f}{\partial \eta}\right|_{(0)} = f'_{\eta}(\eta = 0) = e \tag{III-16}$$

and

$$\left.\frac{\partial f}{\partial q}\right|_{(0)} = f'_{q}(q=q_i) = \frac{e}{q_{(i+2)} - q_{(i)}} \tag{III-17}$$

1. Comments

Selection of an initial perturbation value, q(i + 2), from an initial specified state, q(o) = Y_k(o), is somewhat arbitrary. A value of 1 percent of the initial value has been successfully used for all example problems during the course of the study. In the case where the initial value is null, an infinitesimal value must be chosen. A value of 1×10^{-5} has been accommodated in the digital code. The intermediate choice of $\eta(i + 1) = 1/2$ was selected for other reasons. Consider first that a single evaluation of a partial derivative, $\partial f/\partial Y^i$ is not sufficient to qualify its validity.

An approach has been employed whereby two successive evaluations of $\partial f/\partial Y^i$ obtained by successively cutting the perturbation in half must agree to a predetermined number of significant digits (e.g., 5).* The choice of $\eta(i + 1) = 1/2$ requires but a single new evaluation

*The establishment of the error criteria that will be used to compare successive evaluations of $\partial f/\partial Y^i$ is strongly dependent on computer word size. In special cases, numerical noise can exceed the established error criteria and prevent numerical convergence. This problem can usually be circumvented by changing error criteria limits set in subroutine LINEAR.

for each element in $\dot{Y}^i$ at each successive reduction in the perturbation value. In summary, the linearization employs an iterative technique to establish the desired partial derivatives.

2. System Resonance Properties

The linearization process has provided a system of first-order differential equations that describe the dynamical simulation in terms of perturbation variables about an equilibrium state. The linearized canonical form appears as

$$\Delta\dot{Y}^i = H_{i,j}\Delta Y^j \qquad (i,j = 1,2,\ldots) \tag{III-18}$$

The coefficients, $H_{i,j}$, contain all of the resonance frequency properties of the dynamical system. The standard eigensolution form is indicated by taking the transform of this expression to obtain

$$\left(\delta_i^j s - H_{i,j}\right)\Delta Y^j(s) = 0 \tag{III-19}$$

Extraction of the roots (eigenvalues) from $H_{i,j}$ then gives the roots of the dynamical system. There will be N of these roots, and any complex roots will appear as conjugate pairs because the elements of $H_{i,j}$ are all real. The imaginary part of the complex pairs represents the resonance (or characteristic) frequencies of the system.

C. Exchange of Variables

It is often necessary for the analyst to require additional variables with which to assess the stability characteristics of the dynamical system. These additional variables ordinarily take the form of plant sensor signals and control system output forces and torques. Although the desired variables may not be explicitly contained in the system state vector, Y^i, they are known in terms of the state variables through an expression of the form

$$w^j = g(Y^i) \tag{III-20}$$

Recall also from previous discussions that it has been established either directly or through linearization that

$$\Delta\dot{Y}^i = H_{i,j}\Delta Y^j \tag{III-21}$$

Now, rewriting equation III-20 in matrix form and identifying variables to retain, Y_1, and variables to eliminate, Y_2, gives

$$\{w\} = \left[\begin{array}{c|c} C_1 & C_2 \end{array}\right] \begin{Bmatrix} Y_1 \\ Y_2 \end{Bmatrix} \tag{III-22}$$

and it can readily be established that

$$\{Y\} = [R]\ \{Z\}$$

where

$$[R] = \left[\begin{array}{c|c} I & 0 \\ \hline -C_2^{-1}\ C_1 & C_2^{-1} \end{array}\right] \tag{III-23}$$

and

$$\{Z\} = \begin{Bmatrix} Y_1 \\ w \end{Bmatrix}$$

Thus, the state equations for the dynamical system can be written (in terms of variables that include the desired plant sensor signals and control system forces and torques) as

$$\{\dot{Z}\} = [R]^{-1} \left[H_{i,j}\right] [R]\ \{Z\} \tag{III-24}$$

and the transformation $A_{ij} = R^{-1}\ H_{i,j}\ R$, is commonly referred to as a similarity transformation. The matrix, A_{ij}, is said to be the transform of $H_{i,j}$ by the matrix R (Reference 5).

The similarity transformation, A_{ij}, possesses a unique property in that the eigenvalues of A_{ij} are equal to the eigenvalues of $H_{i,j}$! A simple proof that establishes this point follows:

The characteristic matrix of A_{ij} is given by

$$(A_{ij} - sI) = (R^{-1}\ H_{i,j}\ R - sI) = R^{-1}\ (H_{i,j} - sI)\ R \tag{III-25}$$

It follows that Q(s), the characteristic polynomial of A_{ij}, is

$$Q(s) = \det (A_{ij} - sI) = \det R^{-1} (\det (H_{i,j} - sI)) \det R$$

and, as $(\det R^{-1}) = 1/\det (R)$, it is apparent that

$$Q(s) = \det (H_{i,j} - sI) = P(s)$$

where P (s) is the characteristic polynomial of $H_{i,j}$. Thus, it is evident that the matrices, $H_{i,j}$ and A_{ij}, have the same characteristic equations

$$Q(s) = P(s) = 0$$

and, therefore, the eigenvalues of A_{ij} are equal to the eigenvalues of $H_{i,j}$.

Application of this property now permits isolation of the plant and controller, even for a state-space representation of an inherently nonlinear system that can be linearized about a specified state. Separation of plant and control-system variables is an important facet of linear system stability synthesis.

1. Evaluation of the Similarity Transformation

This discussion relates to a procedural approach for determining the similarity transformation matrix, [R], that will relieve the user from the burden of having to select those variables to eliminate from the original state vector so that the auxiliary variables, B^i and $X_{ss}{}^i$, can become an independent constituent of the modified state vector for use in the linearized studies. With reference to equation III-22, all the C_{ij} coefficients are known because they have been obtained through linearization of the auxiliary equations. The C_{ij} coefficients simply define the dependence of the auxiliary variables, w^j, on the original state variables, Y^i. In general, it is not possible to directly partition the C_{ij} in the C_1 and C_2 partitions as indicated in equation III-22, for the decision has not been made yet as to which state variables to retain and which to discard in preference to introducing the auxiliary variables, w^j. In this light, a *best possible* choice is made with regard to which of the variables to eliminate from the state vector, Y^i, so that the auxiliary variables, w^j, may be included. A one to one variable exchange will often occur between an element of w^j and an element of Y^i. In any case, a variable exchange is necessary for structuring the total system into the desired plant/controller framework whereby the plant and controller can be isolated along with the plant sensor signals and the control-system inputs.

The following approach is used in this simulation to accomplish the desired result (namely, an optimum selection from Y^i as to which variables to eliminate so that w^j can be introduced as a part of the state vector). With reference to equation III-22,

$$\left[C \,\vdots\, -I\right] \begin{Bmatrix} Y^i \\ w^j \end{Bmatrix} = \{0\} \qquad \text{(III-26)}$$

The primary focus of attention is now directed to a systematic examination of the C_{ij} coefficients so that the variable exchange is accomplished in an optimum manner. To help clarify the discussion, some size identifications are noted:

C_{ij} has size NR by NS

Y^i has size NS by 1

w^j has size NR by 1

NJQ = NS + NR

Clearly, at least one nonzero element exists in each row of the C_{ij} array. Otherwise, Y^i does not represent an independent set.

Now, a search through the first NS elements of row 1 in the matrix array

$$\left[C \,\vdots\, -I\right] \qquad \text{(III-27)}$$

will identify the largest element (absolute value) in row 1. Assuming that this element occurs in column JBIG ($1 \leqslant \text{JBIG} \leqslant \text{NS}$) permits the division of each element of row 1 by this largest element, and subsequent elementary row operations on rows 1 through NR will eliminate those elements below the pivotal element in column JBIG. This procedure is repeated for each of the NR rows contained in the matrix, and the following observations are noted:

- The appearance of a one (1.0) in a row identifies a variable that will be eliminated in preference to including an element of w^j.
- The absence of a zero or one in columns of a given row indicates which variables will survive the exchange process.
- All variables in w^j (NR of them) will become part of a new and independent state vector (the modified state vector).
- The transformation, R_{ij} (i, j = 1 . . . NS) can be constructed from the matrix that remains after the procedural approach has exhausted all of the NR rows of expression III-27.

2. *Illustrative Example*

A simple example is presented to further describe the actual mechanics used for evaluating the similarity transformation. Linearization of the auxiliary equations has established that

$$\begin{Bmatrix} w_1 \\ w_2 \end{Bmatrix} = [C] \begin{Bmatrix} Y_1 \\ Y_2 \\ Y_3 \\ Y_4 \end{Bmatrix}$$

and, to implement the proposed algorithm, the C matrix augmented with -I is first written and the elements of C are further identified as

$$\begin{matrix} \overbrace{}^{NS} & \vdots & \overbrace{}^{2} \\ [C & \vdots & -I] \end{matrix} = \left[\begin{array}{cccc|cc} b_{11} & b_{12} & b_{13} & b_{14} & -1 & 0 \\ b_{21} & b_{22} & b_{23} & b_{24} & 0 & -1 \end{array}\right]$$

For illustrative purposes, assume that $|b_{13}| > |(b_{11}, b_{12}, b_{14})|$, and, hence, b_{13} is the pivotal element for the first row. It follows that row 2 is modified by the relation

$$ele_{2j} = - b_{23} \frac{b_{1j}}{b_{13}} + b_{2j}$$

giving the matrix

$$\left[\begin{array}{c|c|c|c|c|c} \dfrac{b_{11}}{b_{13}} & \dfrac{b_{12}}{b_{13}} & 1 & \dfrac{b_{14}}{b_{13}} & -\dfrac{1}{b_{13}} & 0 \\ \hline -b_{23}\dfrac{b_{11}}{b_{13}} + b_{21} & -b_{23}\dfrac{b_{12}}{b_{13}} + b_{22} & 0 & -b_{23}\dfrac{b_{14}}{b_{13}} + b_{24} & \dfrac{b_{23}}{b_{13}} & -1 \end{array}\right]$$

$$= \left[\begin{array}{c|c|c|c|c|c} c_{11} & c_{12} & 1 & c_{14} & c_{15} & 0 \\ \hline c_{21} & c_{22} & 0 & c_{24} & c_{25} & -1 \end{array}\right]$$

The process is continued by first dividing row 2 by the largest element and again using row operations to eliminate the other element in that column. Again, for illustrative purposes, it is assumed that the pivotal element of row 2 (say c_{22}) is known, and row 1 will be modified by row operations as

$$ele_{1j} = - c_{12} \frac{c_{2j}}{c_{22}} + c_{1j}$$

giving

$$d_{ij} = \left[\begin{array}{c|c|c|c|c} -c_{12}\frac{c_{21}}{c_{22}} + c_{11} & 0 & 1 & -c_{12}\frac{c_{24}}{c_{22}} + c_{14} & -c_{12}\frac{c_{25}}{c_{22}} + c_{15} & \frac{c_{12}}{c_{22}} \\ \hline \frac{c_{21}}{c_{22}} & 1 & 0 & \frac{c_{24}}{c_{22}} & \frac{c_{25}}{c_{22}} & -\frac{1}{c_{22}} \end{array}\right]$$

$$= \left[\begin{array}{c|c|c|c|c|c} d_{11} & 0 & 1 & d_{14} & d_{15} & d_{16} \\ \hline d_{21} & 1 & 0 & d_{24} & d_{25} & d_{26} \end{array}\right]$$

from which the desired similarity transformation is established as

$$R_{ij} = \begin{bmatrix} 1 & 0 & 0 & 0 \\ -d_{21} & -d_{24} & -d_{25} & -d_{26} \\ -d_{11} & -d_{14} & -d_{15} & -d_{16} \\ 0 & 1 & 0 & 0 \end{bmatrix}$$

It now follows that the original state variables are written in terms of the modified state variables as

$$\begin{Bmatrix} Y_1 \\ Y_2 \\ Y_3 \\ Y_4 \end{Bmatrix} = \begin{bmatrix} 1 & 0 & 0 & 0 \\ -d_{21} & -d_{24} & -d_{25} & -d_{26} \\ -d_{11} & -d_{14} & -d_{15} & -d_{16} \\ 0 & 1 & 0 & 0 \end{bmatrix} \begin{Bmatrix} Y_1 \\ Y_4 \\ w_1 \\ w_2 \end{Bmatrix}$$

D. System Transfer Functions

The entire system transfer function synthesis can be concisely summarized in a chronological sequence of steps that began with linearization of the coupled mechanical/control law equations that govern the dynamical motion. This process included linearization of additional equations that contained specific variables required for further consideration in the stability analysis (namely, plant sensor signals and control system outputs). A similarity transformation has been introduced that exchanges original state variables for these desired sensor signals and controller outputs so that the resulting modified state vector is still representative of an independent set of state variables. The resulting system of state-space equations is later identified as equation III-28.

The system characteristic matrix, A_{ij}, provides the basis for evaluating the coupled mechanical/control system resonant characteristics (natural frequencies), as well as the fundamental basis for specification and determination of the various types of transfer functions. The next subsection addresses some of the more specific details regarding specific transfer function relationships. A particular transfer function is identified by a *type* along with the desired output/input variable designation. An eigenvalue problem is then stated, which leads to determination of the numerator roots (zeros) and denominator roots (poles) for the particular transfer function. When the poles and zeros are known for a transfer function, this information can be further processed and displayed by any of the conventional display modes: Bode, Nichols, Nyquist, and/or root locus.

The conventional block diagram representation for the coupled plant/controller system (figure 9) provides additional insight for determination of system transfer functions.

The first-order differential equations for the system are written as

$$\dot{Z}^i = A_{ij} Z^j + B_{T_{ij}} R_T{}^j + B_{s_{ij}} R_s{}^j \qquad \text{(III-28)}$$

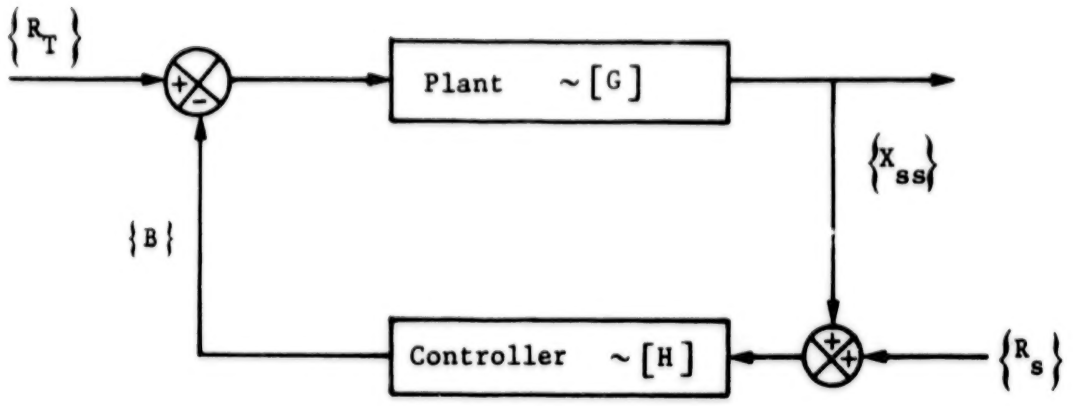

Figure 9. Plant/controller block diagram.

and it is helpful at this point to express the equation in matrix form and indicate the separate partitioned subsets of $\dot{Z}^i$, A_{ij}, Z^j, $B_{T_{ij}}$, $R_T{}^j$, $B_{s_{ij}}$, and $R_s{}^j$ as

$$\begin{Bmatrix} \dot{y} \\ \dot{X}_{ss} \\ \dot{\delta} \\ \dot{B} \end{Bmatrix} = \left[\begin{array}{c|c|c|c} a_{11} & a_{12} & a_{13} & a_{14} \\ \hline a_{21} & a_{22} & a_{23} & a_{24} \\ \hline a_{31} & a_{32} & a_{33} & a_{34} \\ \hline a_{41} & a_{42} & a_{43} & a_{44} \end{array}\right] \begin{Bmatrix} y \\ X_{ss} \\ \delta \\ B \end{Bmatrix} + \begin{bmatrix} b_T 1 \\ b_T 2 \\ b_T 3 \\ b_T 4 \end{bmatrix} \{R_T\} + \begin{bmatrix} b_s 1 \\ b_s 2 \\ b_s 3 \\ b_s 4 \end{bmatrix} \{R_s\} \qquad \text{(III-29)}$$

The following observations are noted

$$\begin{array}{lll} a_{31} = 0 & b_T 1 = -a_{14} & b_s 1 = 0 \\ a_{41} = 0 & b_T 2 = -a_{24} & b_s 2 = 0 \\ a_{13} = 0 & b_T 3 = 0 & b_s 3 = a_{32} \\ a_{23} = 0 & b_T 4 = 0 & b_s 4 = a_{42} \end{array}$$

and equation III-29 can be restated as

$$\begin{Bmatrix} \dot{y} \\ \dot{X}_{ss} \\ \dot{\delta} \\ \dot{B} \end{Bmatrix} = \left[\begin{array}{c|c|c|c} a_{11} & a_{12} & & a_{14} \\ \hline a_{21} & a_{22} & & a_{24} \\ \hline & a_{32} & a_{33} & a_{34} \\ \hline & a_{42} & a_{43} & a_{44} \end{array}\right] \begin{Bmatrix} y \\ X_{ss} \\ \delta \\ B \end{Bmatrix} + \begin{bmatrix} -a_{14} \\ -a_{24} \\ 0 \\ 0 \end{bmatrix} \{R_T\} + \begin{bmatrix} 0 \\ 0 \\ a_{32} \\ a_{42} \end{bmatrix} \{R_s\} \qquad \text{(III-30)}$$

Equation III-30 is the operating basis for stating particular transfer function relationships for the plant/controller system.

The general procedure is to establish a system transfer function between inputs R_T and R_s and outputs X_{ss} and B. Loops may be opened to provide open-loop information by manipulating the A_{ij} coefficients to prohibit certain feedbacks.

To symbolically describe specification of a transfer function, begin by consolidating the b coefficients and taking the Laplace transform of equation III-30 to give

$$[Is]\ \{Z(s)\} = [A]\ \{Z(s)\} + [b]\ \{U(s)\} \qquad \text{(III-31)}$$

or

$$\left[[Is] - [A]\right]\ \{Z(s)\} = [b]\ \{U(s)\} \qquad \text{(III-32)}$$

and then employ Cramer's rule to evaluate a given element, $Z(s)^p$, due to a particular input, $U(s)^q$, where

$$Z(s)^p/U(s)^q = \frac{\text{aug}\,|Is - A|}{|Is - A|} \qquad \text{(III-33)}$$

and where aug | Is – A | is accomplished by placing column q of b into column p of | Is – A |

The Q-R algorithm (References 6 and 7) is a useful tool with which to extract the indicated determinants in equation III-33.

1. *Root Extraction Process*

With reference to equation III-33, evaluation of both the numerator and denominator roots is desired. The denominator root extraction is straightforward in that $p_1, p_2, p_3, \cdots p_n$ is sought from an expression of the form

$$D(s) = \det([I]s - [A])$$

so that

$$D(s) = (s - p_1)(s - p_2) \cdots (s - p_n) = \prod_{i=1}^{n} (s - p_i) \qquad \text{(III-34)}$$

This evaluation is completed by extracting the characteristic roots of the matrix, A_{ij}. In general, these roots will be complex because A_{ij} is not symmetric.

The process used for evaluating the numerator is best illustrated with an example. Consider that we have the (4 by 4) characteristic system matrix,

$$[A_{ij}] = \left[\begin{array}{c|c|c|c} a_{11} & a_{12} & a_{13} & a_{14} \\ \hline a_{21} & a_{22} & a_{23} & a_{24} \\ \hline a_{31} & a_{32} & a_{33} & a_{34} \\ \hline a_{41} & a_{42} & a_{43} & a_{44} \end{array}\right]$$

and the column of coefficients b_i that premultiply the desired input variable, U^q. Further, let it be desired to obtain the transfer function relating output of the third variable in the state equations, y_3, to the input, U^q.

The state equations for this system would appear as

$$\begin{Bmatrix} \dot{y}_1 \\ \dot{y}_2 \\ \dot{y}_3 \\ \dot{y}_4 \end{Bmatrix} = \left[\begin{array}{c|c|c|c} a_{11} & a_{12} & a_{13} & a_{14} \\ \hline a_{21} & a_{22} & a_{23} & a_{24} \\ \hline a_{31} & a_{32} & a_{33} & a_{34} \\ \hline a_{41} & a_{42} & a_{43} & a_{44} \end{array}\right] \begin{Bmatrix} y_1 \\ y_2 \\ y_3 \\ y_4 \end{Bmatrix} + \begin{Bmatrix} b_1 \\ b_2 \\ b_3 \\ b_4 \end{Bmatrix} U^q \qquad \text{(III-35)}$$

and, with reference to equation III-33, the numerator is

$$N(s) = \text{aug} \mid Is - A \mid$$

or

$$N(s) = \det \begin{vmatrix} s - a_{11} & -a_{12} & b_1 & -a_{14} \\ -a_{21} & s - a_{22} & b_2 & -a_{24} \\ -a_{31} & -a_{32} & b_3 & -a_{34} \\ -a_{41} & -a_{42} & b_4 & s - a_{44} \end{vmatrix} \qquad \text{(III-36)}$$

After performing elementary row operations, equation III-36 can be restated in the form

$$N(s) = b_3 \det \begin{vmatrix} s - a_{11} + a_{31} b_1/b_3 & -a_{12} + a_{32} b_1/b_3 & -a_{14} + a_{34} b_1/b_3 \\ -a_{21} + a_{31} b_2/b_3 & s - a_{22} + a_{32} b_2/b_3 & -a_{24} + a_{34} b_2/b_3 \\ -a_{41} + a_{31} b_4/b_3 & -a_{42} + a_{32} b_4/b_3 & s - a_{44} + a_{34} b_4/b_3 \end{vmatrix} \qquad \text{(III-37)}$$

or, in symbolic terms, as

$$N(s) = b_3 \det \mid [Is] - [\tilde{a}] \mid \qquad \text{(III-38)}$$

where the matrix $\tilde{a}$ is given as

$$\left[\begin{array}{c|c|c} a_{11} - a_{31} b_1/b_3 & a_{12} - a_{32} b_1/b_3 & a_{14} - a_{34} b_1/b_3 \\ \hline a_{21} - a_{31} b_2/b_3 & a_{22} - a_{32} b_2/b_3 & a_{24} - a_{34} b_2/b_3 \\ \hline a_{41} - a_{31} b_4/b_3 & a_{42} - a_{32} b_4/b_3 & a_{44} - a_{34} b_4/b_3 \end{array}\right]$$

Note that the previous expression for N (s) is finite only if $b_3 \neq 0$, and the question is: Can b_3 realistically be null? The answer is *yes*, as the following example indicates.

Consider the simple mechanical system consisting of two masses connected by a single spring/dashpot combination as shown in figure 10.

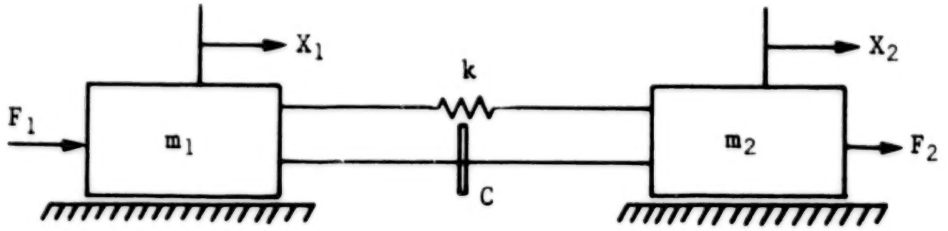

Figure 10. Simple mechanical system.

The state-space representation is

$$\frac{d}{dt}\begin{Bmatrix}\dot{X}_1\\ \dot{X}_2\\ X_1\\ X_2\end{Bmatrix} = \left[\begin{array}{c|c|c|c} -c/m_1 & c/m_1 & -k/m_1 & k/m_1 \\ c/m_2 & -c/m_2 & k/m_2 & -k/m_2 \\ 1 & 0 & 0 & 0 \\ 0 & 1 & 0 & 0 \end{array}\right]\begin{Bmatrix}\dot{X}_1\\ \dot{X}_2\\ X_1\\ X_2\end{Bmatrix} + \begin{bmatrix} 1/m_1 & 0 \\ 0 & 1/m_2 \\ 0 & 0 \\ 0 & 0 \end{bmatrix}\begin{Bmatrix}F_1\\ F_2\end{Bmatrix}$$

and the frequency domain (or transformed) equations in s are

$$\Big[[I]s - [A]\Big]\begin{Bmatrix}\dot{X}_1(s)\\ \dot{X}_2(s)\\ X_1(s)\\ X_2(s)\end{Bmatrix} = \begin{bmatrix} 1/m_1 & 0 \\ 0 & 1/m_2 \\ 0 & 0 \\ 0 & 0 \end{bmatrix}\begin{Bmatrix}F_1\\ F_2\end{Bmatrix}$$

where

$$[A] = \begin{bmatrix} -c/m_1 & c/m_1 & -k/m_1 & k/m_1 \\ c/m_2 & -c/m_2 & k/m_2 & -k/m_2 \\ 1 & 0 & 0 & 0 \\ 0 & 1 & 0 & 0 \end{bmatrix}$$

Now, consider the transfer function, $\dot{X}_1(s)/F_1$, where the augmented numerator is

$$N(s) = \det \begin{vmatrix} 1/m_1 & -c/m_1 & k/m_1 & -k/m_1 \\ 0 & s + c/m_2 & -k/m_2 & k/m_2 \\ 0 & 0 & s & 0 \\ 0 & -1 & 0 & s \end{vmatrix}$$

and the pivot element is the (1, 1) element or $1/m_1 \neq 0$. On the other hand, the transfer function, $X_1(s)/F_1$, has the augmented numerator

$$N(s) = \det \begin{vmatrix} s + c/m_1 & -c/m_1 & 1/m_1 & -k/m_1 \\ -c/m_2 & s + c/m_2 & 0 & k/m_2 \\ -1 & 0 & 0 & 0 \\ 0 & -1 & 0 & s \end{vmatrix}$$

and the pivot element is the (3, 3) element, which is null.

The problem to be addressed now involves evaluation of the numerator determinant, N(s), when the pivotal element is null. The particular mathematical problem may be restated as

$$N(s) = \det \left| [\tilde{I}]s - [\tilde{A}] \right| \qquad \text{(III-39)}$$

where $[\tilde{I}]$ is the identity matrix, [I], of size N with a null diagonal element. Addition and subtraction of the quantity, $[\tilde{I}]\,\chi$, where χ is an arbitrary constant not equal to one of the roots of $[\tilde{A}]$, yields

$$N(s) = \det \left| [\tilde{I}]\,(s - \chi) - \left[[\tilde{A}] - [\tilde{I}]\,\chi \right] \right| \qquad \text{(III-40)}$$

and, if $(s - \chi) \equiv 1/p$ is defined, there results

$$N(s) = \frac{(-1)^N}{p^N} \det \left| \tilde{A} - \tilde{I}\chi \right| \left(\det \left| Ip - (\tilde{A} - \tilde{I}\chi)^{-1} \tilde{I} \right| \right) \qquad \text{(III-41)}$$

The roots, $(p_i,\ i = 1, N)$, are found as the eigenvalues of the expression

$$\left[[\tilde{A}] - [\tilde{I}]\,\chi \right]^{-1} [\tilde{I}] \qquad \text{(III-42)}$$

and the eigensolution permits N(s) to be written as

$$N(s) = \frac{(-1)^N}{p^N} \det \left| \tilde{A} - \tilde{I}\chi \right| \left\{ (p - p_1)(p - p_2) \cdots (p - p_N) \right\} \qquad \text{(III-43)}$$

The following observation can now be made: a p_i equal to zero implies a root at infinity (or a characteristic polynomial having an order less than N). Thus, the null p_i's are eliminated from the expression, giving the characteristic polynomial an order, n, which is less than N. It is a rather common occurrence for the number of zeros (an order of N(s) to be significantly less than the number of poles (order of D(s)). With reference to equation III-43, the numerator expression, N(s), can be written as

$$N(s) = (-1)^N \det \left| \tilde{A} - \tilde{I}\chi \right| \left\{ \left(1 - \frac{p_1}{p}\right)\left(1 - \frac{p_2}{p}\right) \cdots \left(1 - \frac{p_n}{p}\right) \right\} \qquad \text{(III-44)}$$

and, recalling that $p = 1/s\text{-}\chi$, yields

$$N(s) = \frac{(-1)^N}{\prod_{i=1}^{n} (\chi - S_i)} \det \left| \tilde{A} - \tilde{I}\chi \right| \left\{ (s - s_1)(s - s_2) \cdots (s - s_n) \right\} \qquad \text{(III-45)}$$

Next, note that

$$\prod_{i=1}^{n} (\chi - s_i) = \prod_{i=1}^{n} \left(\frac{-1}{p_i} \right) \qquad \text{(III-46)}$$

and it follows that

$$N(s) = (-1)^{N-n} \prod_{i=1}^{n} p_i \det \left| \tilde{A} - \tilde{I}\chi \right| \prod_{i=1}^{n} (s - s_i) \qquad \text{(III-47)}$$

The numerator root gain, k_R, can now be identified as

$$k_R = (-1)^{N-n} \prod_{i=1}^{n} p_i \det \left| \tilde{A} - \tilde{I}\chi \right| \qquad \text{(III-48)}$$

and the Bode gain, k_B, for the numerator is

$$k_B = k_R (-1)^m \prod_{i=1}^{m} s_i$$

where $m \leqslant n$

2. Transfer-Function Classification

With reference to figure 9, it is possible to directly identify six transfer function types, each characterizied by the specific variables involved and by the presence of feedback. In addition, a seventh type will also be described whereby certain control variables feed back and others do not. This type is similar to an open-loop transfer function but treats selected channels of the controller as part of the mechanical system (plant). During the course of this discussion,

it will become apparent that additional transfer function types are easily accommodated by rather simple manipulations with the system characteristic matrix, A_{ij}.*

In general, note that the process of obtaining the desired transfer function involves but a few basic steps. The transfer function characteristic matrix, $\lceil R_{ij}$, and the desired force coefficient vector, b_i, are obtained directly from the system characteristic matrix, A_{ij}. These two matrices are then put in a form so that the Q-R algorithm can be used to extract system roots.

a. Type I (Plant Only)—Type I is the forward path transfer function for the plant with no feedback and is of the form

$$X_{ss}^{p}/R_T^q = G(s) \tag{III-49}$$

The control variables, δ^i, and control outputs, B^i, do not feed back into the plant. The matrix expression depicting the system of interest is

$$\frac{d}{dt}\begin{Bmatrix} y \\ X_{ss} \end{Bmatrix} = \begin{bmatrix} a_{11} & a_{12} \\ a_{21} & a_{22} \end{bmatrix} \begin{Bmatrix} y \\ X_{ss} \end{Bmatrix} + \begin{bmatrix} b_T 1 \\ b_T 2 \end{bmatrix} \{R_T\} \tag{III-50}$$

The matrix, A_{ij}, to use in the general expression given as equation III-33 is referred to as $\lceil R_{ij}$ or the reduced A_{ij} matrix,

$$\lceil R_{ij} = \begin{bmatrix} a_{11} & a_{12} \\ a_{21} & a_{22} \end{bmatrix} \tag{III-51}$$

The augmented $\lceil R_{ij}$ matrix is obtained by removing the column corresponding to the input variable, R_T^q, from the expression, b_T, and inserting this column into the column in $\lceil R_{ij}$, which corresponds to the desired output, X_{ss}^p. The resulting transfer function is then given as

$$X_{ss}^{p}/R_T^q = \frac{\text{aug} \mid Is - \lceil R \mid}{\mid Is - \lceil R \mid} \tag{III-52}$$

*Additional comments pertaining to the exact definitions of various types of transfer functions implemented can be found in subroutine DEF5 Debug 116 in the discussion concerning "Frequency Domain Analysis" (Volume II, Appendix B, page B-332).

b. Type II (Controller Only)—Type II represents the feedback path, H(s), for the controller only. The desired transfer function relates control-system outputs, B^i, to sensor signal inputs, X^j_{ss},

$$B^p/X^q_{ss} = H(s) \tag{III-53}$$

The reduced characteristic matrix, $\mathbb{R}_{ij}$, and the corresponding input coefficients, b_{ik}, are given as

$$\mathbb{R}_{ij} = \begin{bmatrix} a_{33} & a_{34} \\ a_{43} & a_{44} \end{bmatrix}, \quad b_{ik} = \begin{bmatrix} a_{32} \\ a_{42} \end{bmatrix} \tag{III-54}$$

c. Type III (Open Loop, HG)—Type III falls within the framework of the classical open-loop transfer function designation and relates control system outputs, B^i, to external plant inputs, R^j_T. The algebraic expression for a given output variable, B^p, due to an external input, R^q_T, is indicated as

$$B^p/R^q_T = (HG)(s) \tag{III-55}$$

The open-loop system characteristic matrix, $\mathbb{R}_{ij}$, and corresponding input coefficients, b_{ik}, are

$$\mathbb{R}_{ij} = \left[\begin{array}{c|c|c|c} a_{11} & a_{12} & & \\ \hline a_{21} & a_{22} & & \\ \hline & a_{32} & a_{33} & a_{43} \\ \hline & a_{42} & a_{43} & a_{44} \end{array}\right], \quad b_{ik} = \begin{bmatrix} -a_{14} \\ -a_{24} \\ 0 \\ 0 \end{bmatrix} \tag{III-56}$$

It was previously noted that $a_{31} = a_{41} = a_{13} = a_{23} = 0$, and, in addition, the partitions, a_{14} and a_{24}, are set to zero to prohibit the B^i feedback. Thus, the loop is opened to establish HG, and the open-loop transfer function in s. Note that the negative sign in the b_{ik} coefficients simply indicates that the B^i feedback is negative with respect to the external plant inputs, R^j_T.

d. Type IV (Open Loop, GH)—An additional open-loop transfer function is often desired for assessing the plant sensor signal outputs caused by controller noise inputs. The transfer function then relates sensor signal outputs, X_{ss}^{i}, to control system noise inputs, R_{s}^{j}. The plant sensor signal vector does not feed back into the system so that

$$X_{ss}^{p}/R_{s}^{q} = (GH)(s) \tag{III-57}$$

and the system characteristic matrix, $\mathbb{R}_{ij}$, and the external input coefficients, b_{ik}, are identified as

$$\mathbb{R}_{ij} = \left[\begin{array}{c|c|c|c} a_{11} & a_{12} & & a_{14} \\ \hline a_{21} & a_{22} & & a_{24} \\ \hline & & a_{33} & a_{34} \\ \hline & & a_{43} & a_{44} \end{array}\right], \quad b_{ik} = \begin{bmatrix} 0 \\ 0 \\ a_{32} \\ a_{42} \end{bmatrix} \tag{III-58}$$

Note that the a_{32} and a_{42} partitions have been nulled to eliminate sensor signal feedback.

e. Type V (Closed Loop – Control Ratio)—The system control ratio is given as the transfer function that relates plant variable outputs to externally applied plant inputs with the control system entirely active. This transfer function is expressed as

$$X_{ss}^{p}/R_{T}^{q} = \left(\frac{G}{1+GH}\right)(s) \tag{III-59}$$

and the system characteristic matrix, $\mathbb{R}_{ij}$, and the external input coefficients, b_{ik}, are identified as

$$\mathbb{R}_{ij} = \left[\begin{array}{c|c|c|c} a_{11} & a_{12} & & a_{14} \\ \hline a_{21} & a_{22} & & a_{24} \\ \hline & a_{32} & a_{33} & a_{34} \\ \hline & a_{42} & a_{43} & a_{44} \end{array}\right], \quad b_{ik} = \begin{bmatrix} -a_{14} \\ -a_{24} \\ 0 \\ 0 \end{bmatrix} \tag{III-60}$$

The negative sign in the matrix, b_{ik}, indicates that the feedback is negative.

f. Type VI (Closed Loop)—An additional closed-loop transfer function has been accommodated within the digital simulation. Specifically, Type VI relates plant sensor signal outputs to sensor signal noise inputs with all control-system loops active. The transfer function is symbolically indicated as

$$X_{ss}^{p} = (\text{transfer function})\, R_{s}^{q} \tag{III-61}$$

where the system characteristic matrix, $\mathbb{R}_{ij}$, and corresponding input coefficients are identified as

$$\mathbb{R}_{ij} = \begin{bmatrix} a_{11} & a_{12} & & a_{14} \\ a_{21} & a_{22} & & a_{24} \\ & a_{32} & a_{33} & a_{34} \\ & a_{42} & a_{43} & a_{44} \end{bmatrix}, \quad b_{ik} = \begin{bmatrix} 0 \\ 0 \\ a_{32} \\ a_{42} \end{bmatrix} \tag{III-62}$$

g. Type VII (Quasi-Open Loop)—An additional transfer function type is identified here and is referred to as a quasi-open loop (figure 11). It is of the open-loop type in that we are interested in control-system outputs, B^{i}, attributable to plant variable inputs, R_{T}^{j}. For example, suppose that, for a multichannel control system (such as azimuth and elevation), outputs B^{i} are desired on the controller channel that do not feed back and suppose that the other channel is active in that it feeds back into the plant.

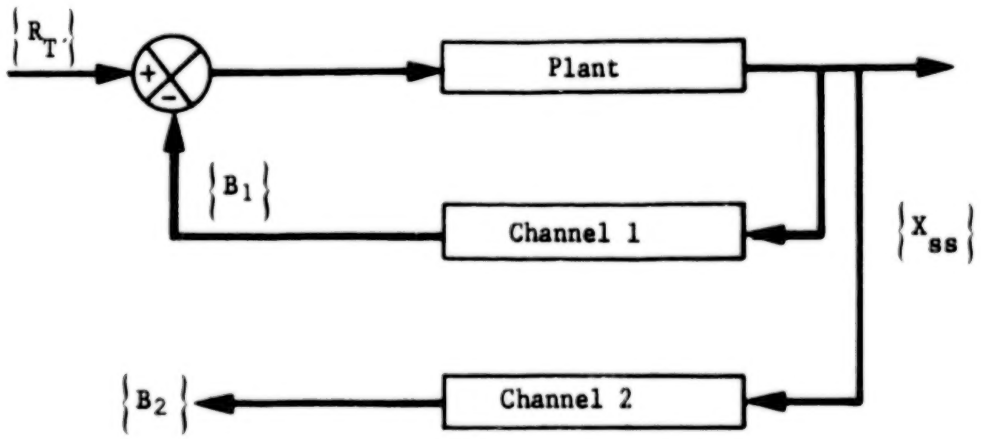

Figure 11. Type VII quasi-open loop block diagram.

For the configuration indicated, a typical Type VII transfer function (TF) would be given by

$$B_2^p = \text{(transfer function)}\ R_T^q$$

and the form of the system characteristic matrix, $\mathbb{R}_{ij}$, and plant input coefficient matrix, b_{ik}, would be

$$\mathbb{R}_{ij} = \left[\begin{array}{c|c|c|c} a_{11} & a_{12} & & \tilde{a}_{14} \\ \hline a_{21} & a_{22} & & \tilde{a}_{24} \\ \hline & a_{32} & a_{33} & a_{34} \\ \hline & a_{42} & a_{43} & a_{44} \end{array}\right], \quad b_{ik} = \begin{bmatrix} -a_{14} \\ -a_{24} \\ 0 \\ 0 \end{bmatrix} \tag{III-63}$$

The subpartitions, $\tilde{a}_{14}$ and $\tilde{a}_{24}$, indicate modification of the original partitions, a_{14} and a_{24}. Specifically, $\tilde{a}_{mn}$ is a subset of a_{ij} that is obtained by keeping only those n columns of a_{mn} that correspond to the B^i variables that feed back to the plant.

3. Transfer Functions—Polynomial Description

This subsection is addressed to implementation of control-system transfer functions described as the ratio of two polynomials in the frequency domain, s. Specifically, consider

$$TF = P(s)/Q(s) \tag{III-64}$$

where

$$Q(s) = a_0 + a_1 s + a_2 s^2 + a_3 s^3 + \cdots + a_n s^n$$

and

$$P(s) = b_0 + b_1 s + b_2 s^2 + \cdots + b_m s^m$$

Because the previously described governing equations have been stated in canonical first-order form, the polynomial description for the transfer function is restated in the form

$$\dot{\delta}^i = A_{ij}\delta^j + B_i U \tag{III-65}$$

The block diagram for the system is

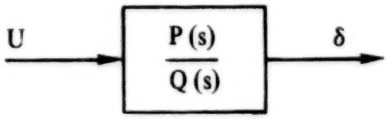

from which we write

$$\delta = \frac{P(s)}{Q(s)}\ U \tag{III-66}$$

and expansion of the implied operator in s results in a differential equation of the form

$$a_n \overset{n}{\delta} + a_{n-1}\overset{n-1}{\delta} + \cdots + a_1\dot{\delta} + a_0\delta = b_m \overset{m}{U} + b_{m-1}\overset{m-1}{U} + \cdots + b_1\dot{U} + b_0 U \tag{III-67}$$

where

$$\overset{n}{\delta} = \frac{d^n\delta}{dt^n}$$

In general, the order of P(s) will be no greater than the order of Q(s) or $m \leqslant n$.

a. $m = n$–Equation III-67 is divided by a_n to obtain

$$\overset{n}{\delta} + C_{n-1}\overset{n-1}{\delta} + \cdots + C_1\dot{\delta} + C_0\delta = d_m \overset{m}{U} + d_{m-1}\overset{m-1}{U} + \cdots + d_1\dot{U} + d_0 U \tag{III-68}$$

where

$$C_i = \frac{a_i}{a_n}$$

and

$$d_i = \frac{b_i}{a_n}$$

The following example is used for illustration:

Consider the equation with m = n = 4,

$$\overset{\cdots\cdot}{\delta} + C_3 \overset{\cdots}{\delta} + C_2 \overset{\cdot\cdot}{\delta} + C_1 \dot{\delta} + C_0 \delta = d_4 \overset{\cdots\cdot}{U} + d_3 \overset{\cdots}{U} + d_2 \overset{\cdot\cdot}{U} + d_1 \dot{U} + d_0 U$$

or, in operator form,

$$s^4\delta + s^3 C_3 \delta + s^2 C_2 \delta + s C_1 \delta + C_0 \delta = s^4 d_4 U + s^3 d_3 U + s^2 d_2 U + s d_1 U + d_0 U$$

This can be rewritten as

$$s^4\left(\delta - d_4 U\right) + s^3\left(C_3\delta - d_3 U\right) + s^2\left(C_2\delta - d_2 U\right) + s\left(C_1\delta - d_1 U\right) + \left(C_0\delta - d_0 U\right) = 0$$

and the substitution

$$\delta_1 = \delta - d_4 U$$

permits a reduction in order to

$$s^3\left(\dot{\delta}_1 + C_3\delta - d_3 U\right) + s^2\left(C_2\delta - d_2 U\right) + s\left(C_1\delta - d_1 U\right) + \left(C_0\delta - d_0 U\right) = 0$$

A new variable can again be introduced:

$$\delta_2 = \left(\dot{\delta}_1 + C_3\delta - d_3 U\right)$$

and the foregoing can be rewritten as

$$s^2 (\dot{\delta}_2 + C_2\delta - d_2U) + s(C_1\delta - d_1U) + (C_0\delta - d_0U) = 0$$

It follows that, if

$$\delta_3 = \dot{\delta}_2 + C_2\delta - d_2U$$

is defined,

$$s(\dot{\delta}_3 + C_1\delta - d_1U) + C_0\delta - d_0U = 0$$

results, and the substitution

$$\delta_4 = \dot{\delta}_3 + C_1\delta - d_1U$$

gives

$$\dot{\delta}_4 = -C_0\delta + d_0U$$

The variable, δ, can now be eliminated from each of the foregoing expressions, and the results can be generalized to n^{th}-order systems.

The result is concisely stated as a matrix equation that is recognized to be of the desired form initially given as equation III-65,

$$\begin{Bmatrix} \dot{\delta}_1 \\ \dot{\delta}_2 \\ \cdot \\ \cdot \\ \cdot \\ \dot{\delta}_{n-1} \\ \dot{\delta}_n \end{Bmatrix} = \left[\begin{array}{c|c|c|c|c|c} -C_{n-1} & 1 & 0 & \cdot & \cdot & 0 \\ -C_{n-2} & 0 & 1 & \cdot & \cdot & 0 \\ \cdot & \cdot & \cdot & & & \cdot \\ \cdot & \cdot & \cdot & & & \cdot \\ \cdot & \cdot & \cdot & & & \cdot \\ -C_1 & 0 & 0 & & & 1 \\ -C_0 & 0 & 0 & \cdot & \cdot & 0 \end{array}\right] \begin{Bmatrix} \delta_1 \\ \delta_2 \\ \cdot \\ \cdot \\ \cdot \\ \delta_{n-1} \\ \delta_n \end{Bmatrix} + \begin{Bmatrix} d_{n-1} - C_{n-1}d_n \\ d_{n-2} - C_{n-2}d_n \\ \cdot \\ \cdot \\ \cdot \\ d_1 - C_1d_n \\ d_0 - C_0d_n \end{Bmatrix} U \qquad \text{(III-69)}$$

where δ_1 and δ, the original variables of the equation, are related as shown previously, and U is the input variable to the transfer function expression as indicated in equation III-65.

b. $m < n$–The general expression for the case where $m < n$ is easily accommodated by restricting the d_i coefficients to reflect the limit m. Commonly, only the d_0 coefficient will be finite.

4. Frequency Response

Transfer-function poles, zeros, and root gain can be converted to the standard Bode form for frequency response by combining time constants, damping, and resonant frequencies as

$$TF = k_B \frac{s^r \prod_{i=1}^{N1} (1 + \tau_i s) \prod_{i=1}^{N2} \left(1 + \frac{2\zeta_i s}{\omega_i} + \frac{s^2}{\omega_i^2}\right)}{\prod_{j=1}^{M1} (1 + \tau_j s) \prod_{j=1}^{M2} \left(1 + \frac{2\zeta_j s}{\omega_j} + \frac{s^2}{\omega_j^2}\right)} \qquad \text{(III-70)}$$

where the Bode gain is

$$k_B = k \frac{\prod_{i=1}^{n} z_i}{\prod_{j=1}^{m} p_j}$$

where

k = root gain

τ = system constants

ζ = system damping at frequency ω

ω = system resonant frequency

The frequency response is then calculated by substituting $j\omega$ for s and evaluating the transfer function expression at various ω's. The digital simulation uses a vernier frequency incrementing approach that automatically introduces smaller frequency increments near the poles

and zeros. This variable frequency incrementing technique permits better transfer-function resolution near the resonances at which amplitude and phase can vary rapidly.*

5. Root Locus

The root-locus method of analysis and design is based on the relationship between the poles and zeros of the closed-loop transfer function and those of the open-loop transfer function. The method is used to determine the location of the roots of the characteristic equation as a function of a single open-loop gain parameter. The locations of these roots are indicative of the relative system stability. The analyst may use the method as a design tool by adjusting the poles, zeros, and the open-loop gain parameters so as to yield a closed-loop system with satisfactory critical frequencies (poles and zeros).

To further describe the theoretical basis for the method, refer to the conventional control ratio for a feedback system as shown in figure 12.

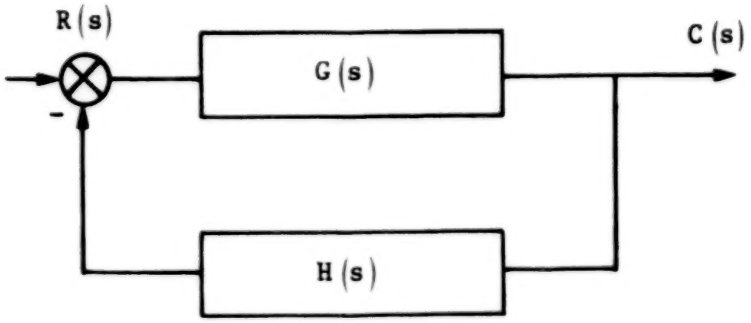

Figure 12. Conventional feedback control system.

The control ratio, C(s)/R(s), is

$$\frac{C(s)}{R(s)} = \frac{G(s)}{1 + G(s)H(s)} \qquad \text{(III-71)}$$

*Eigenvector analysis in conjunction with frequency domain analysis is not a common practice; however, for complex, highly coupled multirigid and flexible-body systems, it becomes a necessity. System roots often shift significantly from body and control frequencies, and are therefore impossible to physically interpret. Eigenvector analysis of the characteristic matrix associated with the transfer function under study can be used to determine a measure of the degree to which each of the body and control-system degrees of freedom couple to form the total system roots and associated modes (eigenvectors). For further information, see subroutine DEF5.

and the open-loop transfer function, G(s) H(s), is identified as a ratio of two functions in s,

$$G(s)H(s) = k\frac{P(s)}{Q(s)} \qquad \text{(III-72)}$$

The characteristic system equation is

$$1 + G(s)H(s) = 0$$

or (III-73)

$$1 + k\frac{P(s)}{Q(s)} = 0$$

The conventional root-locus plot portrays the loci of the values of s that satisfy the characteristic equation as k varies from zero to infinity. Note that

- At k = 0, the roots of the characteristic equation are equal to the roots of Q(s), which are the same as the poles of the open-loop transfer function, k P(s)/Q(s).
- As k approaches infinity, the roots approach the roots of P(s), the open-loop zeros.

Thus, as k varies from 0 to infinity, the loci of the closed-loop poles migrate from the open-loop poles to the open-loop zeros, and the direction of migration depends on the sign of the open-loop gain parameter, k.

Rewriting equation III-73 yields a more conventional expression for the characteristic equation as

$$k\frac{P(s)}{Q(s)} = -1 \qquad \text{(III-74)}$$

and two conditions are required as follows:

$$\left| k\frac{P(s)}{Q(s)} \right| = 1$$

$$\angle P(s)/Q(s) = 180^\circ,\ k \geqslant 0$$

The first of these conditions can be expressed as

$$k = \left| \frac{Q(s)}{P(s)} \right|$$

for those values of s that satisfy the angle criterion. The conditions that govern the migration of the roots in the complex plane can be solved by an iterative procedure. The iterative procedure for evaluating a single root locus* is described in Appendix E.

E. Linear Time-Domain Response

The linearized canonical first-order system of equations can also provide a basis for studying system time history in terms of perturbations about a specified state when the system indeed behaves in a linear manner in the vicinity of the state. The nonhomogeneous form of the equations, the basis for determining system transfer functions, appeared previously as

$$\dot{Z}^i = A_{ij} Z^j + b_{ik} U^k(t) \qquad \text{(III-75)}$$

The external system inputs are the elements of U^k. It is convenient to establish the solution for the foregoing system through the use of a recursive-formula numerical-integration procedure rather than through the Runge-Kutta approach.

Consider the Adams' corrector formula (Reference 8) at time, t + 1,

$$\eta_{t+1} = \eta_t + \frac{h}{24}\left[9\dot{\eta}_{t+1} + 19\dot{\eta}_t - 5\dot{\eta}_{t-1} + \dot{\eta}_{t-2}\right] \qquad \text{(III-76)}$$

where h is the incremented time step.

Application of this formula to our system of equations gives

$$z^i_{t+1} = z^i_t + \frac{h}{24}\left[9 A_{ij} z^j_{t+1} + 9 b_{ik} U^k_{t+1} + 19\dot{z}^i_t - 5\dot{z}^i_{t-1} + \dot{z}^i_{t-2}\right]$$

*Welch, Raymond V. NASA/Goddard Space Flight Center, Branch Report No. 254, October 2, 1973.

and manipulation yields the solution for all the z^i at time step, t + 1,

$$\{z\}_{t+1} = \left[[I] - \frac{3h}{8}[A]\right]^{-1} \left\{\{z\}_t + \frac{h}{24}\left(9[b]\{U\}_{t+1} + 19\{\dot{z}\}_t - 5\{\dot{z}\}_{t-1} + \{\dot{z}\}_{t-2}\right)\right\}$$

Note the requirement for z^i at time step, t - 2; hence, the requirement for a starter (e.g., Runge-Kutta) for initiating the solution process.

Goddard Space Flight Center
National Aeronautics and Space Administration
Greenbelt, Maryland October 1977

REFERENCES

1. Likens, P. W., "Analytical Dynamics and Nonrigid Spacecraft Simulation," Technical Report 32-1593, Jet Propulsion Laboratory, Pasadena, California, July 15, 1974.

2. Fixler, S. Z., "Effects of Solar Environment and Aerodynamic Drag on Structural Booms in Space," *J. Spacecraft*, **4** (3), March 1967.

3. Frisch, H. P., *Coupled Thermally Induced Transverse Plus Torsional Vibrations of a Thin-Walled Cylinder of Open Sections*, NASA TR R-333, March 1970.

4. Goldman, R. L., "Influence of Thermal Distortion on the Anomalous Behavior of a Gravity Gradient Satellite," *AIAA Mechanics and Control of Flight Conference*, Paper No. 74-922, Anaheim, California, August 1974.

5. Hovanessian, S., and L. A. Pipes, *Digital Computer Methods in Engineering*, McGraw-Hill Book Company, New York, 1969.

6. Francis, J. G. F., "The QR-Transformation–A Unitary Analogue to the LR-Transformation," *The Computer Journal*, **4**, Part 1, October 1961.

7. Francis, J. G. F., "The QR-Transformation–A Unitary Analogue to the LR-Transformation," *The Computer Journal*, **5**, Part 2, January 1962.

8. Schied, F., "Theory and Problems of Numerical Analysis." *Schawn's Outline Series*, McGraw-Hill Book Company, New York, 1968.

BLANK PAGE

BLANK PAGE

REFERENCE PAPER I

DYNAMIC RESPONSE AND STABILITY ANALYSIS
OF FLEXIBLE MULTIBODY SYSTEMS
(from DYNAMICS AND CONTROL OF
LARGE FLEXIBLE SPACECRAFT,
Proceedings of a Symposium held
in Blacksburg, Virginia,
June 13-15, 1977)

BLANK PAGE

BLANK PAGE

DYNAMIC RESPONSE AND STABILITY ANALYSIS OF FLEXIBLE, MULTIBODY SYSTEMS

by
Carl S. Bodley and A. Colton Park
Martin Marietta Corporation, Denver, Colorado
A. Darrell Devers
Texas A and M University, College Station, Texas
Harold P. Frisch
Goddard Space Flight Center, Greenbelt, Maryland

Abstract

An approach for dynamic simulation and stability analysis of systems of interconnected flexible bodies is discussed. The overall approach is unique in that any member body of the system can be flexible and the total system is not restricted to a topological tree configuration. The equations of motion are developed using the most general form of Lagrange's equations including auxiliary nonholonomic, rheonomic conditions of constraint. Lagrange multipliers are used as interaction forces/torques to maintain prescribed constraints. Nonlinear flexible/rigid dynamic coupling effects are accounted for in unabridged fashion for individual bodies and for the total system. Elastic deformation can be represented by normal vibration modes or by any adequate series of Rayleigh functions, including so-called quasi-static displacement functions.

A digital computer program system has been developed to numerically implement the modeling and analysis capability for a wide range of dynamic simulations including the nonlinear time domain and/or linear frequency domain. In particular, application has been made to: (1) time domain solution for nonlinear response of systems idealized as a collection of individual bodies; (2) numerical linearization of system governing equations; (3) time domain solution for perturbation response about a nominal state; and (4) frequency domain stability analysis corresponding to the linearized form.

Introduction

State of the art dynamic response analysis of a system of interconnected bodies, typical of current and projected large spacecraft, has

CONTENTS (Continued)

CONTENTS

been restricted until recent years, to rigid bodies interconnected in a topological tree configuration. The formalisms of Hooker and Margulies (Reference 1) and Roberson and Wittenburg (Reference 2) set the precedent with respect to a procedural synthesis and solution of the equations of motion governing such a system of bodies. Computer programs, with associated formalisms, have also been developed by Velman (Reference 3), Frisch (Reference 4) and Farrell, Newton and Connelly (Reference 5). These have proven to be highly applicable and useful tools for studying spacecraft dynamic response in the time domain. Following these earlier formalisms, a host of investigators (for example, References 6, 7, 8 and 9) extended the earlier concepts to include flexible terminal bodies and the capability to deal with environmental effects such as gravity gradient torques.

Almost all current spacecrafts are configured such that existing analytical techniques are completely adequate. That is, a typical spacecraft can be modeled as a rigid central body with flexible terminal bodies interconnected in a topological tree configuration. However, it is anticipated that future spacecraft designs will include configurations that cannot be adequately represented by a topological tree. To be more definitive, a non-topological tree configuration is one wherein there exists re-entrant branches or closed loops of connectivity. Such a system has, in effect, a statically indeterminant load path; this creates special problems for a dynamic analysis formalism.

This paper describes, in summary form, an analytical technique and associated computer program system which deals effectively with the problems of re-entrant connections. The analytical considerations and DISCOS* computer program system are documented in detail in Reference 10.

Definition of the Physical System

The spacecraft, which is subjected to analysis, can be described as a cluster of contiguous, flexible structures, or bodies. In the analytical treatment, the entire spacecraft system, or portions thereof, may be spinning or nonspinning. Member bodies of the system are capable of undergoing large relative excursions such as those of appendage deployment, or rotor/stator motions. Bodies of the system may be interconnected by linear or nonlinear springs and dashpots; they may be interconnected via a mechanism that consists of gimbal and slider block or a servo-actuator, or any combination of the above.

Analytical Considerations - Nonlinear State Equations

In conjunction with this discussion that follows, the interested reader is urged to see Bodley and Park (Reference 11) where attention

---

* Dynamic Interaction and Simulation of COntrols and Structure

is concentrated on development of governing equations of motion for a single flexible body. In the referenced development, ordinary momenta components (as opposed to the generalized momenta of Hamilton's canonical equations) are used as state variables. The ordinary momenta correspond to nonholonomic velocities (or, time derivatives of quasi-coordinates) in the same way that generalized momenta correspond to generalized velocities. The development has been used by the authors to study dynamic behavior of a single flexible body and also it appears to have withstood the test of time with respect to general validity and accuracy.

Presuming the validity of that development, the equations of dynamic equilibrium are

$$\left\{ \dot{p} \right\} = \left\{ G \right\} \tag{1}$$

where $\{p\}$ represents a column vector of ordinary momenta and where $\{G\}$ represents a collection of all external forces, internal restoring and dissipative forces, state dependent inertial forces (i.e., gyroscopic, Coriolis, Euler forces, etc.), and servo-actuator forces/torques. Development of the explicit form of the $\{G\}$ vector is very lengthy and is, therefore, not given here. The interested reader will see Reference 10 where the various contributions to the $\{G\}$ vector are treated with individual detail. Let it suffice to comment that it is possible to account for all state dependent and explicitly time dependent effects in an unabridged fashion.

Now, the vector of ordinary momenta, $\{p\}$ is related to a vector of nonholonomic velocities $\{U\}$ through a deformation dependent mass matrix $[m]$; that is,

$$\left\{ p \right\} = \left[m \right] \left\{ U \right\} , \tag{2}$$

where the elements of $[m]$ generally depend on the displacement coordinates $\{\xi\}$. Thus, the mass matrix has a time derivative. Implementation of the equations of motion of Reference 11 for solution via digital computer did not require evaluation of $[\dot{m}]$ and this was one attractive feature of the formalism. Such is not the case when considering a cluster of interconnected bodies, when the formalism uses Lagrange multipliers (interconnecting constraint forces/torques) and kinematic equations of constraint, as will be seen.

The equations of dynamic equilibrium for the jth body of the system may be extended to include, on the right hand side, the effects of the interconnection forces and torques and thus,

$$\left\{ \dot{p} \right\}_j = \left\{ G \right\}_j + \left[b \right]_j^T \left\{ \lambda \right\} . \tag{3}$$

Also, the equations of kinematic constraint are easily expressed as

$$\sum_j \left[b \right]_j \left\{ U \right\}_j = \left\{ \dot{a} \right\} \tag{4}$$

where $\left[b \right]_j$ represents a matrix of kinematic coefficients for the jth body and where $\left\{ \dot{a}(t) \right\}$ is a column of prescribed time dependent velocities across the interconnection junctions. The subscript j ranges from 1 through the number of bodies of the cluster.

Now, to be able to implement Equations (3) and (4) in a numerical integration solution process, it is necessary to numerically evaluate the highest derivative elements;in this case, evaluate $\left\{ \dot{p} \right\}$, given initial values for $\left\{ p \right\}$. However, before this is possible, it is necessary to view Equations (3) and (4) as simultaneous equations involving $\left\{ \dot{p} \right\}$ and $\left\{ \lambda \right\}$ as sets of unknowns. To simultaneously satisfy Equations (3) and (4), let us differentiate Equation (4) with respect to time and change the variables of Equation (3) as follows:

$$\left\{ \dot{p} \right\} = \frac{d}{dt} \left(\left[m \right] \left\{ U \right\} \right), \tag{5}$$

thus,

$$\begin{aligned} \left\{ \dot{U} \right\}_j &= \left[m \right]_j^{-1} \left(\left\{ G \right\}_j - \left[\dot{m} \right]_j \left\{ U \right\}_j + \left[b \right]_j^T \left\{ \lambda \right\} \right) \\ &\equiv \left[m \right]_j^{-1} \left(\left\{ G^* \right\}_j + \left[b \right]_j^T \left\{ \lambda \right\} \right) \end{aligned} \tag{6}$$

$$\text{and} \sum_j \left[b \right]_j \left\{ \dot{U} \right\}_j = \left\{ \ddot{a} \right\} - \sum_j \left[\dot{b} \right]_j \left\{ U \right\}_j .$$

Now, substituting Equation (6) into Equation (7) yields

$$\begin{aligned} \left\{ \lambda \right\} = &\left(\sum_j \left[b \right]_j \left[m \right]_j^{-1} \left[b \right]_j^T \right)^{-1} \\ &\left[\left\{ \ddot{a} \right\} - \sum_j \left(\left[\dot{b} \right]_j \left\{ U \right\}_j + \left[b \right]_j \left[m \right]_j^{-1} \left\{ G \right\}_j \right) \right] \end{aligned} \tag{8}$$

The numerically evaluated $\{\lambda\}$ given by Equation (8), when substituted into Equation (6), provides complete numerical definition of $\{\dot{U}\}$, which represents a vector of time derivatives of nonholonomic velocities (accelerations as seen by the observer moving and rotating with the reference frame of the jth body). The collection of $\{U\}_j$ vectors for the n bodies of the cluster serves as a portion of the complete state vector. Now, as the expression to evaluate the $\{\lambda\}$ and $\{G^*\}$ vectors and the $[m]_j$ matrix must involve dependence on the elements of $\{U\}_j$ and on position and displacement coordinates $\{\beta\}$ and $\{\xi\}_j$, there must be additional differential equations to provide $\{\beta\}$ and $\{\xi\}_j$ feedback. These are of the form:

$$\{\dot{\beta}\} = \sum_j [B]_j \{U\}_j \tag{9}$$

and

$$\{\dot{\xi}\}_j = [S]_j \{U\}_j \tag{10}$$

where $\{\beta\}$ represents a vector of position coordinates (gimbal angles and cartesian position vector components) and where $\{\xi\}_j$ represents displacement coordinates corresponding to assumed displacement functions (eigenfunctions, or any other kinematically admissible functions that are consistent with the boundary conditions). In Equation (9) the $[B]_j$ represents a matrix of kinematic coefficients of very similar form to the $[b]_j$ of Equation (6). That is, the elements of $[b]_j$ and $[B]_j$ are each dependent on the elements of $\{\beta\}$ and $\{\xi\}$. Finally, in Equation (10), the $[S]_j$ matrix simply provides a selection operation as $\{\dot{\xi}\}_j$ is a subvector of $\{U\}_j$.

The collection of $\{\xi\}_j$ vectors, for the n bodies, and the $\{\beta\}$ vector are <u>truly the generalized coordinates</u> of the structural system (they provide a complete configuration description of the system of bodies). We note that the equations of dynamic equilibrium (6) involve generalized coordinates and velocities in an implicit fashion, while generalized accelerations are not evident.

To complete the definition of the state equations, one must account for additional differential equations such as those linking control actuator torques to combinations of state elements (attitudes, their rates and time integrals) through an appropriate control law. These are of the form

$$\{\dot{\delta}\} = f(\{\beta\}, \{\xi\}, \{U\}, \{\delta\}, t). \tag{11}$$

The explicit form of the "controller", Equation (11), must be provided by a prospective DISCOS program user in that there is an unlimited variety of additional differential equations he may desire to use. We note that the functional dependence of $\{\dot{\delta}\}$ on state vector elements is not restricted to linear form. In fact, the additional differential equations may include sample data systems, hysteresis, deadbands and any other type nonlinearity or discontinuity that can be numerically represented.

The required kinematic and selection transformations, the equations of dynamic equilibrium, and the additional controller equations collected together are:

$$\begin{aligned}
\{\dot{U}\}_j &= [m]_j^{-1}\left(\{G^*\}_j + [b]_j^T\{\lambda\}\right), \\
\{\dot{\beta}\} &= \sum_j [B]_j \{U\}_j \\
\{\dot{\xi}\}_j &= [S]_j \{U\}_j \\
\{\dot{\delta}\} &= f(\{\beta\},\{\xi\},\{U\},\{\delta\}, t)
\end{aligned} \tag{12}$$

where the subscript j ranges from 1 through the number of cluster bodies. These first order differential equations thus represent the state equations governing a system of controlled, interconnected flexible bodies. They are clearly of the form

$$\dot{y}_k = f_k\,(y_1, y_2, \ldots y_n, t) \tag{13}$$

which is easily adaptable to numerical integration.

Numerical Linearization for Frequency Domain Studies

If an equilibrium state is known, and if it is desired to examine stability characteristics with respect to that state, then numerical perturbation techniques can be employed. Considering an autonomous system, such that $f_k = 0$; and expanding Equation (13) in a Taylor's series (in Δy_k) yields the linear, perturbation equations

$$\{\Delta\dot{y}\} = [A]\{\Delta y\} \tag{14}$$

with

$$A_{ij} = \frac{\partial f_i}{\partial y_j} \cdot \tag{15}$$

The DISCOS program system obtains the partial derivatives A_{ij} numerically (see Reference (10)). Now, as the original system states don't necessarily include observed outputs of the "plant", the program system also linearizes additional functions that relate observed outputs and control actuator torques (forces) to the original states, such that

$$\left\{\Delta w\right\} = \left[\, C \,\right] \left\{\Delta y\right\} . \tag{16}$$

The partial derivatives, C_{ij}, having been numerically defined, provide a means of eliminating as many of the original perturbated states as there are elements of $\left\{\Delta w\right\}$, and thus, a replacement similarity transformation on the linear equations (Equation (14)) can be executed. That is, it is possible to develop

$$\left\{\Delta y\right\} = \left[\, R \,\right] \left\{ z \right\} \tag{17}$$

such that

$$\left[\, R \,\right]^{-1} \left[\, R \,\right] \left\{ \dot{z} \right\} = \left[R \right]^{-1} \left[\, A \,\right] \left[\, R \,\right] \left\{ z \right\} ,$$

or

$$\left\{ \dot{z} \right\} = \left[\, A^* \,\right] \left\{ z \right\} . \tag{18}$$

The linear equations (Equations (18)) represent the exact same system as Equation (14), ($\left[A^*\right]$ is similar to $\left[A\right]$), but the new perturbated states now include observed outputs and actuator torques. The advantage of transforming the system's linear equations to the form of Equation (18) is that now a plant-controller concept is inherent. Thus, subpartitions of $\left[A^*\right]$ can be easily manipulated so as to create characteristic matrices corresponding to forward-loop, return-loop and loop-gain definitions of the dynamic system. In summary, $\left[A^*\right]$ contains all of the required numerical information to provide the general format of:

$$\left\{ \dot{x} \right\} = \left[\, a \,\right] \left\{ x \right\} + \left[\, b \,\right] \left\{ u \right\} \tag{19}$$

corresponding to any open or closed-loop block diagram of the dynamic

system. Thus, there is provision for conducting frequency domain studies that support stability analysis and control system design.

Analysis of a Multibody Spacecraft

An analytical investigation utilizing the DISCOS digital simulation code was conducted to investigate the dynamical behavior of a typical satellite configuration. The configuration chosen was a spinning vehicle possessing four doubly hinged solar array assemblies, as shown in Figure 1. The vehicle was symmetric but consisted of two types of solar array subassemblies. Upon deployment, the x-z plane assemblies deployed such that $\alpha_x \triangleq 90^o$ and $\gamma_x \triangleq 180^o$. The y-z assemblies deployed in a similar fashion; however, they also articulated such that upon deployment, $\psi_y \triangleq 90^o$.

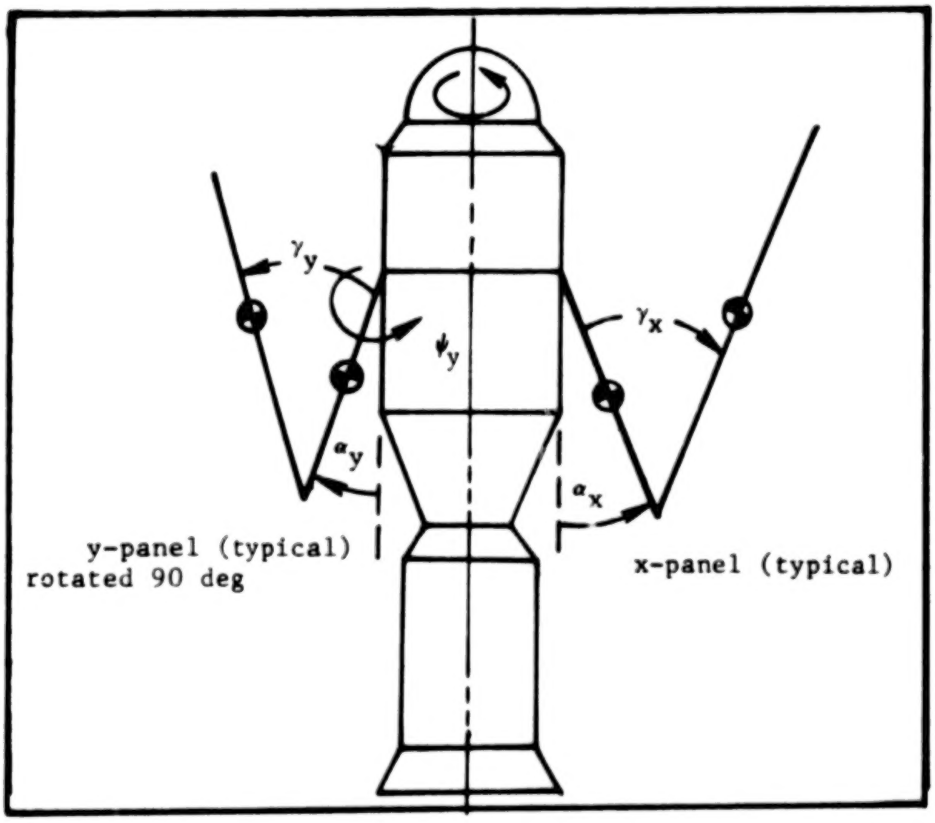

Figure 1. Spacecraft Schematic

The analytical investigation was two-fold in that a nominal configuration without the array constraint was first exercised to verify simu-

lation of the deployment mechanism. The spacecraft was despun by applying a torque directly to the main body and, as the despin occurred, the arrays were simultaneously deployed. The array deployment then resulted from both spin induced dynamics and the spring/dashpot/cable deployment mechanism characteristics. Nondimensionalized results for the nominal despin/deployment are presented in Figure 2. The figure also shows a comparison with results from the NBOD simulation of Frisch (Reference 4). The variation in x and y array deployment characteristics represents the time delay of y assembly deployment initiation due to the "yo-yo" despin cables uncovering first the x arrays and then the y arrays.

The constrained array analysis employed a flexible linkage between adjacent arrays to affect the desired non-topological tree type configuration. Flexible modal properties were also considered for the panel portion of the array assemblies. The spacecraft and the spar portion of the arrays were considered as rigid. Results for the despin/deployment dynamics of the non-topological configuration are given in Figure 3. The ψ_x for the x assembly arises because of flexibility between the opposing x assemblies. There is no ψ_x restraint between the spacecraft and the x assembly.

A test program was conducted to qualify the analytical results. Comparison of test data and analysis was generally very good, however, test results indicated more symmetry between x and y assembly positions than did analytical results. This was attributed, in part, to tolerance accumulation in the structural joints.

Discussion of Selected Applications

The system governing equations of motions, as incorporated in the DISCOS program system, have been applied to numerical analysis of a wide range of dynamic systems. The results thereof have been used as both design aids and to confirm ground test and flight data. The following text briefly describes selected efforts and is included here to provide the analyst with insight as to general applicability.

Appendage Deployment

The SCATHA (Spacecraft Charging At High Altitude) spacecraft will deploy five dual element tubular experiment booms in three sequential events. The vehicle is spin stabilized; no active control system exists.

Spacecraft/boom design was accomplished following development of the deployment time history; the deployment profile influences stability considerations and deployment rates at boom latch were used to size the boom tubes and the boom latch mechanism. Additionally, the analyses were used to show that the acceleration environment caused by the boom latch event would not be detrimental to the experiments.

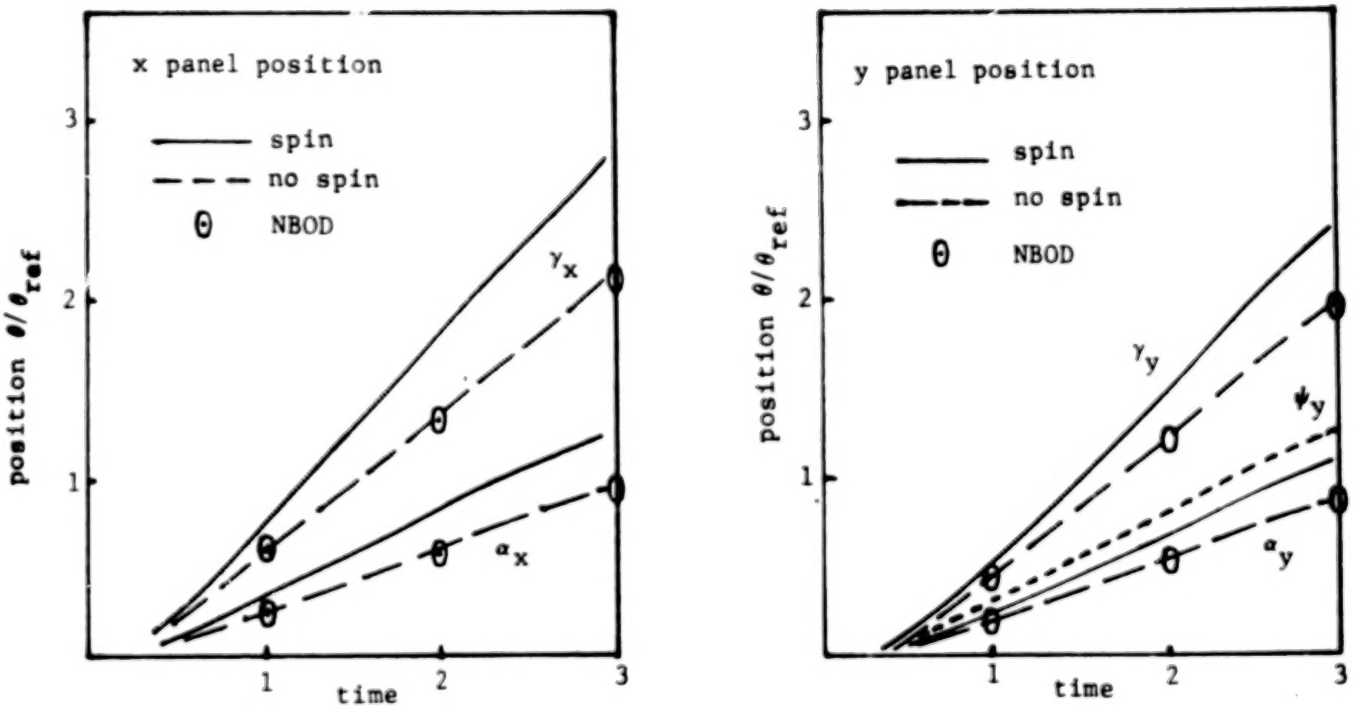

Figure 2. Nominal Deployment Time Histories

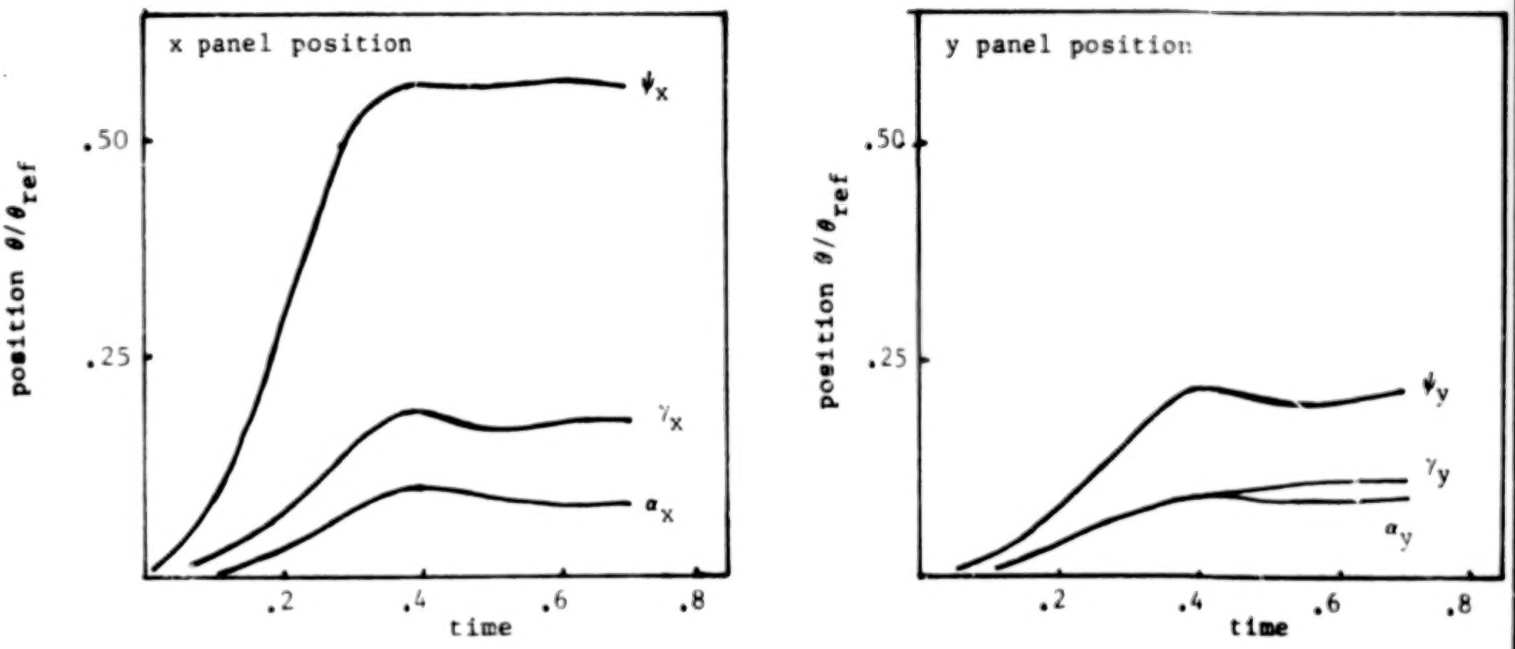

Figure 3. Constrained Deployment Time Histories

Staging

The SCATHA mission has the requirement to jettison the Apogee Insertion Motor (AIM) following its burnout. The AIM jettison system consists of a single-point spring separation device; there are no guide rails to constrain motion. The separation analysis of the two-body system is further complicated by the fact that the spacecraft is spinning with a finite coning angle, neither separating body is inertially symmetric, and the separation device (spring) may have a lateral force component. Bounds on the design coning angle at separation, allowable inertial asymmetry and separation device tolerances were established to preclude the possibility of short term recontact of the AIM. Additionally, an envelope of the separation relative velocities was developed for use in long term recontact studies.

Orbital Docking

The orbital docking maneuver of the proposed Space Tug was investigated in order to establish the effects of large amplitude fluid motion which might occur during the impact event. A variable length pendulum analog was implemented to account for fluid mass motions and the time histories of gross vehicle motions and interaction forces were established to serve as an aid to impact attenuation mechanism design.

Digital Control Law

The Block 5-D spacecraft served as the prototype for the TIROS-N satellite and was analyzed in order to provide a valid simulation model directly applicable to investigation of the TIROS-N on orbit attitude dynamics. The configuration consisted of a central body with an articulated solar array subject to a four channel controller: (1) a three axis digital autopilot employing sample-and-hold and computational delay logic and (2) an array drive motor to compensate for spacecraft motions and provide a fixed inertial orientation for the solar array. The control law (furnished by Goddard Space Flight Center in block diagram format) was cast in first order form and interfaced with the spacecraft equations of motion. Response to initial attitude errors were determined.

Other Applications

The versatility of the DISCOS program system admits its use for a wide range of dynamic studies. The nonlinear time domain response analysis capability has been, or will be used (in addition to those items described previously) to investigate (1) space fabrication techniques envisioned for future large space structures, (2) launch vehicle performance associated with the Titan III, Stage II post-SECO event, and (3) the librational motion of a very large satellite subject to gravity gradient excitation and orbital transfer maneuvers. The frequency response analysis capability has been successfully exercised in the development of stability criteria for the Titan III, Stage I POGO event.

Concluding Remarks

A cursory description of nonlinear differential equations of state that govern dynamic behavior of a system of interconnected flexible bodies has been given, along with discussion of an available digital computer code that synthesizes and numerically solves the equations in time and frequency domains. A few of the numerous possible applications of the program code are discussed. A comprehensive expose' of the analytical and programming considerations is not possible herein, due to space limitations and, of course, that has not been the objective of this discussion. The objective has been to highlight some of the attendant features of the formalism and program code so as to provide insight into the motivation and rationale behind them.

Lagrange multipliers have been used for every constraint of the system, not just the ones involved in the closed loops. This has resulted in increased program flexibility, in that some of the rheonomic constraint conditions can be unilateral.

In conclusion, the authors feel that the nature of the formalism and associated program code, DISCOS, is sufficiently general to cover a broad range of future applications.

References

1. Hooker, W. W. and Margulies, G., "The Dynamical Attitude Equations for an n-body Satellite", Journal of the Astronautical Sciences, Vol. XII, No. 4, (1965).

2. Roberson, R. E. and Wittenburg, J., "A Dynamical Formalism for an Arbitrary Number of Interconnected Rigid Bodies, with Reference to the Problem of Satellite Attitude Control", Proceeding of the Third International Congress of Automatic Control (London, 1966), Butterworth and Company, Ltd., London, (1967).

3. Velman, J. R., "Simulation Results for a Dual Spin Spacecraft", Proceedings of the Symposium on Attitude Stabilization and Control of Dual-Spin Spacecraft, Report No. TR-0158(3307-01)-16, Aerospace Corp., El Segundo, California, pp. 11-21, (1967).

4. Frisch, H. P., "A Vector-Dyadic Development of the Equations of Motions for N Coupled Rigid Bodies and Point Masses", Report No. NASA TN D-7767, Goddard Space Flight Center, Greenbelt, Maryland, (1975).

5. Farrell, J. L., Newton, J. K., and Connelly, J. J., "Digital Program for Dynamics of Non-rigid Gravity Gradient Satellites", NASA CR-1119, National Aeronautics and Space Administration, Washington, D.C., (1968).

6. Ness, D. J., and Farrenkopf, R. L., "Inductive Methods for Generating the Dynamic Equations of Motion for Multibodied Flexible Systems, Part 1 Unified Approach", Presented at the Winter Annual Meeting of the ASME, Washington, D.C., (1971).

7. Likens, P. W., "Dynamic Analysis of a System of Hinge-Connected Rigid Bodies with Nonrigid Appendages", International Journal of Solids and Structures, 9, pp. 1473-1487, (1973).

8. Ho, J. Y. L., "Direct Path Method for Flexible Multibody Spacecraft Dynamics", Journal of Spacecraft, 14, pp. 102-110, (1977).

9. Williams, C. J. H., "Dynamics Modeling and Formulation Techniques for Non-Rigid Spacecraft", Symposium on the Dynamics and Control Non-Rigid Spacecraft, Frascali, Italy, pp. 55-70, (1976).

10. Bodley, C. S., Devers, A. D. and Park, A. C., "Computer Program System for Dynamic Simulation and Stability Analysis of Passive and Actively Controlled Spacecraft", MCR-75-17, Martin Marietta Corporation, Denver, Colorado, April, (1975).

11. Bodley, C. S. and Park, A. C., "The Influence of Structural Flexibility on the Dynamic Response of Spinning Spacecraft", AIAA Paper 72-348, San Antonio, Texas, 1972.

REFERENCE PAPER II

INFLUENCE OF STRUCTURAL FLEXIBILITY ON THE DYNAMIC RESPONSE OF SPINNING SPACECRAFT

(from AIAA PAPER 72-348, San Antonio, Texas, 1972)

THE INFLUENCE OF STRUCTURAL FLEXIBILITY ON THE DYNAMIC RESPONSE OF SPINNING SPACECRAFT

C. S. Bodley[1] and A. C. Park[2]
Martin Marietta Corporation
Denver, Colorado

Abstract

A unique approach to dynamic response analysis of highly flexible, rotating spacecraft is presented. Formulation of applicable equations of motion includes dynamic coupling between elastic deformations and spacecraft rotation rates. Coupling is shown to be a closed-loop effect, in which elastic deflections significantly influence vehicle angular rates, and conversely, elastic response is strongly influenced by (if not entirely caused by) vehicle spin rates. Angular motion is shown to be most strongly influenced by changes in inertial characteristics caused by elastic deformation, and this deformation is in turn influenced by centrifugal and Coriolis forces. Equations of motion are nonlinear, first-order differential equations of first degree. State variables include projections of translational and rotational momentum vectors onto the rotating vehicle frame and the generalized momenta and deflections corresponding to a set of normal vibration modes. Additional state variables include inertial position coordinates and quaternion (Euler 4-parameter) elements to characterize vehicle attitude. Numerical results for a typical spacecraft are presented, and the influence of flexibility is evaluated.

Introduction

A variety of mathematical formulations and computational procedures related to dynamic behavior of spinning flexible satellites has appeared in recent literature. Most investigators have been concerned with rotational stability of nearly rigid vehicles undergoing small elastic deformation. In addition to intrinsic dynamical features of a freely rotating flexible vehicle, other authors have considered the effects of external disturbances such as gravity gradient and attitude control.

Approaches to derivation of governing differential equations of motion are diverse. Likins[1] has classified analytical procedures in three categories: (1) discrete coordinate methods, (2) hybrid coordinate methods, and (3) vehicle normal coordinate methods, and has found each to have an area of applicability. With his hybrid coordinate method, Likins separates a vehicle into a number of idealized structural subsystems, each of which is classified either as a flexible appendage or as a rigid body or particle. Applications are presented[2,3] to demonstrate the method's utility in design of an attitude control system, and in analyzing a dual-spin spacecraft with solar panels and a damped linear oscillator that simulates a nutation damper.

[1]Senior Staff Engineer, Dynamics and Loads

[2]Staff Engineer, Dynamics and Loads

The Eulerian N-body dynamic formulation of Hooker-Margulies[4] and Roberson-Wittenburg[5] has been programmed for general use by Farrell, Newton, and Connelly.[6] With this method, the vehicle is considered as a set of N interconnected rigid bodies. In a recently published two-part paper, Ness and Farrenkopf[7] and Ho and Gluck[8] extend the N-body concept with two methods. The first, called the unified approach, features an automated synthesis of the governing differential equations of motion of a multibodied flexible spacecraft system. With this method, terminal bodies of the topological tree configuration (no closed loop) may be flexible, but interior bodies must be rigid. The second method, called the perturbation approach, is more general in that any body is allowed to deform, but spacecraft motion due to flexibility is treated as a small perturbation of nominal motion, resulting in piecewise linear differential equations.

Keat[9] describes a method analogous to the N-body approach that is applicable when satellite nonrigidity is characterized by generalized coordinates Other approaches to derive governing differential equations include a formal application of Lagrange's equation by Newton and Farrell.[10] Meirovitch[11] uses Hamilton's principle, where body motion is described by a "hybrid" system of equations (not to be confused with the hybrid coordinates of Likins) consisting of both ordinary and partial differential equations.

This paper presents a new derivation of applicable differential equations of motion. The approach considers a more fundamental basis, namely the use of D'Alembert's principle. This approach is somewhat similar to a method reported by Likins[12] in one of his earlier papers. However, the procedure presented here results in a system of first-order ordinary differential equations, akin to Hamilton's canonical equations. It also does not require use of normal modes of deformation for either the spacecraft as a whole or for appendages as separate structural components, but may use normal modes to facilitate numerical solutions.

The method has the following advantages: (1) the final format of governing differential equations is similar to classical Newton-Euler rigid-body equations, (2) derivation of equations is uncomplicated, (3) vehicle strain energy, kinetic energy, and total angular momentum can be easily monitored, (4) equations are particularly amenable to programming for digital simulation.

We have limited the scope of this study to exclude effects of external environment, being content to examine the behavior of a freely spinning flexible satellite in the time domain. Extension of the analysis to consider attitude control, gravitational forces, and other disturbances presents no great difficulty.

Development of the Analysis

Governing nonlinear differential equations of motion for spinning flexible spacecraft result from direct application of D'Alembert's principle. Lanczos[13] states that "all the different principles of mechanics are merely mathematically different formulations of D'Alembert's principle." He implies that D'Alembert's principle is a truly fundamental principle, particularly useful when using "kinematical variables" to characterize the motion.

In studies of rigid-body dynamics, it is considerably more convenient to use angular velocity components that are projections of the spin vector onto the moving axes. We believe it is more convenient to use kinematical variables when considering the dynamics of a flexible spinning spacecraft.

Geometry and Kinematics

Consider the geometry of a deformable spinning spacecraft, as shown in Figure 1.

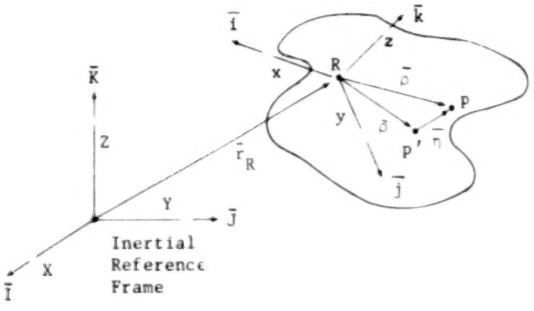

Figure 1 Geometry of Deformable Spinning Spacecraft

We use two rectangular Cartesian frames of reference; an inertially fixed (Newtonian) axis system (X,Y,Z) and a moving frame (x,y,z). We should emphasize that reference point R does not necessarily coincide with the mass center of the deformable body, nor is it necessarily fixed to some material point of the body, although it could be either. We represent body deformation as a single-valued displacement field $\bar{\eta}$ to be measured in the moving reference frame. In the figure, material point p is shown in a deformed configuration specified by the instantaneous position vector $\bar{\rho}$. The corresponding point p′ is in the undeformed configuration and is specified by the position vector $\bar{\rho}$ fixed to the moving reference frame. These geometric notions are in line with traditional treatment of a system of particles,[14,15] although our development considers a continuous structure.

In view of these geometric considerations, we may now specify an absolute velocity field, $\bar{v}$, associated with the deformable body, and by kinematic principles, express velocity of the typical point p as

$$\bar{v} = \bar{v}_R + \bar{\omega} \times \bar{\rho} + (\dot{\bar{\rho}})_r$$

where $\bar{v}_R$ denotes the absolute velocity of reference point R, $\bar{\omega}$ represents angular velocity of the moving reference frame, and $(\cdot)_r$ represents the time derivative of the enclosed quantity, as seen by an observer rotating with the moving reference frame. In particular, in Eq 1 the term $(\dot{\bar{\rho}})_r$ can be written as

$$(\dot{\bar{\rho}})_r = (\dot{\bar{\eta}})_r = \bar{i}\,\dot{\eta}_x + \bar{j}\,\dot{\eta}_y + \bar{k}\,\dot{\eta}_z \quad . \tag{2}$$

The displacement field, $\bar{\eta}$, can be further developed as a linear combination of a finite number of single-valued displacement functions (of x, y, and z), so that we can write

$$\bar{\eta}\,(x,y,z,t) = \sum_k \bar{\phi}_k\,(x,y,z)\;\xi_k(t) \tag{3}$$

and it follows that

$$(\dot{\bar{\eta}})_r = \sum_k \bar{\phi}_k\,(x,y,z)\;\dot{\xi}_k(t) \quad . \tag{4}$$

We can also express the acceleration field, $\bar{a}$, associated with the deformable body as

$$\bar{a} = (\dot{\bar{v}})_r + \bar{\omega} \times \bar{v} \tag{5}$$

which will be needed in subsequent expressions of equilibrium. We have tacitly implied that components of all vector quantities (except $\bar{r}_R$, the position vector to reference point R of Fig. 1) are projections onto the rotating reference frame ($\bar{i}$, $\bar{j}$, $\bar{k}$), thus we can write

$$\left.\begin{aligned}
\bar{v}_R &= \bar{i}u + \bar{j}v + \bar{k}w \\
\bar{\omega} &= \bar{i}\omega_x + \bar{j}\omega_y + \bar{k}\omega_z \\
\bar{\rho} &= \bar{i}\left(x + \sum_k \phi_{xk}\,\xi_k\right) + \bar{j}\left(y + \sum_k \phi_{yk}\,\xi_k\right) \\
&\quad + \bar{k}\left(z + \sum_k \phi_{zk}\,\xi_k\right) \quad .
\end{aligned}\right\} \tag{6}$$

With the preceding definitions and notations, we are in a position to develop applicable state equations.

Development of State Equations by Direct Application of D'Alembert's Principle

Equations of motion for any dynamical system are derived, in one way or another, from considerations of equilibrium; some authors use the term equations of equilibrium synonymously with equations of motion. A system of impressed forces is not generally in equilibrium, and motion of the system (implying accelerations and additional inertial forces) results in an overall system of forces (impressed and inertial) that is in balance.

D'Alembert's principle states that any system of impressed and inertial forces is in equilibrium, and therefore, the total virtual work of the system is zero for reversible virtual displacements that satisfy the given kinematical conditions, or

$$\delta W = \int_V \delta\bar{r} \cdot (\bar{f} - \sigma\bar{a})\, dV = 0 \quad . \tag{7}$$

D'Alembert's principle, restated as Eq 7, is the basis from which we derive applicable equations of state.

The given kinematical conditions with which the virtual displacements must be consistent are represented by the velocity expression of Eq 1. Elements of this expression are kinematical variables (sometimes referred to as nonholonomic velocities) because we stipulated that all vector quantities would be represented as projections onto the rotating axis system. These nonholonomic velocities (u, v, w, ω_x, ω_y, ω_z) are not time derivatives of actual position coordinates. Multiplying the nonholonomic velocities by differential time (dt) leaves a set of infinitesimal quantities (dr_x, dr_y, dr_z, $d\theta_x$, $d\theta_y$, $d\theta_z$) that are not differentials, but are quantities referred to as "differentials of quasi coordinates".(15,16,17) Because they are infinitesimal quantities, they correspond to a set of virtual infinitesimal displacements (δr_x, δr_y, δr_z, $\delta\theta_x$, $\delta\theta_y$, $\delta\theta_z$) and, in view of Eq 1, 6 and 7, we can write the virtual displacement field as

$$\begin{aligned}\delta\bar{r} = {} & \bar{i}\left(\delta r_x + \delta\theta_y \rho_z - \delta\theta_z \rho_y + \sum_k \phi_{xk}\, \delta\xi_k\right) \\ & + \bar{j}\left(\delta r_y + \delta\theta_z \rho_x - \delta\theta_x \rho_z + \sum_k \phi_{yk}\, \delta\xi_k\right) \\ & + \bar{k}\left(\delta r_z + \delta\theta_x \rho_y - \delta\theta_y \rho_x + \sum_k \phi_{zk}\, \delta\xi_k\right) \quad .\end{aligned} \tag{8}$$

Combining Eq 7 and 8 results in

$$\int_V \left|(\dot{\bar{v}})_r + \bar{\omega} \times \bar{v}\right| \sigma dV = \int_V \bar{f}\, dV \tag{9}$$

$$\int_V \bar{\rho} \times \left|(\dot{\bar{v}})_r + \bar{\omega} \times \bar{v}\right| \sigma dV = \int_V \bar{\rho} \times \bar{f}\, dV \tag{10}$$

$$\int_V \bar{\phi}_k \cdot \left|(\dot{\bar{v}})_r + \bar{\omega} \times \bar{v}\right| \sigma dV = \int_V \bar{\phi}_k \cdot \bar{f}\, dV \tag{11}$$

because virtual displacements δr_x, δr_y, $\cdots$, $\delta\xi_k$ are arbitrary and independent quantities. These results are familiar expressions of equilibrium if we recall some results from studies of dynamics of a system of particles.

Let us now define the following momenta

$$\bar{p}_v = \int_V \bar{v}\, \sigma dV \tag{12}$$

$$\bar{p}_\omega = \int_V \bar{\rho} \times \bar{v}\, \sigma dV \tag{13}$$

$$p_{\dot{\xi}_k} = \int_V \bar{\phi}_k \cdot \bar{v}\, \sigma dV \quad . \tag{14}$$

If we differentiate left and right members of Eq 12 through 14 and compare the results with Eq 9 through 11, we arrive at the following state equations

$$\left.\begin{aligned}\left(\dot{\bar{p}}_\omega\right)_r &= \int_V \bar{\rho} \times \bar{f}\, dV - \bar{\omega} \times \bar{p}_\omega - \bar{v}_R \times \bar{p}_v \\ \left(\dot{\bar{p}}_v\right)_r &= \int_V \bar{f}\, dV - \bar{\omega} \times \bar{p}_v \\ \dot{p}_{\dot{\xi}_k} &= \int_V \bar{\phi}_k \cdot \bar{f}\, dV + \bar{\omega} \cdot \int_V \left(\bar{\phi}_k \times \bar{v}\right) \sigma dV\end{aligned}\right\} \tag{15}$$

We see immediately that, if ξ_k are suppressed, the first two of Eq 15 represent the rigid-body equations of motion. The third of Eq 15 is, neglecting the second term on the right, a familiar equation of motion for the kth normal coordinate if we consider $\int_V \bar{\phi}_k \cdot \bar{f}\, dV$ to include effects of structural damping and restoring forces and if we define ξ_k to be a normal coordinate.

Referring to Eq 12 through 15, and using the momentum components defined by Eq 16, viz.,

$$\begin{aligned}\bar{p}_\omega &= \bar{i}y_1 + \bar{j}y_2 + \bar{k}y_3 \\ \bar{p}_v &= \bar{i}y_4 + \bar{j}y_5 + \bar{k}y_6 \\ p_{\dot{\xi}_k} &= y_{k+6}\end{aligned} \tag{16}$$

allows us to write the state equations as

$$\begin{aligned}\dot{y}_1 &= G_1 - (\omega_y y_3 - \omega_z y_2) - (vy_6 - wy_5) \\ \dot{y}_2 &= G_2 - (\omega_z y_1 - \omega_x y_3) - (wy_4 - uy_6) \\ \dot{y}_3 &= G_3 - (\omega_x y_2 - \omega_y y_1) - (uy_5 - vy_4) \\ \dot{y}_4 &= G_4 - (\omega_y y_6 - \omega_z y_5) \\ \dot{y}_5 &= G_5 - (\omega_z y_4 - \omega_x y_6) \\ \dot{y}_6 &= G_6 - (\omega_x y_5 - \omega_y y_4) \\ \dot{y}_{k+6} &= G_{k+6} \quad .\end{aligned} \tag{17}$$

It can now be seen that the (6+n) state equation given by Eq 17 are expressed as functions of

the state variables themselves and other undetermined quantities. It is therefore necessary to develop a means to establish these quantities in terms of known state variables.

If we substitute Eq 1 in Eq 12 through 14, respectively, there results

$$\bar{p}_v = \int_V \left(\bar{v}_R + \bar{\omega} \times \bar{\rho} + \sum_k \bar{\phi}_k \dot{\xi}_k \right) \sigma dV \tag{18}$$

$$\bar{p}_\omega = \int_V \left| \bar{\rho} \times \bar{v}_R + \bar{\rho} \times (\bar{\omega} \times \bar{\rho}) + \sum_k (\bar{\rho} \times \bar{\phi}_k) \dot{\xi}_k \right| \sigma dV \tag{19}$$

$$p_{\dot{\xi}_k} = \int_V \left| \bar{\phi}_k \cdot \bar{v}_R + \bar{\omega} \cdot (\bar{\rho} \times \bar{\phi}_k) + \sum_j \bar{\phi}_k \cdot \bar{\phi}_j \dot{\xi}_j \right| \sigma dV \quad . \tag{20}$$

Integrating the first of these (over the volume V) term-by-term allows us to write

$$\bar{p}_v = m \bar{v}_R + \bar{\omega} \times \int_V \bar{\rho} \, \sigma dV + \sum_k \left(\int_V \bar{\phi}_k \, \sigma dV \right) \dot{\xi}_k$$

$$= m \bar{v}_R + \bar{\omega} \times \bar{S} + \sum_k \bar{a}_k \dot{\xi}_k \tag{21}$$

where m is the total system mass, $\bar{S}$ is the "static" moment vector.

In a similar manner, the other equations yield

$$\bar{p}_\omega = \bar{S} \times \bar{v}_R + \bar{h} + \sum_k \bar{d}_k \dot{\xi}_k \tag{22}$$

$$p_{\dot{\xi}_k} = \bar{a}_k \cdot \bar{v}_R + \bar{d}_k \cdot \bar{\omega} + \sum_j e_{kj} \dot{\xi}_j \tag{23}$$

where $\bar{h}$ is a momentum vector referred to the moving coordinate system and is defined as

$$\bar{h} = \lfloor \bar{i} \; \bar{j} \; \bar{k} \rfloor \, [J] \, \{\omega\} \tag{24}$$

and $\bar{d}_k$ and e_{kj} are undetermined coefficients. Comparison of Eq 21 through 23 with Eq 16 yields the matrix relationship between the state variables $(y_1, y_2, \cdots, y_{6+k})$ and the kinematic variables $(\omega_x, \omega_y, \cdots, \dot{\xi}_{6+k})$ as

$$\begin{bmatrix} y_1 \\ y_2 \\ y_3 \\ y_4 \\ y_5 \\ y_6 \\ y_7 \\ \vdots \\ y_{6+n} \end{bmatrix} = \left[\begin{array}{ccc|ccc|ccc} J_{xx} & -J_{xy} & -J_{xz} & & -S_z & S_y & d_{x1} & \cdots & d_{xn} \\ & J_{yy} & -J_{yz} & S_z & & -S_x & d_{y1} & \cdots & d_{yn} \\ & & J_{zz} & -S_y & S_x & & d_{z1} & \cdots & d_{zn} \\ \hline & & & m & & & a_{x1} & \cdots & a_{xn} \\ & & & & m & & a_{y1} & \cdots & a_{yn} \\ & & & & & m & a_{z1} & \cdots & a_{zn} \\ \hline & & & & & & e_{11} & \cdots & e_{1n} \\ & & \text{(Symmetric)} & & & & & e_{22} \; \cdots & \vdots \\ & & & & & & & & e_{nn} \end{array}\right] \begin{bmatrix} \omega_x \\ \omega_y \\ \omega_z \\ u \\ v \\ w \\ \dot{\xi}_1 \\ \vdots \\ \dot{\xi}_n \end{bmatrix} \tag{25}$$

where the coefficients in the above array are defined to be

$$J_{\alpha\alpha} = (J_{\alpha\alpha})_o + 2 \sum_j^n \left(b_{\beta\beta j} + b_{\gamma\gamma j} \right) \xi_j + \sum_j^n \sum_k^n \left(c_{\beta j \beta k} + c_{\gamma j \gamma k} \right) \xi_j \, \xi_k \tag{26}$$

when $\begin{cases} \alpha = x & \beta = y & \gamma = z \\ \alpha = y & \beta = z & \gamma = x \\ \alpha = z & \beta = x & \gamma = y \end{cases}$;

$$J_{\alpha\beta} = (J_{\alpha\beta})_o + \sum_j^n \left(b_{\alpha\beta j} + b_{\beta\alpha j} \right) \xi_j + \sum_j^n \sum_k^n c_{\alpha j \beta k} \, \xi_j \, \xi_k \tag{27}$$

where $\alpha, \beta = x, y, z$ and $\alpha \neq \beta$;

$$S_\alpha = (S_\alpha)_o + \sum_j^n a_{\alpha j} \, \xi_j \tag{28}$$

where $\alpha = x, y, z$;

$$d_{\alpha k} = b_{\beta\gamma k} - b_{\gamma\beta k} + \sum_{j}^{n} \left(c_{\beta j \gamma k} - c_{\gamma j \beta k} \right) \xi_j \qquad (29)$$

$$\text{when} \begin{cases} \alpha = x & \beta = y & \gamma = z \\ \alpha = y & \beta = z & \gamma = x \\ \alpha = z & \beta = x & \gamma = y \end{cases} ;$$

$$e_{jk} = c_{xjxk} + c_{yjyk} + c_{zjzk} \qquad (30)$$

where $j,k = 1, 2, \cdots, n$;

and

$$m = \int_V \sigma dV \quad . \qquad (31)$$

In the definitions above, we have used

$$(J_{\alpha\alpha})_o = \int_V (\beta^2 + \gamma^2)\, \sigma dV \qquad (32)$$

$$\text{when} \begin{cases} \alpha = x & \beta = y & \gamma = z \\ \alpha = y & \beta = z & \gamma = x \\ \alpha = z & \beta = x & \gamma = y \end{cases} ;$$

$$(J_{\alpha\beta})_o = \int_V \alpha\beta\sigma dV \qquad (33)$$

where $\alpha,\beta = x,y,z$ and $\alpha \neq \beta$;

$$(S_\alpha)_o = \int_V \alpha\sigma dV \qquad (34)$$

where $\alpha = x,y,z$;

$$\left.\begin{aligned} a_{\alpha k} &= \int_V \phi_{\alpha k}\, \sigma dV \\ b_{\alpha\beta k} &= \int_V \alpha \phi_{\beta k}\, \sigma dV \\ c_{\alpha k \beta j} &= \int_V \phi_{\alpha k}\, \phi_{\beta j}\, \sigma dV \end{aligned}\right\} \qquad (35)$$

where $\alpha,\beta = x,y,z$; $j,k = 1,2,\cdots, n$.

Solution for unknown velocities on the right-hand side of Eq 25 in terms of state variables is now straightforward.

The first six forces (torques) in the state equations are components of the resultant impressed force (torque), namely

$$\left.\begin{aligned} G_i &= \int_V (\bar{\rho} \times \bar{f})\, dV \\ G_{i+3} &= \int_V \bar{f}\, dV \end{aligned}\right\} i = 1,2,3 \quad . \qquad (36)$$

Remaining n forces acting in deformation coordinates, ξ, are defined to be

$$G_{k+6} = g_{k+6} + h_{k+6} \qquad k = 1,2,\cdots, n \qquad (37)$$

where

$$g_{k+6} = \int_V \bar{\phi}_k \cdot \bar{f}\, dV \qquad (38)$$

and

$$\begin{aligned} h_{k+6} = {} & \omega_x^2 \left| b_{yyk} + b_{zzk} + \sum_{j}^{n} (c_{ykyj} + c_{zkzj})\, \xi_j \right| \\ & + \omega_y^2 \left| b_{zzk} + b_{xxk} + \sum_{j}^{n} (c_{zkzj} + c_{xkxj})\, \xi_j \right| \\ & + \omega_z^2 \left| b_{xxk} + b_{yyk} + \sum_{j}^{n} (c_{xkxj} + c_{ykyj})\, \xi_j \right| \\ & - \omega_x\omega_y \left| b_{xyk} + b_{yxk} + \sum_{j}^{n} (c_{xkyj} + c_{ykxj})\, \xi_j \right| \\ & - \omega_x\omega_z \left| b_{xzk} + b_{zxk} + \sum_{j}^{n} (c_{xkzj} + c_{zkxj})\, \xi_j \right| \\ & - \omega_y\omega_z \left| b_{yzk} + b_{zyk} + \sum_{j}^{n} (c_{ykzj} + c_{zkyj})\, \xi_j \right| \\ & + \omega_x \left[wa_{yk} - va_{zk} \right] + \omega_y \left[ua_{zk} - wa_{xk} \right] \\ & \quad + \omega_z \left[va_{xk} - ua_{yk} \right] \\ & + \omega_x \sum_{j}^{n} (c_{ykzj} - c_{zkyj})\, \dot{\xi}_j \\ & + \omega_y \sum_{j}^{n} (c_{zkxj} - c_{xkzj})\, \dot{\xi}_j \\ & + \omega_z \sum_{j}^{n} (c_{xkyj} - c_{ykxj})\, \dot{\xi}_j \quad . \end{aligned} \qquad (39)$$

All previously defined coefficients depend on the ξ_k variables, and therefore, the state equations must be augmented to establish values for the respective ξ_k. This can be done by integrating the $\dot{\xi}_k$, which are obtained from solution of the simultaneous equations given by Eq 25. The final form of the (2n+6) state equations is

$$\dot{y}_j = f_j\, (y_1, y_2, \cdots, y_{2n+6}, t) \quad . \qquad (40)$$

This presentation of the state equations is complete in that all variables required to characterize vehicle elastic response have been included. However, it is often necessary, or at least desirable, to monitor the vehicle's position and attitude with respect to the inertially fixed reference frame. This can be done by addition of supplementary state variables. The position of reference point R can be monitored through definition of the three projections of the vector $\bar{r}_R$ onto the inertial axes. These can be obtained by integrating components of $\bar{v}_R$ along the inertial axes. The inertial attitude of the moving reference frame can be monitored by using quaternion (Euler 4-parameter) elements. We have found this to be more practical than use of Euler angles because the potential of "gimble lock" associated with large excursions is eliminated.

Application

Equations of motion previously described were programmed for solution on a digital computer. The program was then used to analyze the dynamic response of a representative elastic spacecraft, the Phase A version of the proposed Planetary Explorer (Fig. 2). This investigation was intended to establish the influence of variations in flexibility on overall response.

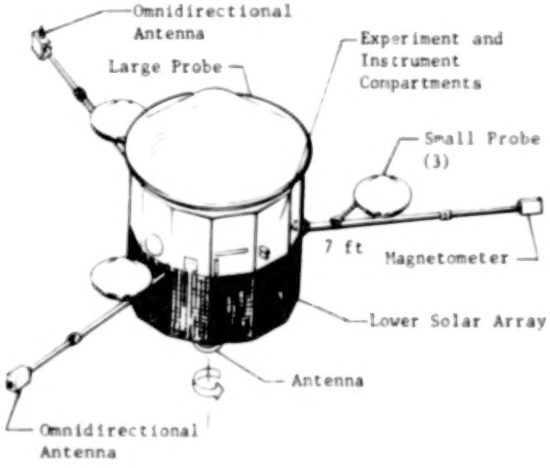

Figure 2 Planetary Explorer Venus Multi-Probe Configuration

Dynamic Model and Response Analyses

Three response simulations were performed. The first, Case 1, considered the body to be rigid, and the other two considered variations in overall structural flexibility. Case 2 assumed nominal flexibility derived from a finite-element representation of the structure, and Case 3 assumed a 25% increase in flexibility. Modal characteristics required as input to the response analyses were obtained from the 60-degree-of-freedom model shown in Figure 3. The first six elastic modes are shown in Figure 4.

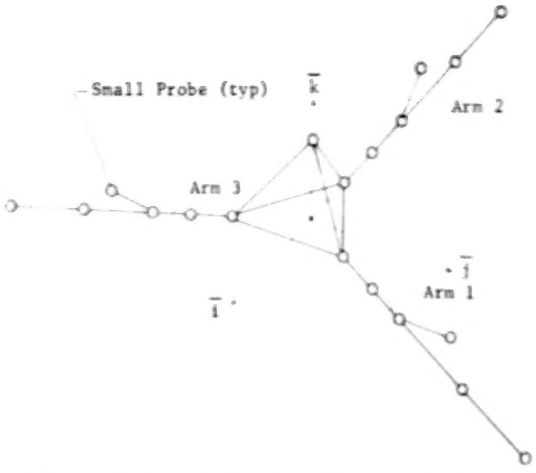

Figure 3 Dynamic Model of Planetary Explorer

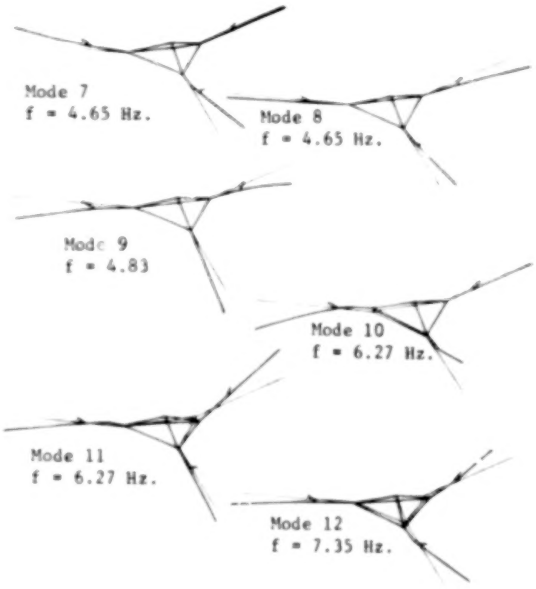

Figure 4 Elastic Modes for Planetary Explorer

The structure was assumed to be free from the influence of external forces (torques); elastic response was excited from the undeformed state through imposition of initial reference-axis angular velocity components

$$\bar{\omega} = [\bar{i}\ \bar{j}\ \bar{k}] \begin{Bmatrix} 0 \\ \pi \\ 10\pi \end{Bmatrix} \quad \text{(rad/sec)}$$

Because normal vibration modes were used, and reference point R was initially at the center of mass, vectors $\bar{a}_k$ and $\bar{S}_o$ are zero ($\bar{a}_k = 0$ from

orthogonality considerations of the unsupported vibration modes). Therefore, the mass center and reference point remain coincident throughout the simulation.

Results

The three principal inertias and projections of the spin vector onto the principal axes are shown in Figures 5a through 5c and Figures 5d through 5f, respectively. These inertias, as a function of time, are determined by extraction of characteristic values (eigenvalues) of the inertia dyadic, J, of Eq 24 and 25. Here we note with no great amazement that, for the rigid case, the principal inertias are constant, and spin vector components on the intermediate and minor principal axes are oscillatory; one trace leading the other by 90°. The frequency of these oscillations agrees with that predicted from the rigid-body expression[14]

$$\omega_n = \Omega_z \sqrt{\frac{(J_{zz} - J_{xx})(J_{zz} - J_{yy})}{J_{xx} J_{yy}}} ,$$

obtained by considering the stability of perturbations in $\underline{\omega}$.

Examination of the principal inertias for the two flexible cases again indicates an oscillatory nature, the steady-state value of the major axis inertia being somewhat increased over the initial value. This is consistent with the characteristics of the spin vector components, where we see that the steady-state projection on the major axis is decreased from the initial value. This is a direct result of conservation of angular momentum. We note further that the projections on the intermediate and minor axes indicate a null value at steady state. It can therefore be concluded that, in the presence of flexibility (and implied structural damping), the spin vector tends to align with the major principal inertia axis.

The orientation time history of the z-reference axis ($\bar{k}$ of Fig. 1) to the principal axis system is shown (Fig. 6) for the two flexible cases. These plots indicate angles determined from three direction cosines extracted from the orthogonal rotation transformation that relates reference and principal axis systems.

For nominal flexibility (Case 2), we note that the reference axis is nearly coincident with the principal axis system and that steady-state excursion will be less than 1°. Case 3 shows markedly larger excursions, for here we note that although one angle is approximately 90°, angles between the reference axis and the other two principal axes have a significant value. In fact, the steady-state excursion is seen to be about 10°. This increase in reference-axis excursion results from increased structural flexibility, although it is not possible to specify the exact relationship between flexibility and reference-axis excursion.

Figure 7 shows three characteristic motion variables for the two flexible cases. Figures 7a and 7b indicate the projection of the spin vector onto the momentum vector, which, as we prescribed no external torques, is known to be fixed in inertial space. This projection is oscillatory and approaches a steady-state value whose magnitude is somewhat less than the initial value, implying a steady spin condition. Inspection of the steady-state value and comparison with Figures 5e and 5f, where the spin vector tends toward alignment with the axis of maximum principal inertia, allows us to conclude that the major principal axis tends to coalesce with the momentum vector. This conclusion is verified through inspection of Figures 7c and 7d, where we have shown the time history of the angle between the spin and momentum vectors. Note that the angle is a measure of the nutation and that structural flexibility (damping) acts as a nutation damper; the damping increasing with increasing activity in the deformation coordinates

The angle between the z-reference axis and Z-inertial axis ($\bar{K}$ of Fig. 1) is shown in Figures 7e and 7f. These data indicate the relative excursion of the spacecraft with respect to the inertial frame.

The elastic displacements at the three satellite points (the probes in Fig. 2 and 3) are shown in Figure 8. For nominal (Case 2) flexibility, the magnitudes of the three η_z deflections are approximately equal and the η_x and η_y deflections indicate the almost symmetrical axial extension of the booms. This result is not surprising, for the imposed initial conditions resulted in a spin rate that was in close agreement with observed natural frequency of the third elastic mode, and the effect of this spin rate has been to excite an almost pure mode. No such observation is evident for the modified flexibility case because the resultant system natural frequencies are much lower in value than the imposed spin rate. Increased structural deformation with increased flexibility is, however, quite evident.

Figure 9 shows time variations of the flexible system energies, where we noted the constant rigid-body value on the kinetic-energy history. Kinetic energy (Fig. 9a & 9b) is seen to decrease and approach a steady-state value. This further validates previous assertions with respect to variations in principal inertias and angular velocity components. The steady-state value can be verified through inspection of Figure 5. Figures 9c and 9d indicate the corresponding strain energy arising from structural deformation. Once again we see the tendency toward the steady-state value that will be achieved as elastic motion is finally dissipated. Case 3 indicates the higher value of strain energy expected because of the nature of elastic deflection histories shown in Figure 8.

In conclusion, we point out that total system energy (Fig. 9e & 9f) is monotonically decreasing to a value equal to the sum of the steady-state kinetic and strain energies.

The results--that the spin vector coalesces with the axis of maximum principal inertia--are in agreement with the precept that a spinning system will, in the presence of damping, seek the lowest possible energy level consistent with a constant angular momentum.

Conclusions

We have used a direct application of D'Alembert's principle to arrive at canonical state equations and have shown that these equations have minimal coupling. The similarity of this development to classical Newton-Euler equations for a rigid body clarifies assessment of effects of deformation on the overall motion. This clarity is not so evident when the equations are derived by application of Lagrange's equations or Hamilton's principle.

Numerical examples yield results that agree with previous knowledge regarding behavior of flexible spinning vehicles. In particular, coalesence (in the steady-state configuration) of the spin vector, momentum vector, and major principal inertia axis was observed. Total system energy was shown to decay to a steady-state value consistent with a constant angular momentum. Results clearly show that initial and final principal axes can be misaligned depending on relative values of spin rate and structural vibration frequencies. The steady-state configuration is not necessarily axisymmetric, even though the undeformed configuration was.

We have purposely limited the numerical investigation by excluding effects of gravity or any other external disturbances. In so doing, we have been able to isolate mutual effects of vehicle spin and deformation; in themselves complex phenomena.

By concentrating on a freely rotating flexible vehicle we have established a practical and mathematically rational procedure for analyzing more complex dynamical systems. In particular, extension of the methodology to include gravity gradient, attitude control, or dynamics of an interconnected system of flexible vehicles (e.g., articulating appendages, multispin configurations, etc) can be accomplished in an orderly fashion. Another extension might be linearization of the equations to examine stability in the frequency domain.

In conclusion, we note that the procedure can consider a rigid main body and, therefore, might be used to support a test program in which one or more flexible structures is attached to a rigid spin platform.

Acknowledgement

The authors wish to express their appreciation to Dr. M. B. McGrath who provided the vibration characteristics used in the numerical studies.

References

1. Likins, P. W., "Dynamics and Control of Flexible Space Vehicles", Technical Report 32-1329 (Revision 1), Jet Propulsion Laboratory, Pasadena, California, January 1970.

2. Likins, P. W., and Fleischer, G. E., "Results of Flexible Spacecraft Attitude Control Studies Utilizing Hybrid Coordinates", AIAA Paper No. 70-20, Presented at the AIAA 8th Aerospace Sciences Meeting, New York, 1970.

3. Gale, A. H., and Likins, P. W., "Influence of Flexible Appendages on Dual-Spin Spacecraft Dynamics and Control", *Journal of Spacecraft and Rockets*, Vol 7, No. 9, September, 1970.

4. Hooker, W. W. and Margulies, G., "The Dynamical Attitude Equations for an n-body Satellite", *Journal of the Astronautical Sciences*, Vol XII, No. 4, 1965.

5. Roberson, R. E. and Wittenburg, J., "A Dynamical Formalism for an Arbitrary Number of Interconnected Rigid Bodies, with Reference to the Problem of Satellite Attitude Control", *Proceedings of the Third International Congress of Automatic Control* (London, 1966), Butterworth & Co., Ltd., London, 1967.

6. Farrell, J. L., Newton, J. K., and Connelly, J. J., "Digital Program for Dynamics of Nonrigid Gravity Gradient Satellites", NASA CR-1119, National Aeronautics and Space Administration, Washington, D. C., 1968.

7. Ness, D. J., and Farrenkopf, R. L., "Inductive Methods for Generating the Dynamic Equations of Motion for Multibodied Flexible Systems, Part 1, Unified Approach", Presented at the Winter Annual Meeting of the ASME, Washington, D. C., 1971.

8. Ho, J. Y. L., and Gluck, R., "Inductive Methods for Generating the Dynamic Equations of Motion for Multibodied Flexible Systems, Part 2, Perturbation Approach", Presented at the Winter Annual Meeting of the ASME, Washington, D. C., 1971.

9. Keat, J. E., "Dynamical Equations of Nonrigid Satellites", *AIAA Journal*, Vol 8, No. 7, 1970.

10. Newton, J. K., and Farrell, J. L., "Natural Frequencies of a Flexible Gravity Gradient Satellite", *Journal of Spacecraft and Rockets*, Vol 5, No. 5, 1968.

11. Meirovitch, L., "Stability of a Spinning Body Containing Elastic Parts via Liapunov's Direct Method", *AIAA Journal*, Vol 8, No. 7, 1970.

12. Likins, P. W., "Modal Method for Analysis of Free Rotations of Spacecraft", *AIAA Journal*, Vol 5, No. 7, 1967.

13. Lanczos, C., *The Variational Principles of Mechanics* (3rd edition), University of Toronto Press, 1966.

14. Greenwood, D. T., *Principles of Dynamics*, Prentice Hall, Inc., 1965.

15. Meirovitch, L., *Methods of Analytical Dynamics*, McGraw-Hill, Inc., 1970.

16. Whittaker, E. T., *Analytical Dynamics*, Cambridge University Press, London, 1917.

17. Kane, T. R., and Wang, C. G., "On the Derivation of Equations of Motion", *Journal of the Society of Industrial and Applied Mathematics*, Vol 13, No. 2, 1965.

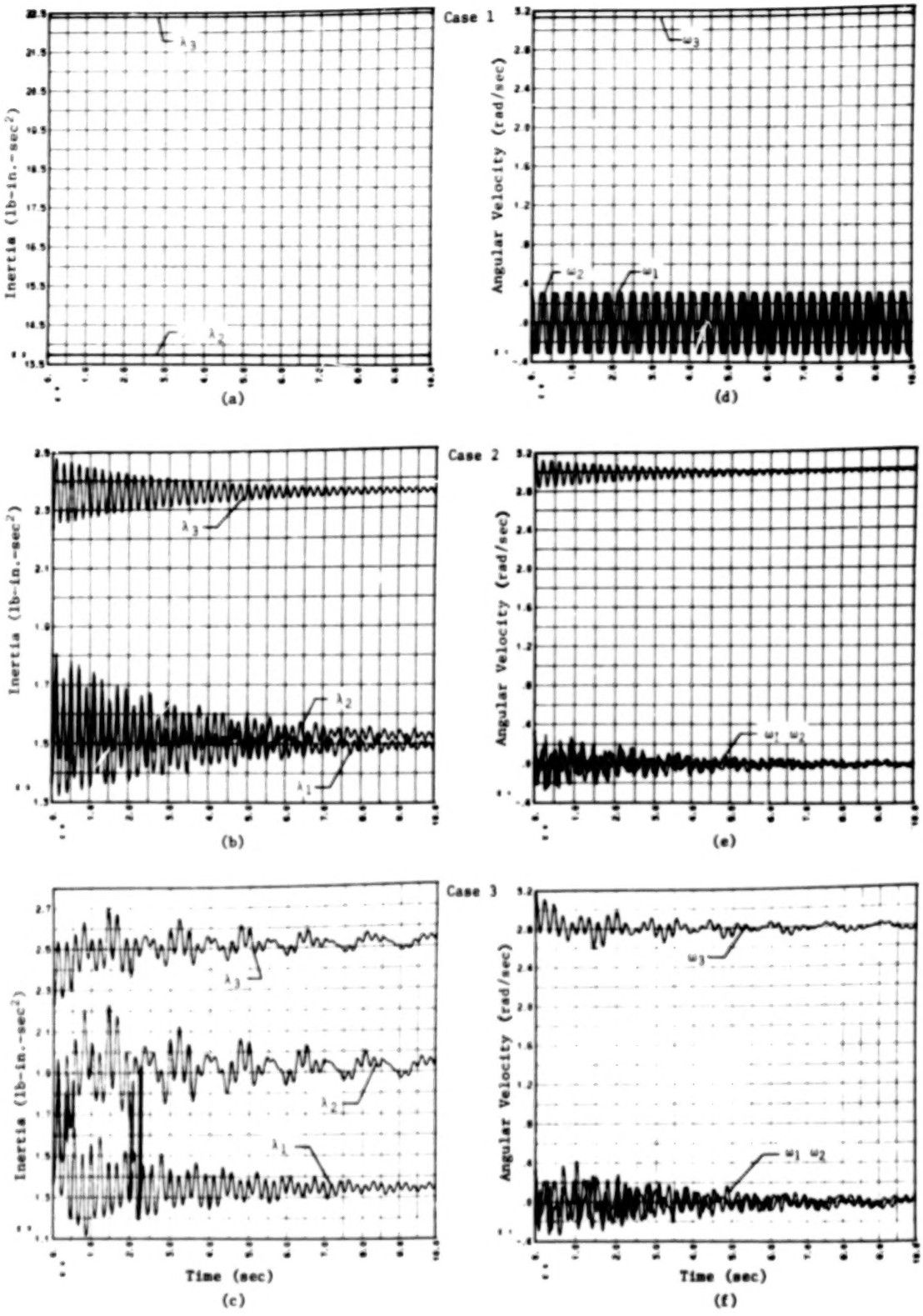

Figure 5, Principal Inertias and Principal Axes Angular Velocity Components

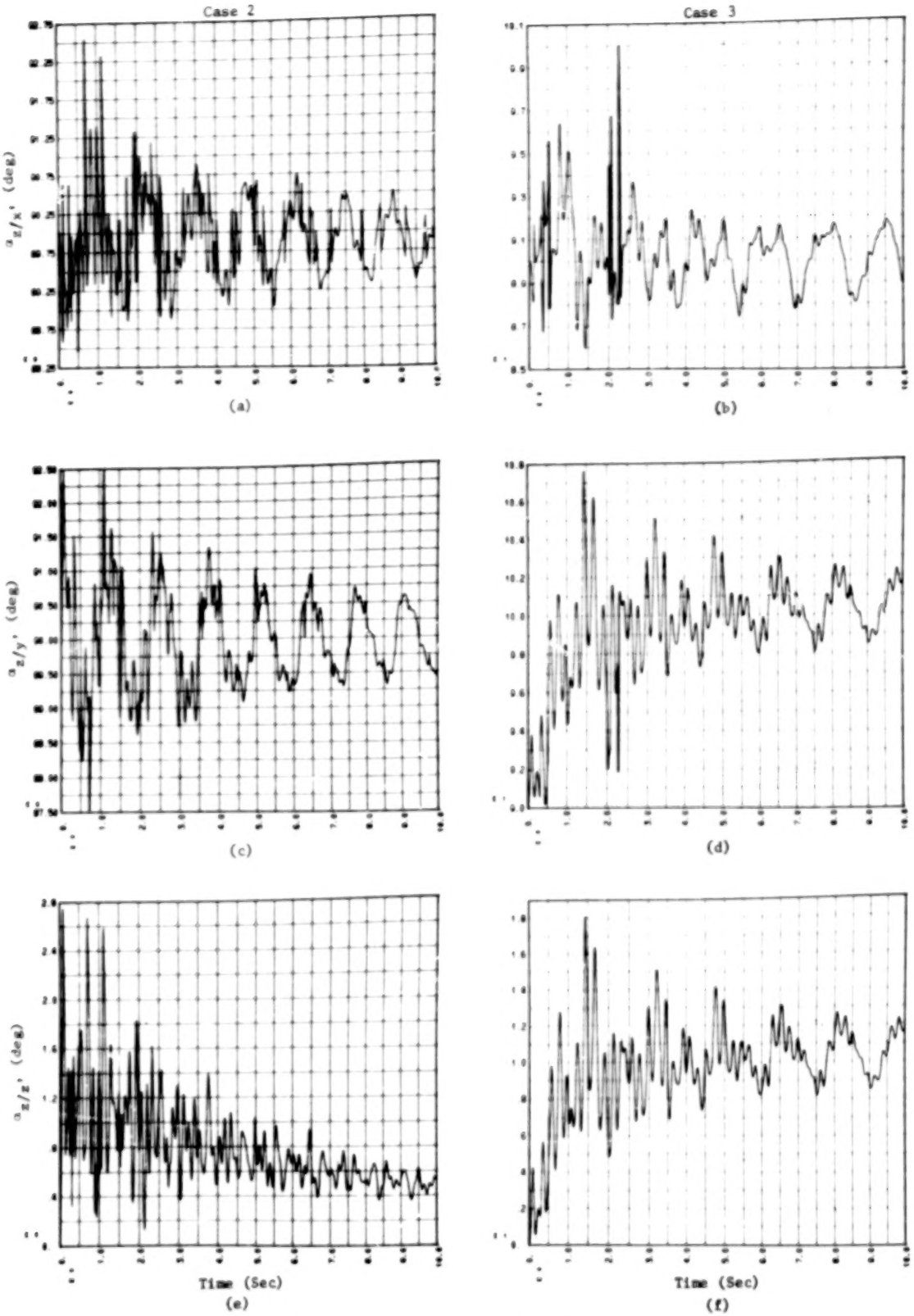

Figure 6. Orientation of Z-Reference Axis to Principal Axes

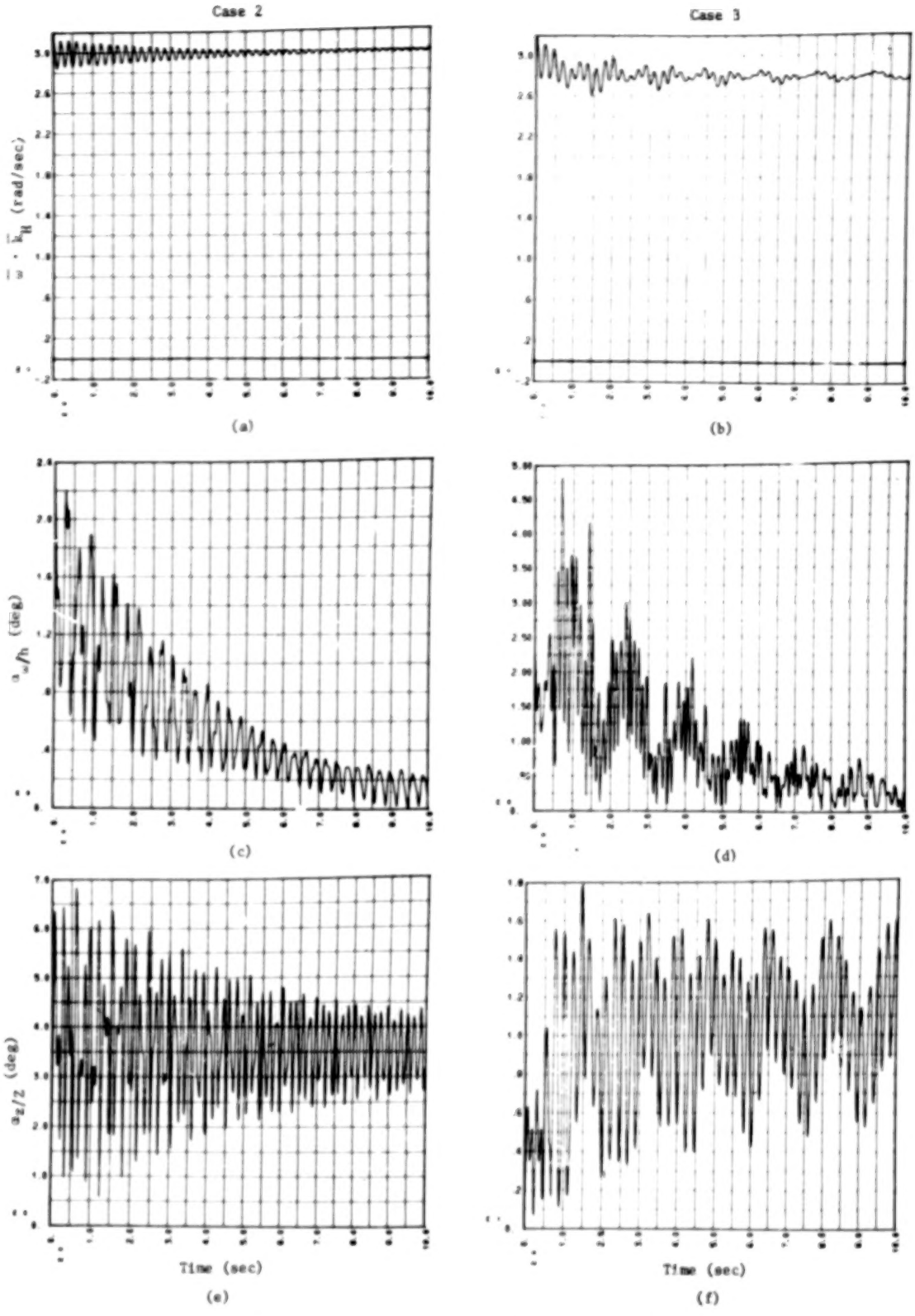

Figure 7. Characteristic Scalar Motion Variables

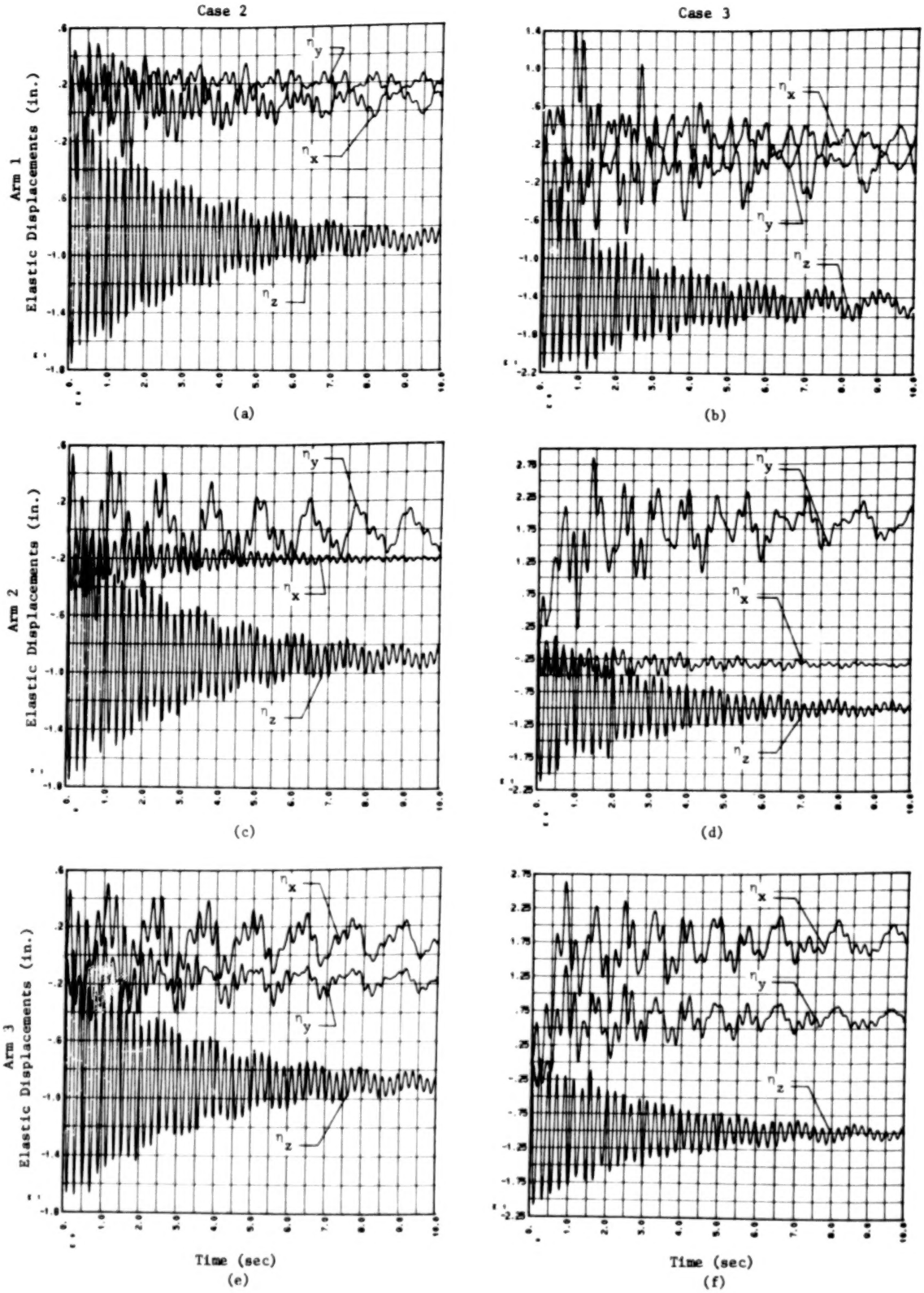

Figure 8. Elastic Displacements at Satellites

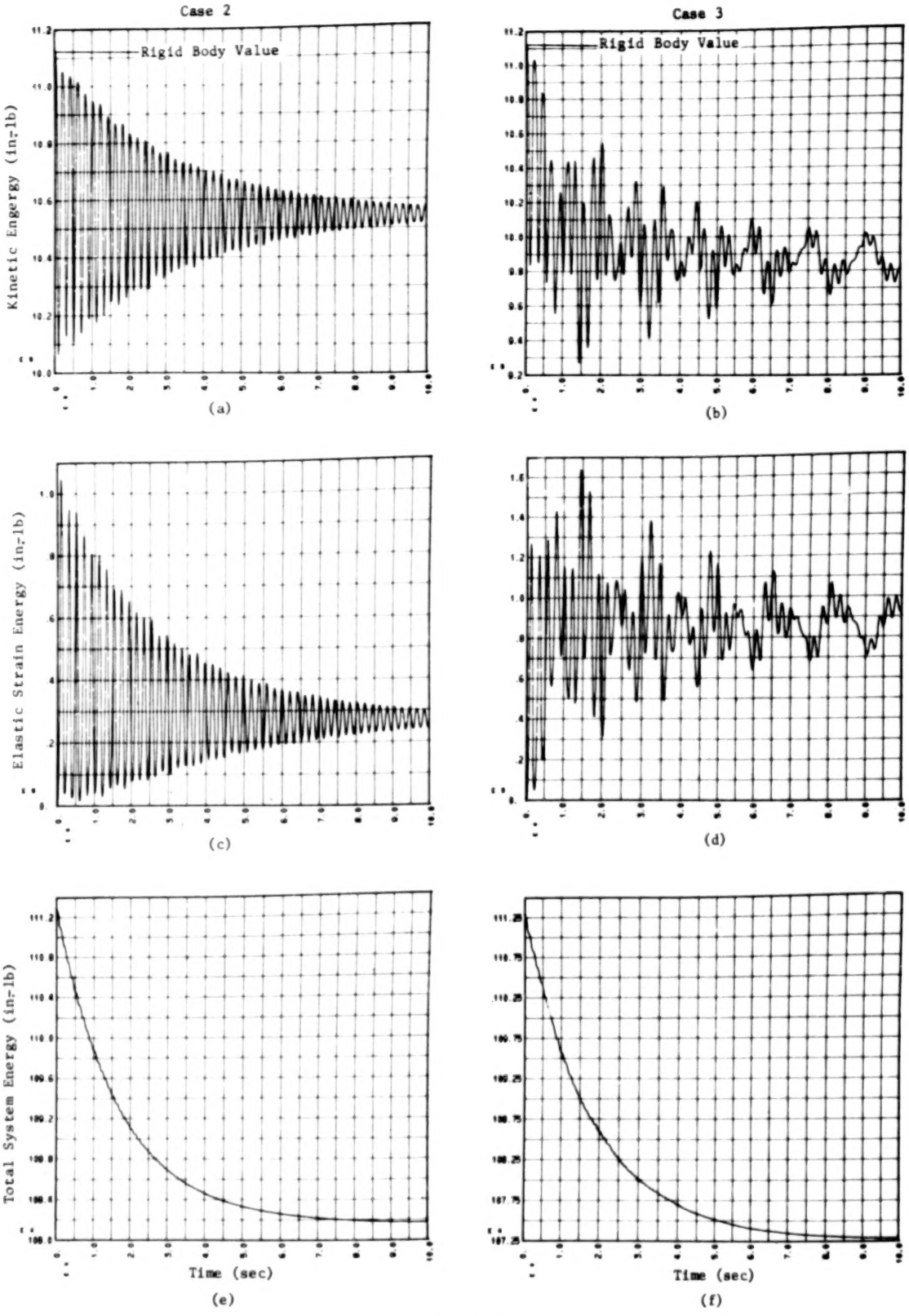

Figure 9. System Energies

APPENDIX A

DEVELOPMENT OF THE INERTIAL INTEGRALS

APPENDIX A

DEVELOPMENT OF THE INERTIAL INTEGRALS

In developing the equations of motion (paragraphs II.B and II.D of the main text), certain inertial integrals are identified that are required to account for the deformation-dependent inertia matrix and that are involved in calculating the effects of centrifugal and Coriolis forces.

The basis for calculating these integrals is a triple-matrix product that involves a so-called discrete mass matrix, [M], which is assembled by finite element techniques and which may be used in calculating vibration modes. The other constituent of the triple-matrix product is a modal transformation that transforms ordinary velocities associated with the finite-element model to the velocities of the $\{U\}_j$ vector.

Referring to the transformation as $[\phi]$, the triple-matrix product is therefore

$$[m] = [\phi]^T [M] [\phi] \qquad \text{(A-1)}$$

which is the basis of the kinetic-energy expression of equation II-21 of the main text. Now, the mass matrix, [M], is invariable with respect to the body's deformation. However, the modal transformation, $[\phi]$, depends on the $\{\xi\}$ in a linear fashion, or $[\phi]$ may be expanded as

$$[\phi] = [\phi]_o + [\Delta\phi] \qquad \text{(A-2)}$$

where $[\phi]_o$ is a matrix of constant elements, and $[\Delta\phi]$ is variable with respect to deformation.

On substituting equation A-2 into equation A-1 and referring to equation II-86 of the main text, it follows that

$$[m_o] = [\phi_o]^T [M] [\phi_o] \qquad \text{(A-3)}$$

$$[m_1]_j \xi_j = [\Delta\phi]^T [M] [\phi_o] + [\phi_o]^T [M] [\Delta\phi] \qquad \text{(A-4)}$$

and

$$[m_2]_{jk}\,\xi_j\,\xi_k = [\Delta\phi]^T\,[M]\,[\Delta\phi] \tag{A-5}$$

Assume that the finite-element model of the body has a "global" Cartesian frame in which the ordinary velocities are measured, and further assume that the generalized coordinates of the finite-element model are grouped (or ordered) so that all the x-translations are together, followed by all the y- and then z-translations and that the translations are followed by sets of x-, y-, and z-rotations. With this implied ordering, it follows that the discrete mass matrix is partitioned in the form:

$$[M] = \begin{bmatrix} m_{xx} & m_{xy} & m_{xz} & m_{xp} & m_{xq} & m_{xr} \\ & m_{yy} & m_{yz} & m_{yp} & m_{yq} & m_{yr} \\ & & m_{zz} & m_{zp} & m_{zq} & m_{zr} \\ & & & m_{pp} & m_{pq} & m_{pr} \\ & \text{(symmetric)} & & & m_{qq} & m_{qr} \\ & & & & & m_{rr} \end{bmatrix} \tag{A-6}$$

with p, q, and r corresponding to rotation coordinates about x-, y-, and z-axes, respectively. Similarly, the modal transformation is partitioned as

$$[\phi] = \begin{bmatrix} & \{z+\eta_z\} & -\{y+\eta_y\} & \{1\} & & & [h_x] \\ -\{z+\eta_z\} & & \{x+\eta_x\} & & \{1\} & & [h_y] \\ \{y+\eta_y\} & -\{x+\eta_x\} & & & & \{1\} & [h_z] \\ \{1\} & & & & & & [\sigma_x] \\ & \{1\} & & & & & [\sigma_y] \\ & & \{1\} & & & & [\sigma_z] \end{bmatrix} \tag{A-7}$$

Each square subpartition of equation A-6 has rows equal to the number of structural joints (collocation points) of the finite-element model, as does each subpartition of equation A-7.

The submatrices in the last column partition of equation A-7, ($[h_x]$, $[h_y]$, ••, $[\sigma_z]$), have columns equal to the number of deformation modes used to represent the body and are matrices of modal translation and rotation amplitudes.

The forms of $[\phi_o]$ and $[\Delta\phi]$ are seen immediately from equation A-7 in that the only nonzero parts of $[\Delta\phi]$ are attributable to the $\{\eta\}$ vectors. The $[\phi]$ matrix is effectively a kinematic velocity transformation consistent with the form of equation II-25 of the main text, and it follows that

$$\begin{aligned} \{\eta_x\} &= [h_x]\ \{\xi\} \\ \{\eta_y\} &= [h_y]\ \{\xi\} \\ \{\eta_z\} &= [h_z]\ \{\xi\} \end{aligned} \tag{A-8}$$

Equation A-4 shows the product of two constant matrices; namely, $[M]\ [\phi_o]$. The two triple products on the right of equation A-4 require evaluation of only the first three row partitions of $[M]\ [\phi_o]$. Thus, the following is defined

(The first three row partitions of $[M]\ [\phi_o]$) =

$$\left[\begin{array}{ccccccc} \{P_{x1}\} & \{P_{x2}\} & \{P_{x3}\} & \{P_{x4}\} & \{P_{x5}\} & \{P_{x6}\} & [P_{xk}] \\ \{P_{y1}\} & \{P_{y2}\} & \{P_{y3}\} & \{P_{y4}\} & \{P_{y5}\} & \{P_{y6}\} & [P_{yk}] \\ \{P_{z1}\} & \{P_{z2}\} & \{P_{z3}\} & \{P_{z4}\} & \{P_{z5}\} & \{P_{z6}\} & [P_{zk}] \end{array}\right] \tag{A-9}$$

with, for example,

$$\{P_{x1}\} = [m_{xp}]\ \{1\} + [m_{xz}]\ \{y\} - [m_{xy}]\ \{z\} \tag{A-10}$$

and

$$\begin{aligned} [P_{xk}] = {} & [m_{xx}]\ [h_x] + [m_{xy}]\ [h_y] + [m_{xz}]\ [h_z] \\ & + [m_{xp}]\ [\sigma_x] + [m_{xq}]\ [\sigma_y] + [m_{xr}]\ [\sigma_z] \end{aligned} \tag{A-11}$$

It is unnecessary to expand each partition of equation A-9; the partial product is numerically obtained, and the examples of equations A-10 and A-11 are for purposes of illustration only.

Now, with reference to the intermediate constant matrices given in equation A-9 and the definitions of equations A-4 and A-5, the following inertial integrals* are developed:

$$[\alpha_1] = [P_{z4}]\ [h_y] - [P_{y4}]\ [h_z] \tag{A-12}$$

$$[\alpha_2] = [P_{z5}]\ [h_y] - [P_{y5}]\ [h_z] \tag{A-13}$$

$$[\alpha_3] = [P_{z6}]\ [h_y] - [P_{y6}]\ [h_z] \tag{A-14}$$

$$[\alpha_4] = [P_{x4}]\ [h_z] - [P_{z4}]\ [h_x] \tag{A-15}$$

$$[\alpha_5] = [P_{x5}]\ [h_z] - [P_{z5}]\ [h_x] \tag{A-16}$$

$$[\alpha_6] = [P_{x6}]\ [h_z] - [P_{z6}]\ [h_x] \tag{A-17}$$

$$[\alpha_7] = [P_{y4}]\ [h_x] - [P_{x4}]\ [h_y] \tag{A-18}$$

$$[\alpha_8] = [P_{y5}]\ [h_x] - [P_{x5}]\ [h_y] \tag{A-19}$$

$$[\alpha_9] = [P_{y6}]\ [h_x] - [P_{x6}]\ [h_y] \tag{A-20}$$

$$[b_1] = [P_{z1}]\ [h_y] - [P_{y1}]\ [h_z] \tag{A-21}$$

$$[b_2] = [P_{x2}]\ [h_z] - [P_{z2}]\ [h_x] \tag{A-22}$$

$$[b_3] = [P_{y3}]\ [h_x] - [P_{x3}]\ [h_y] \tag{A-23}$$

*The reader is advised to refer to paragraph II.D, particularly equations II-88 and II-89, of the main text.

$$[b_4] = [P_{z1}]\,[h_x] - [P_{x1}]\,[h_z] + [P_{y2}]\,[h_z] - [P_{z2}]\,[h_y] \quad \text{(A-24)}$$

$$[b_5] = [P_{x1}]\,[h_y] - [P_{y1}]\,[h_x] + [P_{y3}]\,[h_z] - [P_{z3}]\,[h_y] \quad \text{(A-25)}$$

$$[b_6] = [P_{x2}]\,[h_y] - [P_{y2}]\,[h_x] + [P_{z3}]\,[h_x] - [P_{x3}]\,[h_z] \quad \text{(A-26)}$$

$$[C_{yz}] = [h_y]^T\,[P_{zk}] - [h_z]^T\,[P_{yk}] \quad \text{(A-27)}$$

$$[C_{zx}] = [h_z]^T\,[P_{xk}] - [h_x]^T\,[P_{zk}] \quad \text{(A-28)}$$

$$[C_{xy}] = [h_x]^T\,[P_{yk}] - [h_y]^T\,[P_{xk}] \quad \text{(A-29)}$$

$$[C_{11}] = [h_y]^T\,[m_{zz}]\,[h_y] - [h_y]^T\,[m_{zy}]\,[h_z] - [h_z]^T\,[m_{yz}]\,[h_y] + [h_z]^T\,[m_{yy}]\,[h_z] \quad \text{(A-30)}$$

$$[C_{22}] = [h_z]^T\,[m_{xx}]\,[h_z] - [h_z]^T\,[m_{xz}]\,[h_x] - [h_x]^T\,[m_{zx}]\,[h_z] + [h_x]^T\,[m_{zz}]\,[h_x] \quad \text{(A-31)}$$

$$[C_{33}] = [h_x]^T\,[m_{yy}]\,[h_x] - [h_x]^T\,[m_{yx}]\,[h_y] - [h_y]^T\,[m_{xy}]\,[h_x] + [h_y]^T\,[m_{xx}]\,[h_y] \quad \text{(A-32)}$$

$$[C_{12}] = -[h_y]^T\,[m_{zx}]\,[h_z] + [h_y]^T\,[m_{zz}]\,[h_x] + [h_z]^T\,[m_{yx}]\,[h_z] - [h_z]^T\,[m_{yz}]\,[h_x] \quad \text{(A-33)}$$

$$[C_{13}] = - [h_y]^T [m_{zy}] [h_x] + [h_y]^T [m_{zx}] [h_y] + [h_z]^T [m_{yy}] [h_x] - [h_z]^T [m_{yx}] [h_y] \quad \text{(A-34)}$$

$$[C_{23}] = - [h_z]^T [m_{xy}] [h_x] + [h_z]^T [m_{xx}] [h_y] + [h_x]^T [m_{zy}] [h_x] - [h_x]^T [m_{zx}] [h_y] \quad \text{(A-35)}$$

APPENDIX B

DEVELOPMENT OF ROTATION TRANSFORMATIONS

APPENDIX B

DEVELOPMENT OF ROTATION TRANSFORMATIONS

In terms of Euler angles, the analyst may choose from twelve possible orthonormal rotation transformations in order to orient one orthogonal triad with respect to another. For each of these orthonormal rotation transformations, there is an associated rotation transformation that is not orthonormal and that is used to transform angular velocity projections (onto a nonorthogonal vector basis), which are time derivatives of Euler angles, to projections (onto an orthogonal vector basis) that are commonly referred to as time derivatives of angular quasi-coordinates (ω_x, ω_y, and ω_z).

For digital computation, these transformations can be generated automatically, given a selected order of rotation. The purpose of this appendix is to indicate the steps and numerical manipulations that are required. To this end, consider one of the twelve types (e.g., a 2-3-2 permutation) as an illustrative example.

Consider the two orthogonal vector bases, whose relative orientation we want to describe, to be

$$\{\bar{a}\} = \begin{bmatrix} I \\ J \\ K \end{bmatrix} \tag{B-1}$$

and

$$\{\bar{e}\} = \begin{bmatrix} \bar{i} \\ \bar{j} \\ \bar{k} \end{bmatrix} \tag{B-2}$$

Now, if θ_1, θ_2, and θ_3 are the three successive Euler rotations about axes (2-3-2), respectively, it then follows that

$$\{\bar{a}\} = [T_1]\{\bar{e}'\} \tag{B-3}$$

$$= \begin{bmatrix} \cos\theta_1 & 0 & \sin\theta_1 \\ 0 & 1 & 0 \\ -\sin\theta_1 & 0 & \cos\theta_1 \end{bmatrix} \begin{bmatrix} \bar{i}' \\ \bar{j}' \\ \bar{k}' \end{bmatrix} \qquad \text{(B-3) continued}$$

$$\{\bar{e}'\} = [T_2]\{\bar{e}''\} \qquad \text{(B-4)}$$

$$= \begin{bmatrix} \cos\theta_2 & -\sin\theta_2 & 0 \\ \sin\theta_2 & \cos\theta_2 & 0 \\ 0 & 0 & 1 \end{bmatrix} \begin{bmatrix} \bar{i}'' \\ \bar{j}'' \\ \bar{k}'' \end{bmatrix}$$

and

$$\{\bar{e}''\} = [T_3]\{\bar{e}\} \qquad \text{(B-5)}$$

$$= \begin{bmatrix} \cos\theta_3 & 0 & \sin\theta_3 \\ 0 & 1 & 0 \\ -\sin\theta_3 & 0 & \cos\theta_3 \end{bmatrix} \begin{bmatrix} \bar{i} \\ \bar{j} \\ \bar{k} \end{bmatrix}$$

On combining equations B-3, B-4, and B-5, there results

$$\{\bar{a}\} = [T_1][T_2][T_3]\{\bar{e}\} \qquad \text{(B-6)}$$

Now, a 2-3-2 permutation means that the first rotation, (θ_1), is about the second axis of the $\{\bar{a}\}$ basis, the second rotation, (θ_2), is about the third axis of the $\{\bar{e}'\}$ basis, and the third rotation, (θ_3), is about the second axis of the $\{\bar{e}''\}$ basis.

Consider the correlation between Euler rotations and the corresponding axis (table B-1). It is now clear that the elementary rotation transformations, ($[T_1]$, $[T_2]$, and $[T_3]$), always involve θ_1, θ_2, and θ_3, respectively, but any of them may have three different forms, depending on the axis associated with its rotation. That is, when θ_i (i = 1, 2, 3) is about

Table B-1
Correlation of Euler Rotations and Axes

Type	1	2	3	4	5	6	7	8	9	10	11	12
θ_1 about	1,I	1,I	1,I	1,I	2,J	2,J	2,J	2,J	3,K	3,K	3,K	3,K
θ_2 about	2,$\bar{j}'$	2,$\bar{j}'$	3,$\bar{k}'$	3,$\bar{k}'$	3,$\bar{k}'$	3,$\bar{k}'$	1,$\bar{i}'$	1,$\bar{i}'$	1,$\bar{i}'$	1,$\bar{i}'$	2,$\bar{j}'$	2,$\bar{j}'$
θ_3 about	3,$\bar{k}''$	1,$\bar{i}''$	1,$\bar{i}''$	2,$\bar{j}''$	1,$\bar{i}''$	2,$\bar{j}''$	2,$\bar{j}''$	3,$\bar{k}''$	2,$\bar{j}''$	3,$\bar{k}''$	3,$\bar{k}''$	1,$\bar{i}''$

axis (1), then

$$[T_i] = \begin{bmatrix} 1 & 0 & 0 \\ 0 & \cos\theta_i & -\sin\theta_i \\ 0 & \sin\theta_i & \cos\theta_i \end{bmatrix} \tag{B-7}$$

when θ_i is about axis (2),

$$[T_i] = \begin{bmatrix} \cos\theta_i & 0 & \sin\theta_i \\ 0 & 1 & 0 \\ -\sin\theta_i & 0 & \cos\theta_i \end{bmatrix} \tag{B-8}$$

and, finally, when θ_i is about axis (3),

$$[T_i] = \begin{bmatrix} \cos\theta_i & -\sin\theta_i & 0 \\ \sin\theta_i & \cos\theta_i & 0 \\ 0 & 0 & 1 \end{bmatrix} \tag{B-9}$$

Thus, it is evident that, to create the required orthonormal rotation transformation, equation B-6, only a rotation type (table B-1) and the three Euler rotations need to be specified.

The associated rotational velocity transformations are developed as follows. Consider, again, the 2-3-2 permutation. For this case, it is possible to express the angular velocity vector $\bar{\omega}$ in two ways:

$$\bar{\omega} = \bar{i}\,\omega_x + \bar{j}\,\omega_y + \bar{k}\,\omega_z \tag{B-10}$$

and

$$\bar{\omega} = \bar{j}'\dot{\theta}_2 + \bar{k}''\dot{\theta}_2 + \bar{j}''\dot{\theta}_3 \tag{B-11}$$

On combining equations B-10 and B-11, there results

$$\{\omega\} = [\pi]\,\{\dot{\theta}\}$$

or

$$\begin{bmatrix} \omega_x \\ \omega_y \\ \omega_z \end{bmatrix} = \begin{bmatrix} \cos\theta_3 & 0 & -\sin\theta_3 \\ 0 & 1 & 0 \\ \sin\theta_3 & 0 & \cos\theta_3 \end{bmatrix} \begin{bmatrix} \sin\theta_2 & 0 & 0 \\ \cos\theta_2 & 0 & 1 \\ 0 & 1 & 0 \end{bmatrix} \begin{bmatrix} \dot{\theta}_1 \\ \dot{\theta}_2 \\ \dot{\theta}_3 \end{bmatrix} \tag{B-12}$$

or

$$[\pi] = [T_3]^T\,[A]^T \tag{B-13}$$

Now, the inverse transformation of equation B-12 is required for hinge kinematics applications, or it is necessary to express

$$\begin{aligned} [\pi]^{-1} &= [A]^{T^{-1}}\,[T_3] \\ &= \left([E]^{-1}\,[E]\,[A]^T\right)^{-1}\,[T_3] \\ &= \left([E]\,[A]^T\right)^{-1}\,[E]\,[T_3] \end{aligned} \tag{B-14}$$

with [E], an elementary row interchange transformation that, for the (2-3-2) example, is

$$[E] = \begin{bmatrix} 1 & 0 & 0 \\ 0 & 0 & 1 \\ 0 & 1 & 0 \end{bmatrix} \tag{B-15}$$

and causes $\left([E]\ [A]^T\right)$ to be of the form:

$$[E]\ [A]^T = \begin{bmatrix} \alpha & 0 & 0 \\ 0 & 1 & 0 \\ \beta & 0 & 1 \end{bmatrix} \tag{B-16}$$

so that

$$\left([E]\ [A]^T\right)^{-1} = \begin{bmatrix} 1/\alpha & 0 & 0 \\ 0 & 1 & 0 \\ -\beta/\alpha & 0 & 1 \end{bmatrix} \tag{B-17}$$

with $\alpha = \sin\theta_2$ and $\beta = \cos\theta_2$.

The purpose of introducing [E] was to make the form of equation B-17 the same for all twelve types of Euler rotations. This is convenient with respect to programming considerations. It follows that:

- For types 1, 5, and 9, $\alpha = \cos\theta_2$, $\beta = \sin\theta_2$.
- For types 2, 6, and 10, $\alpha = \sin\theta_2$, $\beta = \cos\theta_2$.
- For types 3, 7, and 11, $\alpha = -\sin\theta_2$, $\beta = \cos\theta_2$.
- For types 4, 8, and 12, $\alpha = \cos\theta_2$, $\beta = \sin\theta_2$.

Also, for each of the twelve types, there is an elementary row interchange transformation, [E], that can be constructed from simple inspection of the permutation integers of table B-1 (e.g., 2-3-2). In fact, it is not necessary to actually construct [E] because information to construct it is merely applied to $[T_3]$ (interchanging its rows), which produces $[E]\ [T_3]$. Thus, the velocity transformation of equation B-14 can be created for any of the twelve possible types with comparative ease.

APPENDIX C

TIME DERIVATIVES OF KINEMATIC COEFFICIENTS

APPENDIX C

TIME DERIVATIVES OF KINEMATIC COEFFICIENTS

The formulation and numerical implementation of motion equations for the system of interconnected bodies involves a vector of Lagrange multipliers, $\{\lambda\}$. (Refer to equations II-1 and II-6 of the main text.) In order to numerically evaluate $\{\lambda\}$, time derivatives of kinematic coefficients (velocity transformations) associated with hinges must be calculated.

With reference to paragraph II.C of the main text, note that, for each hinge, there is a $[b_p]$ and a $[b_q]$ matrix of kinematic coefficients. The basic form of these matrices is repeated here, followed by the sequence of steps necessary for developing their time derivatives.

The $[b_p]$ array is

$$[b_p] = -\left[\begin{array}{c|c|c} [\pi]^{-1}\,[{}_qR_m] & [0] & [\pi]^{-1}\,[{}_qR_m]\,[\sigma_p] \\ \hline [{}_pR_m]\,[S^{(m)}_{mp}] & [{}_pR_m] & [{}_pR_m]\,[h_p] \end{array}\right] \qquad \text{(C-1)}$$

and

$$[b_q] = \left[\begin{array}{c|c|c} [\pi]^{-1}\,[{}_qR_n] & [0] & [\pi]^{-1}\,[{}_qR_n]\,[\sigma_q] \\ \hline [{}_pR_n]\,[S^{(n)}_{nq}] & [{}_pR_n] & [{}_pR_n]\,[h_q] \end{array}\right] \qquad \text{(C-2)}$$

To develop $[\dot{b}_p]$ and $[\dot{b}_q]$, it is necessary to expand the following as

$$\frac{d}{dt}\left([\pi]^{-1}\,[{}_qR_m]\right) = [\dot{\pi}^{-1}]\,[{}_qR_m] + [\pi]^{-1}\left([{}_q\dot{R}_p]\,[{}_pR_m] + [{}_qR_p]\,[{}_p\dot{R}_m]\right) \qquad \text{(C-3)}$$

$$\left(\frac{d}{dt}\ [{}_pR_m]\ [S^{(m)}_{mp}]\right) = [{}_p\dot{R}_m]\ [S^{(m)}_{mp}] + [{}_pR_m]\ [\dot{S}^{(m)}_{mp}] \tag{C-4}$$

$$\frac{d}{dt}\left([\pi]^{-1}\ [{}_qR_n]\right) = [\dot{\pi}^{-1}]\ [{}_qR_n] + [\pi]^{-1}\ [{}_q\dot{R}_n] \tag{C-5}$$

and

$$\frac{d}{dt}\left([{}_pR_n]\ [S^{(n)}_{nq}]\right) = [{}_p\dot{R}_n]\ [S^{(n)}_{nq}] + [{}_pR_n]\ [\dot{S}^{(n)}_{nq}] \tag{C-6}$$

The 3 by 3 matrix time derivatives defined by equations C-3 through C-6 have factors (also 3 by 3 matrix time derivatives) that are expanded in terms of previously defined quantities as follows:

$$[{}_p\dot{R}_m] = [SK^*\left([{}_pR_m]\ [\sigma_p]\ \{\dot{\xi}_m\}\right)\ ]\ [{}_pR_m] \tag{C-7}$$

$$[{}_q\dot{R}_n] = [SK^*\left([{}_qR_n]\ [\sigma_q]\ \{\dot{\xi}_n\}\right)\ ]\ [{}_qR_n] \tag{C-8}$$

$$[{}_p\dot{R}_q] = [\Omega^{(p)}_{p/q}]\ [{}_pR_q] \tag{C-9}$$

with

$$\begin{aligned}[\Omega^{(p)}_{p/q}] = SK^*\Big(&[{}_pR_m]\ \left(\{\omega_m\} + [\sigma_p]\ \{\dot{\xi}_m\}\right) \\ &- [{}_pR_q]\ [{}_qR_n]\ \left(\{\omega_n\} + [\sigma_q]\ \{\dot{\xi}_n\}\right)\Big)\end{aligned} \tag{C-10}$$

$$[{}_p\dot{R}_n] = [{}_p\dot{R}_q]\ [{}_qR_n] + [{}_pR_q]\ [{}_q\dot{R}_n] \tag{C-11}$$

$$[\dot{S}^{(m)}_{mp}] = \left[SK^*\left([h_p]\ \{\dot{\xi}_m\}\right)\right] \tag{C-12}$$

$$[\dot{S}^{(n)}_{nq}] = \left[SK^{*}\left([h_q]\ \{\dot{\xi}_n\}\right)\right] \tag{C-13}$$

Finally, the time derivative of $[\pi]^{-1}$ requires additional consideration. (Refer to Appendix B.) The rotation transformation, $[\pi]^{-1}$, is developed as

$$[\pi]^{-1} = \left([E]\ [A]^{T}\right)^{-1}\ [E]\ [T_3] \tag{C-14}$$

and it is shown that the form

$$\left([E]\ [A]^{T}\right)^{-1} = [\tilde{A}] = \begin{bmatrix} 1/\alpha & 0 & 0 \\ 0 & 1 & 0 \\ -\beta/\alpha & 0 & 1 \end{bmatrix} \tag{C-15}$$

holds for each of the twelve possible Euler rotations. In that [E] is constant, $[\tilde{A}]$ depends *only* on θ_2, and $[T_3]$ depends on θ_3 *only*. It follows that

$$\frac{d}{dt}\ [\pi]^{-1} = \dot{\theta}_2\ \frac{\partial}{\partial\theta_2}\ [\tilde{A}]\ [E]\ [T_3] + \dot{\theta}_3\ \left([\tilde{A}]\ [E]\right)\ \frac{\partial}{\partial\theta_3}\ [T_3] \tag{C-16}$$

where the Euler angle rates, $\dot{\theta}_2$ and $\dot{\theta}_3$, are numerically evaluated before their use in equation C-16 through application of equation II-3 of the main text (that is, they reside in that part of the state-vector time derivative, $\{\dot{y}\}$, that has been evaluated).

APPENDIX D

MONITOR OF SYSTEM MOMENTA AND ENERGIES

APPENDIX D

MONITOR OF SYSTEM MOMENTA AND ENERGIES

Developing state equations for predicting dynamic response of a system of interconnected flexible bodies involves a considerable amount of complicated formulation and programming codes regardless of the particular method of analytical mechanics selected for basing development.

The inherent complexity of such a digital simulation program gives rise to the question: Is there any way to check the program validity? In an attempt to answer this question, one suggestion is to compare results with those of other dynamic simulations or hardware tests. If such a comparison is positive, credibility (to a degree) is established. However, another absolutely necessary (if not sufficient) condition must be passed to establish validity. For a dynamic system free of external forces and torques, angular and linear momenta must be conserved, and total energy (kinetic plus potential) must not increase in time.

A desirable feature for such a digital simulation program is to have a built-in monitor of momenta and energy. The purpose of this appendix is to develop (in terms of previously identified state variables and system parameters) the expressions for total system angular and linear momentum vectors and the total system energy.

The total angular momentum about the inertial reference can be expressed (from definition) as

$$\bar{H} = \sum_{j=1}^{NB} \int_{V_j} (\bar{x} \times \bar{v})\, dm \qquad \text{(D-1)}$$

with the summation over the number of bodies, NB, of the system, with $\bar{x}$ being the vector positioning the elemental mass, dm, from the inertial origin, with $\bar{v}$ being the absolute velocity of dm, and with integration taken over the volume of the j^{th} body, V_j. Also, from definition, the total linear momentum with respect to the inertial frame is

$$\bar{L} = \sum_{j=1}^{NB} \int_{V_j} \bar{v}\, dm \qquad \text{(D-2)}$$

Now, consistent with the notion of a body fixed-axis system and with a consistent velocity field assumed (paragraph II.B of the main text), it follows that, over the volume of the j^{th} body,

$$\bar{x} = \bar{x}_{Rj} + \bar{\rho}_0 + \bar{\eta} \tag{D-3}$$

and

$$\bar{v} = \bar{v}_{Rj} + \bar{\omega}_j \times (\bar{\rho}_0 + \bar{\eta}) + \bar{\phi}_k \dot{\xi}_k \tag{D-4}$$

On substituting equations D-3 and D-4 into D-1 and D-2 and integrating, it becomes clear that the first six elements of the product

$$\begin{aligned} \{p\}_j &= [m]_j \{U\}_j \\ &= \begin{bmatrix} \{p_\omega\} \\ \{p_v\} \\ \{p_\xi^*\} \end{bmatrix}_j \end{aligned} \tag{D-5}$$

are projections of the j^{th} body's angular and linear momentum vectors onto the moving-body axis system. In fact, $\{p_\omega\}$ includes the effect of momentum wheels (equation II-109 of the main text), which must be accounted for. Thus, the angular momentum of the j^{th} body about its body origin is

$$\bar{h}_j = [\bar{e}_j] \{p_\omega\}_j \tag{D-6}$$

whereas the linear momentum of the j^{th} body is

$$\bar{\ell}_j = [\bar{e}_j] \{p_v\}_j \tag{D-7}$$

where $[\bar{e}_j]$ is the unit-vector basis associated with the body fixed-reference triad.

Rotation transformations that relate vector components in each body system to the inertial system exist, and position vector from the inertial origin to the reference point of each body exists. It follows that

$$\begin{aligned} \bar{L} &= \sum_{j=1}^{NB} \bar{\ell}_j \\ &= \sum_{j=1}^{NB} \left[{}_0R_j \right] \left\{ p_v \right\}_j \end{aligned} \tag{D-8}$$

and that

$$\begin{aligned} \bar{H} &= \sum_{j=1}^{NB} \left(\bar{h}_j + \bar{X}_{Rj} \times \bar{\ell}_j \right) \\ &= \sum_{j=1}^{NB} \left(\left[{}_0R_j \right] \left\{ p_\omega \right\}_j + \left[SK^* \left(\left[{}_0R_j \right] \left\{ p_v \right\} \right) \right] \left\{ x_R \right\}_j \right) \end{aligned} \tag{D-9}$$

The total angular and linear momentum vectors are calculated by the program in the manner indicated in equations D-8 and D-9. For a variety of torque/force-free configurations that have been examined, momentum has been conserved within acceptable numerical tolerances.

The total energy is calculated (equations II-38 and II-42 of the main text) as

$$T + V = \tfrac{1}{2} \sum_{j=1}^{NB} \left(\left\{ U \right\}_j \left[m \right]_j \left\{ U \right\}_j + \left\{ \xi \right\}_j \left[k \right]_j \left\{ \xi \right\}_j \right) \tag{D-10}$$

The kinetic energy contribution of embedded momentum wheels is included (as it must be) because $[m]_j$ includes momentum-wheel inertial coupling terms and $\{U\}_j$ includes momentum-wheel spin rates ($\dot{\theta}_s$).

Potential energy, in addition to that shown in equation D-10, comes about if there is a "sprung" hinge (e.g., associated with the β_k coordinate). If the spring force/torque is linear with β_k, additional potential energy is

$$V_{(additional)} = \tfrac{1}{2} \sum_k K_k \beta_k^2 \tag{D-11}$$

APPENDIX E

ROOT-LOCUS SOLUTION TECHNIQUES

APPENDIX E

ROOT-LOCUS SOLUTION TECHNIQUES

INTRODUCTION

The root-locus solution procedure that is included in the digital program was supplied by Goddard Space Flight Center (GSFC) personnel and is included here for completeness. The following discussion has been extracted from GSFC Branch Report No. 254, dated October 2, 1973 (Raymond V. Welch, author).

Two expressions are identified as the basis for initiating the solution process:

$$\left| K \frac{P(s)}{Q(s)} \right| = 1 \qquad \text{(E-1)}$$

$$\angle \frac{P(s)}{Q(s)} = 180^\circ \; K \geq 0 \qquad \text{(E-2)}$$

Expressions E-1 and E-2 contain polynomial expressions for the conventional open-loop expression,

$$KG(s)\,H(s) = KP(s)/Q(s) \qquad \text{(E-3)}$$

The solution process requires a starting point (known to lie somewhere on the loci) from which to generate the desired locus; therefore, assume that a known value of s exists, (e.g., s_0) so that

$$\angle \frac{P(s_0)}{Q(s_0)} = 180^\circ \qquad \text{(E-4)}$$

(i.e., s_0 is a point on the locus). A good starting point might be an open-loop pole or zero because these points are usually known *a priori*; however, any point along the branch of the locus to be determined may be used. The locus is then traced, using the following procedure.

STEP 1

Draw a "small" circle of radius, r, centered at s_o, and define s_c to be the values of s which lie on this circle (figure E-1). These values of s_c are determined analytically by

$$s_c = s_o + re^{j\theta} \tag{E-5}$$

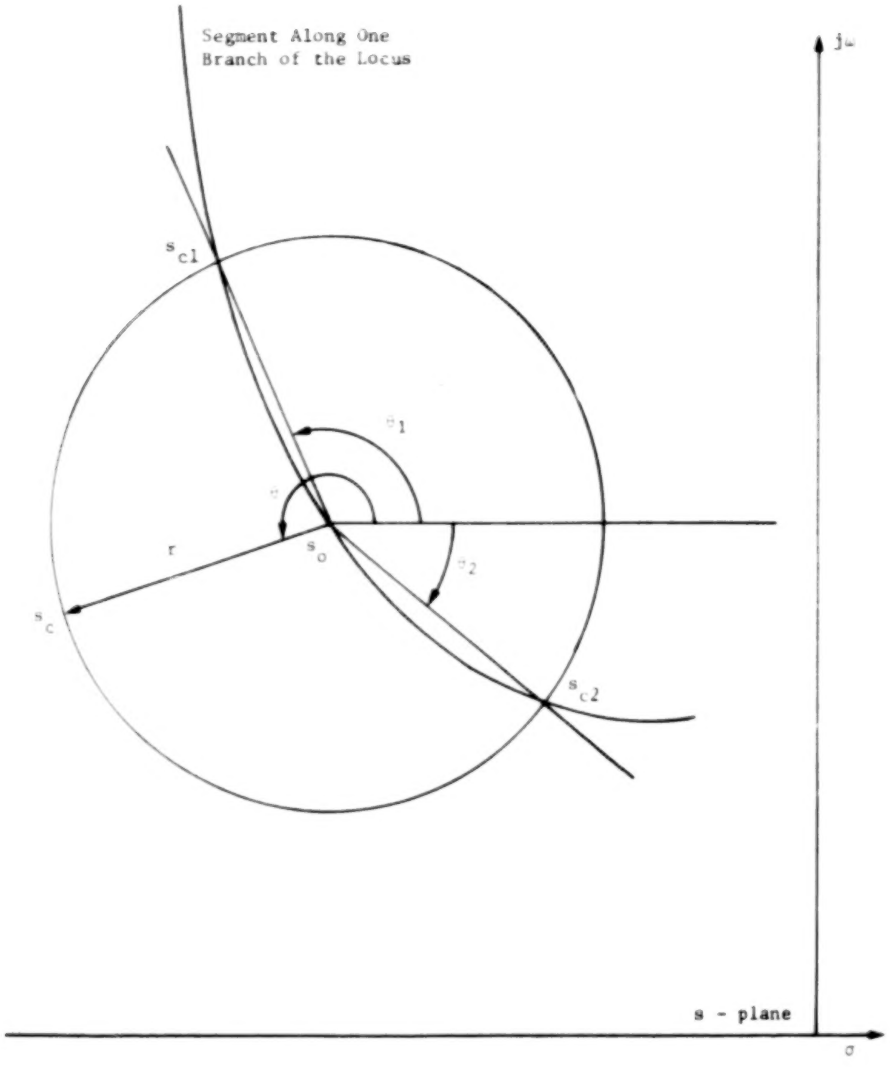

Figure E-1. Variable definitions at starting point of locus.

where θ is measured as the angle generated by a counterclockwise rotation from the positive real axis of the s-plane. If the locus does not terminate inside the circle, at least two values of θ must exist between zero and 360 degrees so that

$$\angle \frac{P(s_c)}{Q(s_c)} = 180^\circ \qquad \text{(E-6)}$$

(More than two values of θ will exist that satisfy this equation if breakway points of the locus are encircled or if the circle is large enough to intersect other branches of the locus. Consequently, to avoid changing branches, r must be kept smaller than the distance between the branches of the locus.) If, for $\theta = \theta_1$ and $\theta = \theta_2$, the foregoing equation is satisfied, s_{c1} and s_{c2} are points on the locus (figure E-1) where

$$\begin{aligned} s_{c1} &= s_o + re^{j\theta_1} \\ s_{c2} &= s_o + re^{j\theta_2} \end{aligned} \qquad \text{(E-7)}$$

These roots are found by an iterative process.

STEP 2

Define $\psi(\theta)$ by

$$\psi(\theta) = \angle \frac{P(s_c)}{Q(s_c)} \qquad \text{(E-8)}$$

where s_c is defined above and θ is any arbitrary angle. If $\psi(\theta)$ does not equal 180°, increment θ by $\Delta\theta$ and reevaluate $\psi(\theta)$. Continue this process until $\psi(\theta)$ passes through 180°. Because $\psi(\theta)$ is a monotonic function across the locus, $\psi(\theta)$ crossing 180° implies that the locus has been crossed. When $\psi(\theta)$ passes through 180°, redefine $\Delta\theta$ as

$$\Delta\theta_{new} = -K\Delta\theta_{old}; \quad 0 < K < 1 \qquad \text{(E-9)}$$

and again calculate $\psi(\theta)$. If $\psi(\theta)$ does not equal 180° for this point, increment θ by this new $\Delta\theta$ and recalculate $\psi(\theta)$. Continue this process until $\psi(\theta)$ again crosses 180°. Reduce $\Delta\theta$

again by the foregoing process, and repeat the previous operation until $\Delta\theta = \delta$, where δ is some predefined small positive number. At this time, $\psi(\theta)$ will be $180 \pm\epsilon^{\circ}$, where ϵ is a "small" angle whose size is a function of δ; thus, a root on the locus has been found that is either s_{c1} or s_{c2}, depending on the initial choice of θ and on the initial sign of $\Delta\theta$. For this subprogram, the initial value of θ is optional, but, if no choice is made, a value of 180° is used. Also, the initial increment, $\Delta\theta$, is set at 10° with the change in $\Delta\theta$ for every 180° crossing defined by

$$\Delta\theta_{new} = -\frac{1}{10}\,\Delta\theta_{old} \tag{E-10}$$

It was found that $\delta = 10^{-8^{\circ}}$ was small enough to ensure $\epsilon < 0.001^{\circ}$ except for possibly values of s near the open-loop poles or zeros. Assume that θ is chosen initially so that the root found is located at the point, s_{c1}, as previously defined and as shown in figure E-1, and suppose that it is desired to continue the locus in this direction.

STEP 3

Draw a circle of radius, r , centered at s_{c1}. Again, if the locus does not terminate inside the circle, the locus will intersect the circle in at least two points. Because the circles located at s_o and s_{c1} are of equal radius, one of these points is s_o as shown in figure E-2. This root is eliminated from the search routine by restricting the range of θ to

$$\theta_1 - 120^{\circ} < \theta < \theta_1 + 120^{\circ} \tag{E-11}$$

These limits are chosen because they are the points at which the circles located at s_o and s_{c1} intersect. Thus, the search for a new root is conducted only in a previously unsearched region. The initial angle is chosen at $\theta = \theta_1 - 120^{\circ}$ $\Delta\theta$>o, and Step 2 is repeated until $\Delta\theta = \delta$ (i.e., another root is found).

STEP 4

Draw a circle of radius, r, centered at the root found in the previous step, and repeat Step 2 with the restrictions on θ as defined in Step 3.

Repeat Step 4 to determine the roots along one branch of the locus. The value of the gain, K, for each of these roots is calculated from

$$K = \left|\frac{Q(s)}{P(s)}\right| \tag{E-12}$$

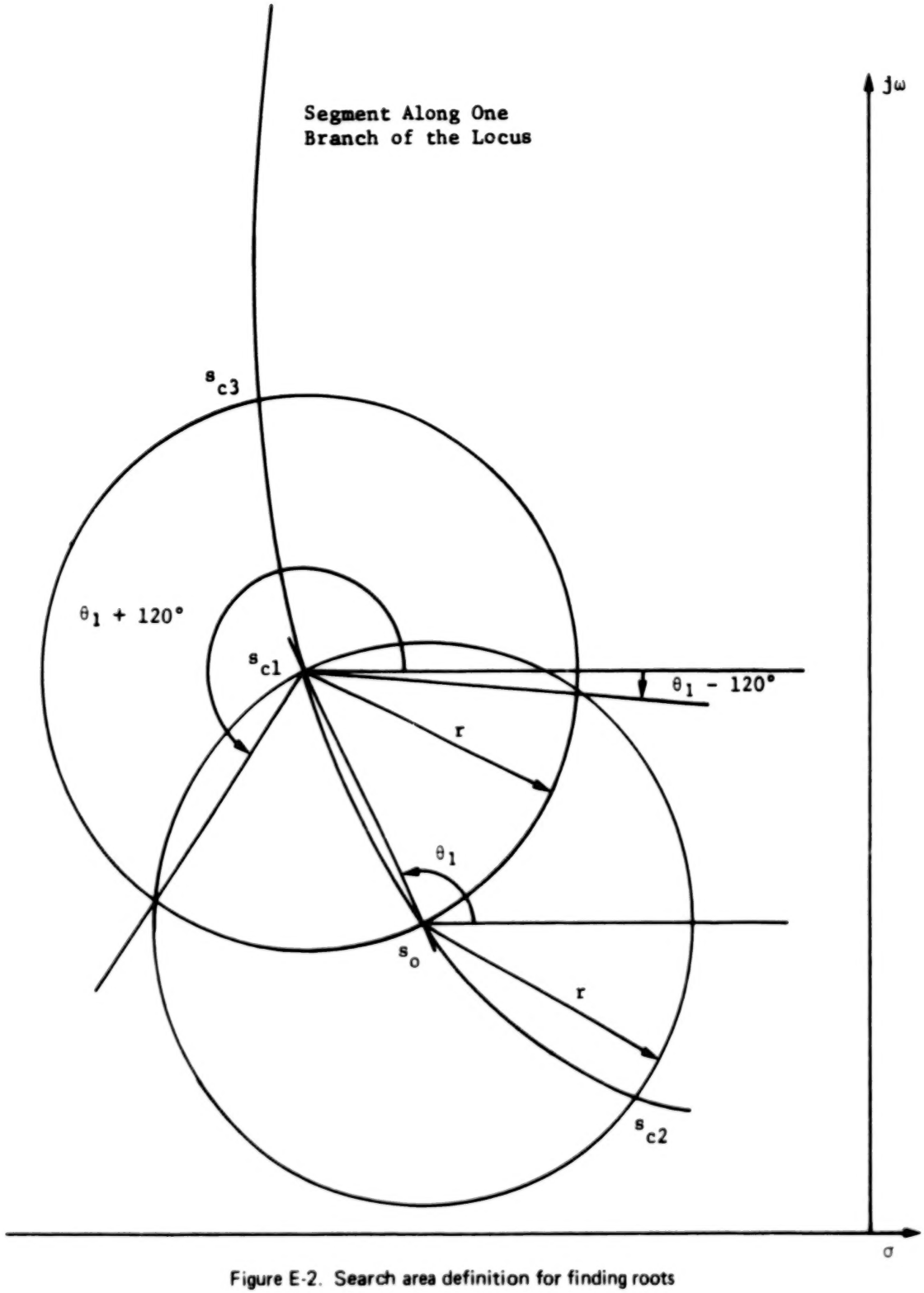

Figure E-2. Search area definition for finding roots after the first root is found.

APPENDIX F

SIMULATION NOMENCLATURE

BLANK PAGE

BLANK PAGE

TYPICAL MULTIBODY CONFIGURATION

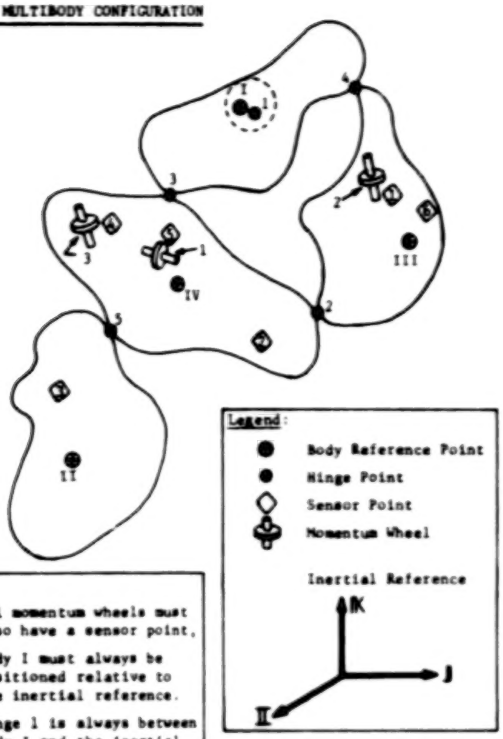

Note:

1. All momentum wheels must also have a sensor point,
2. Body I must always be positioned relative to the inertial reference.
3. Hinge 1 is always between Body I and the inertial reference.

TYPICAL TWO BODY/HINGE POINT ARRANGEMENT

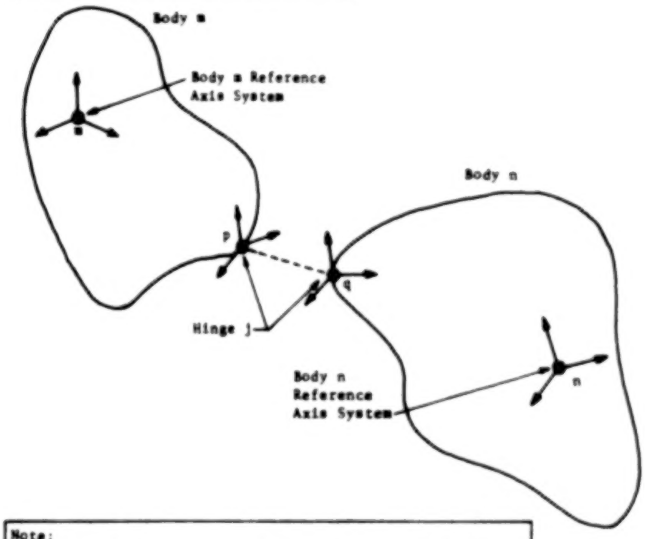

Note:

1. Motion of the q frame on Body n is measured relative to the p frame on Body m,
2. The p and q frames are positioned with respect to Body m and n reference axis systems,
3. Hinge j is identified via array ITOPOL,
4. Array IHDATA contains additional hinge information.

PROGRAM SIMULATION INTEGER ARRAYS

ITOPOL — Topology, Size = 2 x NH

Hinge No.	1	2	3	4	5
Body No.	1	3	4	3	2
	0	4	1	1	4

Body n has frame q
Body m has frame p

Example: Refer to Column 3 (Hinge 3) and note Body 4 interfaces with Body 1 via Hinge 3.

IRGFLX — No. of Elastic Modes/Body, Size = 1 x NB

Body No.	1	2	3	4
	5	0	0	2

Example: Body No. 4 has 2 elastic modes, Body No. 2 has no elastic modes.

IFTSMx — Sensor Point Locations, Size = 1 x NS

Sensor Pt.	1	2	3	4	5	6
	3	4	2	4	4	3

Example: Sensor Point (5) is located on Body 4 (as are Sensor Points (2) and (4))

IHDATA — Hinge Information, Size = 7 x NH

ITYPE	1	2	3	4	5 ← Hinge No.
	3	1	7	2	11
$\dot{\theta}_1$	0	0	0	1	0
$\dot{\theta}_2$	0	0	0	1	2
$\dot{\theta}_3$	0	0	0	0	1
$\dot{x}$	0	1	1	1	1
$\dot{y}$	0	1	0	1	1
$\dot{z}$	0	1	1	1	0

Note:
1. ITYPE = Euler Type
2. Elements in rows 2-7 identify hinge constraint type.

0: Free/forced
1: Fixed Constraint (Zero relative velocity)
2: Rheonomic Constraint (time dependent)

Additional Remarks:

1. The number of Betas in the state vector equals the sum of "zeros" plus the sum of the "twos" (excluding row 1) in the array.
2. The number of Lambdas (constraints) equals the number of "nonzeros" (excluding row 1) in the array.

IMO — Momentum Wheel Information, Size = 3 x NOFMO and 2 x NOFMO

AMO

Momentum Wheel No.	1	2	3
Sensor Point No.	5	1	4
Spin Axis (1, 2, or 3)	2	1	3
1 = Active; 0 = Constant Speed	1	1	0
Wheel Rates (Initial)	$\dot{\theta}_1$	$\dot{\theta}_2$	$\dot{\theta}_3$
Wheel Inertia about Spin Axis	J_1	J_2	J_3

EULER ANGLE PERMUTATION CANDIDATES - ITYPE

	ITYPE =	1	2	3	4	5	6	7	8	9	10	11	12
1st Rotation	Axis of θ_1	1	1	1	1	2	2	2	2	3	3	3	3
2nd Rotation	Axis of θ_2	2	2	3	3	3	3	1	1	1	1	2	2
3rd Rotation	Axis of θ_3	3	1	1	2	1	2	2	3	2	3	3	1

Example Using ITYPE = 6

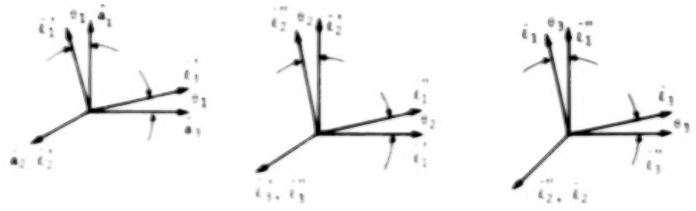

θ_1 about axis 2 θ_2 about axis 3 θ_3 about axis 2

$$\begin{Bmatrix} \hat{i}_1 \\ \hat{i}_2 \\ \hat{i}_3 \end{Bmatrix} \begin{bmatrix} C_3 & 0 & -S_3 \\ 0 & 1 & 0 \\ S_3 & 0 & C_3 \end{bmatrix} \begin{bmatrix} C_2 & S_2 & 0 \\ -S_2 & C_2 & 0 \\ 0 & 0 & 1 \end{bmatrix} \begin{bmatrix} C_1 & 0 & -S_1 \\ 0 & 1 & 0 \\ S_1 & 0 & C_1 \end{bmatrix} \begin{Bmatrix} \hat{a}_1 \\ \hat{a}_2 \\ \hat{a}_3 \end{Bmatrix}$$

also

$$\hat{i}_1 = {}_1R_1 \, \hat{i}_1$$

CONSOLIDATION OF KINEMATICAL COEFFICIENTS

(The "b" Coefficients)

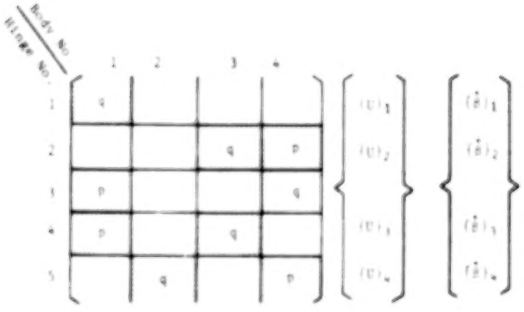

Note:

1. Only a single entry is in partition for Hinge 1 and it is a q type partition from the connection kinematical array above.
2. All other row partitions have both a p and a q constituent for each "hinge" between contiguous bodies

CONNECTION KINEMATICS - TYPICAL HINGE

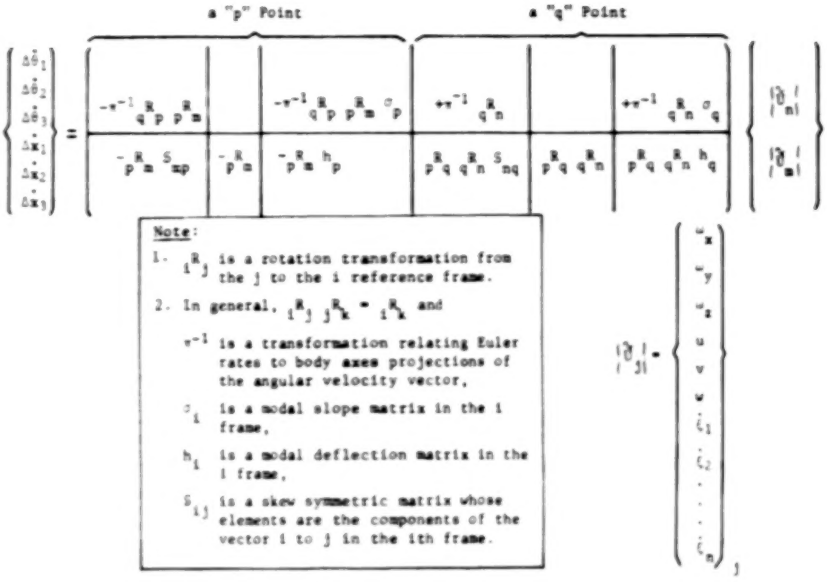

CONSTRAINT FORCE/TORQUE VECTOR

$$\{\lambda\} = \begin{Bmatrix} \lambda_1 \\ \lambda_2 \\ \lambda_3 \\ \lambda_4 \\ \lambda_5 \\ \lambda_6 \\ \lambda_7 \\ \lambda_8 \\ \lambda_9 \\ \lambda_{10} \\ \lambda_{11} \\ \lambda_{12} \\ \lambda_{13} \\ \lambda_{14} \end{Bmatrix} \begin{matrix} (F_x)_2 \\ (F_y)_2 \\ (F_z)_2 \\ (F_x)_3 \\ (F_z)_3 \\ (T_1)_4 \\ (T_2)_4 \\ (F_x)_4 \\ (F_y)_4 \\ (F_z)_4 \\ (T_2)_5 \\ (T_3)_5 \\ (F_x)_5 \\ (F_y)_5 \end{matrix}$$

$(F_x)_i$ refers to Hinge i

STATE VECTOR ARRANGEMENT

$$\{y\} = \begin{Bmatrix} (U)_1 \\ (U)_2 \\ (U)_3 \\ (U)_4 \\ (\zeta)_1 \\ (\zeta)_2 \\ (\zeta)_3 \\ (\zeta)_4 \\ \theta_1 \\ \theta_2 \\ \theta_3 \\ \theta_4 \\ \theta_5 \\ \theta_6 \\ \theta_7 \\ \theta_8 \\ \theta_9 \\ \theta_{10} \\ \theta_{11} \\ \theta_{12} \\ \theta_{13} \\ \theta_{14} \\ \theta_{15} \\ \theta_{16} \\ \theta_{17} \\ \xi_1 \\ \xi_2 \\ \xi_3 \end{Bmatrix} ; \quad \{\dot{y}\} = \begin{Bmatrix} (\dot{U})_1 \\ (\dot{U})_2 \\ (\dot{U})_3 \\ (\dot{U})_4 \\ (\dot{\zeta})_1 \\ (\dot{\zeta})_2 \\ (\dot{\zeta})_3 \\ (\dot{\zeta})_4 \\ \dot{\theta}_1 \\ \dot{\theta}_2 \\ \dot{\theta}_3 \\ \dot{\theta}_4 \\ \dot{\theta}_5 \\ \dot{\theta}_6 \\ \dot{\theta}_7 \\ \dot{\theta}_8 \\ \dot{\theta}_9 \\ \dot{\theta}_{10} \\ \dot{\theta}_{11} \\ \dot{\theta}_{12} \\ \dot{\theta}_{13} \\ \dot{\theta}_{14} \\ \dot{\theta}_{15} \\ \dot{\theta}_{16} \\ \dot{\theta}_{17} \\ \dot{\xi}_1 \\ \dot{\xi}_2 \\ \dot{\xi}_3 \end{Bmatrix}$$

where $(U)_j = \begin{Bmatrix} \omega_x \\ \omega_y \\ \omega_z \\ u \\ v \\ w \\ \dot{\zeta}_1 \\ \dot{\zeta}_2 \\ \cdot \\ \cdot \\ \cdot \\ \dot{\zeta}_{NE} \\ \dot{\theta}_1 \\ \dot{\theta}_2 \\ \cdot \\ \cdot \\ \cdot \\ \dot{\theta}_M \end{Bmatrix}_j$

← For this example, prescribed as function of time, i.e., a rheonomic constraint as noted in INDATA

1. Report No. NASA TP-1219	2. Government Accession No.	3. Recipient's Catalog No.
4. Title and Subtitle A Digital Computer Program for the Dynamic Interaction Simulation of Controls and Structure (DISCOS), Volume I		5. Report Date May 1978 6. Performing Organization Code 712
7. Author(s) Carl S. Bodley, A. Darrell Devers, A. Colton Park, and Harold P. Frisch		8. Performing Organization Report No. G7702-F26
9. Performing Organization Name and Address Goddard Space Flight Center Greenbelt, Maryland 20771		10. Work Unit No. 506-17-31 11. Contract or Grant No.
12. Sponsoring Agency Name and Address National Aeronautics and Space Administration Washington, D.C. 20546		13. Type of Report and Period Covered Technical Paper 14. Sponsoring Agency Code
15. Supplementary Notes		

16. Abstract

This document presents a theoretical development and associated digital computer program system for the dynamic simulation and stability analysis of passive and actively controlled spacecraft. The dynamic system (spacecraft) is modeled as an assembly of rigid and/or flexible bodies not necessarily in a topological tree configuration. The computer program system may be used to investigate total system dynamic characteristics, including interaction effects between rigid and/or flexible bodies, control systems, and a wide range of environmental loadings. In addition, the program system may be used for designing attitude-control systems and for evaluating total dynamic system performance, including time-domain response and frequency-domain stability analyses.

17. Key Words (Selected by Author(s))	18. Distribution Statement		
Spacecraft attitude dynamics, Stabilization and control, Flexible body dynamics, Applied mathematics	STAR Category 18 Unclassified–Unlimited		
19. Security Classif. (of this report) Unclassified	20. Security Classif. (of this page) Unclassified	21. No. of Pages 168	22. Price* $8.00

*For sale by the National Technical Information Service, Springfield, Virginia 22161.

NASA-Langley, 1978